REGENERATIVE AIR ENERGY STORAGE FOR RENEWABLE ENERGY INTEGRATION: SYSTEM MODELING AND OPTIMIZATION

by

Sebastian Callaghan Manchester

Submitted in partial fulfilment of the requirements
for the degree of Master of Applied Science

at

Dalhousie University
Halifax, Nova Scotia
April 2014

This thesis is dedicated to the billions of people who are, or will soon be, facing the adversities of climate change.

TABLE OF CONTENTS

LIST OF TABLES

LIST OF FIGURES

ABSTRACT

As energy systems shift away from fossil-fuel based electricity, the non-dispatchability of renewable energy converters (REC) continue to stress the grid infrastructure and conventional thermal generating units. These hybrid electricity systems require energy storage systems to buffer the variabilities of electricity supply and demand. Regenerative air energy storage (RAES) is an emerging technology that shows promise to overcome the barriers of REC variability. RAES uses a novel compressor/expander that approaches isothermal operation by spraying water into the piston/cylinder to absorb/release heat. RAES can be sized for power and energy independently, and has a high round-trip efficiency that can be boosted using low grade waste heat. Because of its novelty, new numerical models are necessary to investigate the sizing and performance of RAES systems. In this thesis a numerical simulation tool is developed to allow flexible and intuitive analysis of a range of hybrid energy systems involving RAES. The model allows inputs of various time series datasets to simulate RAES operation and uses a parametric sweep to optimize for user-defined objectives. Two case studies are presented to demonstrate the operation of the model and the viability of RAES as a means to further integrate REC.

LIST OF ABBREVIATIONS AND SYMBOLS USED

Acronyms

CAES	Compressed Air Energy Storage
CE	Compressor/expander
CHP	Combined heat and power
DG	Diesel generator
ESS	Energy storage system
LSC	LightSail Canada
LSE	LightSail Energy
MAL	Minimum annual load
NGCC	Natural gas combined cycle
PV	Photovoltaic
RAES	Regenerative air energy storage
RE	Renewable energy
SOC	State of charge
TES	Thermal energy storage
WEC	Wind energy converter
WHR	Waste heat recovery

Symbols

A	Swept area (m^2)
CP	Power coefficient
C_p	Specific heat capacity (kJ/kg/K)
d	Differential
E	Electrical energy (kWh)
F	Fuel consumption (kWh)
$\dot{F}$	Fuel consumption rate (L/hr)
H	Enthalpy (kJ/kg/K)
HR	Heat recovery effectiveness coefficient
M	Mass (kg)
m	Mass ratio
$\dot{m}$	Mass flow rate (kg/s)
N	Quantity (number of)
n	Exponential compression/expansion coefficient
P	Power (kW)
PR	Penetration rate
p	Pressure (Pa)
U	Wind speed (m/s)
Q	Heat (kWh)
$\dot{Q}$	Heat rate (kW)
$\dot{q}$	Heat rate coefficient (kW/K)
q	Specific heat (kWh/kg)
R	Ideal gas constant (J/mol/K)

S	Entropy (J/K)
T	Temperature (K)
t	Time step duration (hr)
V	Volume (m^3)
w	Specific work (kJ/kg)
z	Height (m)

Subscripts

1	Pre-compression state
2	Compressed state
3	Expanded stage
a	Air
w	Water
amb	Ambient
anem	Anemometer
CC	Cycle charging set-point
CHP	Combined heat and power
chg	Charge
comp	Compression process
curt	Curtailment
DG	Diesel generator power
dschg	Discharge
hub	WEC hub
L	Community electrical load
Loss	Heat loss coefficient
max	Maximum
min	Minimum
NP	Name-plate capacity
Power	Power of storage
RAES	Regenerative air energy storage
SOC	State of charge of storage
start	DG start-up
steam	Steam properties
TES	Thermal energy storage
therm	Thermodynamic
WEC	Wind generated electrical power
WH	Waste heat

Greek symbols

Δ	Change
ρ	Density
α	Wind shear coefficient
η	Efficiency

ACKNOWLEDGEMENTS

Foremost, I would like to express my endless gratitude and appreciation for my supervisor Dr. Lukas Swan, whose tireless support and guidance not only made this research possible, but also made it great. I owe many thanks to my co-supervisor Dr. Dominic Groulx, who lent his knowledge and experience to help this research succeed. Special thanks to Dr. Marek Kujath and Dr. Timothy Little, for their oversight as supervisory committee members, and to the faculty, administration, and staff of the Department of Mechanical Engineering at Dalhousie for all of your support along the way. I would also like to acknowledge the rest of the Renewable Energy Storage Lab team, past and present, for their mentorship and encouragement.

Thank you to everyone at LightSail Energy and LightSail Canada, whose amazing work has been a source of inspiration throughout the duration of my Master's degree. Thank you for your technical support in this research, and for giving me the opportunity to work alongside you. Likewise, thank you to everyone else who provided technical support for this research including (but certainly not limited to) Nova Scotia Power, Brooklyn Power, Emera, Watts Wind, Frontier Power Systems, Natural Resources Canada, and Fundy Tidal Inc.

This research was made possible thanks to the support of the Natural Sciences and Engineering Research Council, and the Nova Scotia Productivity and Innovation Voucher Program. I would also like to thank the Nova Scotia Department of Energy and the Offshore Energy Research Association for giving me the opportunity to collaborate with the University of Edinburgh's Institute for Energy Systems (a team that also deserves many thanks).

Finally, I infinitely thank my family, friends, and roommates. Your love and support keeps me motivated and balanced.

CHAPTER 1 INTRODUCTION

Global concern over the effects of anthropogenic climate change has led to increased activity in the research and development of renewable energy (RE) technology as alternatives to fossil fuel based energy systems. The fastest growing sources of RE in terms of installed capacity are wind energy converters (WEC) followed by solar photovoltaic (PV) modules [1]. The penetration rate of non-dispatchable RE electricity converters has become, or is poised to become, significant in many jurisdictions (i.e. greater than 30% by capacity) [2]. WEC and PV farms are displacing electricity generation formerly fueled by coal, oil, diesel, and natural gas.

As the installed RE generating capacity continues to grow, the inherent variability of wind and solar resources cause WEC and PV to stress present energy systems. For most large-scale grid-interconnected RE generators installed to date, the grid acts as an infinite sink for energy. For grids that have a high penetration of RE and insufficient local energy consumption, the solution to deal with RE variability is to export electricity to a proximal grid with shared transmission infrastructure. For many cases of RE integration, the grid cannot absorb energy and export is not a possibility. In these cases, curtailment or other mechanisms are necessary to buffer the output of variable RE generators to ensure the demand for electricity is exactly supplied with a high standard for quality. Commonly, conventional fossil fuel based generation meets the continuously variable electricity demand by ramping power up and down. This same mechanism is effective in buffering the variabilities of both demand and RE generation, but results in lower fuel efficiencies and higher wear in fossil fuel generators due to increased power output ramping and thermal stresses [3]. As the contribution from RE in electricity generation portfolios continues to grow, energy storage systems (ESS) will provide the grid with the flexibility required to manage variable electricity generation [1]. Modern ESS encompass a wide array of technologies at various levels of development (from conception to maturity) that are effective at buffering supply and demand as well as offering other ancillary services including but not limited to energy arbitrage, power quality, voltage control, ramp rate compensation and black starting.

Many of the earliest energy systems requiring storage were isolated microgrids with both conventional fossil fuel and RE generating capacity. Their relatively small and isolated system architecture makes them most susceptible to energy dispatch issues. While most microgrids are still powered by diesel generators (DG), a growing number are adopting RE generation and will require ESS as penetration rates grow. Even in large electricity grids, the necessity for ESS is becoming either an attractive alternative to grid infrastructure upgrades or a necessity to ensure grid reliability. This is commonly the case for RE generation feeding into distribution level grids and is a foreseeable issue for transmission level grids.

Compressed air energy storage (CAES) is well suited to accommodate increased penetration of renewables, especially wind energy [4-6] and has already been implemented in commercial applications. Regenerative air energy storage (RAES) is an alternative to conventional CAES that improves the efficiency and energy density of storage by minimizing the temperature increase during compression using a second fluid [7]. RAES is a flexible energy storage technology that consists of a near-isothermal compressor/expander unit and above-ground pressure vessels and water tanks for storage. The power and energy of the system can be scaled independently, thus enabling RAES to meet diverse performance objectives for various applications. RAES can also use low-grade waste heat to boost efficiency and mitigate thermal losses.

1.1 Research Objectives

Because it is a new technology, no numerical models exist for the purposes of investigating the sizing and performance of RAES systems while integrated with RE generators. New modeling is required for RAES because it has unique operating characteristics, the simulations of which are beyond the capabilities of existing hybrid energy system analysis tools. The objective of this thesis is to present the theory, method, development, and practical application of an energy storage modeling and simulation tool. Although the model can be modified to analyze any ESS technology, the embodiment presented herein has been developed specifically for RAES, a technology lacking significant representation in literature, yet highly promising in industry. Several

assumptions are made in order to characterize RAES performance, since the technology is still in development. This numerical model can be applied to a variety of renewable energy integration scenarios. It is used to determine optimal system sizes, analyze the effectiveness of control strategies, perform parametric analyses for different operating characteristics of RAES, and evaluate the effectiveness of integrating waste heat into a RAES system. These capabilities make it more flexible than commercial ESS analysis tools such as HOMER, HYBRID 2, and RETScreen, and more intuitive than tools such as Dymola/Modelica and TRNSYS. The majority of this research has been carried out in association with industrial research collaborators LightSail Canada (LSC) and LightSail Energy (LSE), the inventors and developers of a unique and patented RAES system [7].

This thesis is divided into six sections. This introductory chapter is followed by a background on applications for ESS describing both microgrid and grid scenarios. Chapter 2 also describes the state of the art and relevant literature for ESS technology with a focus on CAES and RAES. Chapter 3 describes the development of the numerical model and the analysis methodology used in this research. The modeling methodology is divided into 3 sections: the electricity grid and load, the generation, and RAES. The fourth and fifth chapters describe two case studies for which the model was employed along with their results. Each case study evaluates a unique opportunity for RAES integration in RE systems where waste heat is available. In the first case study, it is proposed to install RAES in remote microgrid communities to achieve the following objectives:

- buffer the variations in community electricity load and WEC output;
- operate DG at its optimal efficiency;
- use waste heat from the DG to boost its efficiency.

In the second case study, a WEC and RAES system is proposed that is interconnected to a capacity constrained grid and co-located with a combined heat and power (CHP) plant. In this case, the RAES has a different set of objectives:

- buffer the output of the WEC to remain below the grid capacity;
- use heat from the CHP to boost its efficiency.

The final chapter concludes the work and recommends advancements for the model.

CHAPTER 2 BACKGROUND AND LITERATURE REVIEW

Recent reviews of storage discuss the many technologies and compare their characteristics. The technologies include: pumped hydro, CAES, batteries, flywheels, hydrogen, and capacitors [8, 9]. These employ a range of methods for storing energy, including: kinetic, potential, chemical, and electric field. A comprehensive comparison of technology characteristics includes values of: energy capacity; peak and average power; cycle efficiency and self-discharge; cycle and calendar life; capital and operating costs; technological maturity and availability of supply; as well as direct and life cycle environmental impact assessment [10]. In addition, the performance of a storage technology to suit a specific project is based upon the effectiveness of the services it provides, and the effect it has on the project from a technical, economic, and/or greenhouse gas (GHG) emissions perspective [11], as well as local community perspectives [12].

Academic research into RAES (or "isothermal CAES") is limited, as it is an emerging technology. As such, no published research, other than the author's own [13], has ever analyzed RAES deployment to assist in the integration of RE generation. The most widely used software for analyzing gird-integrated and microgrid energy systems incorporating RE and ESS is HOMER [14, 15], which was developed by the National Renewable Energy Laboratory. While it is straightforward and easy to use, recent reviews of the software available for hybrid energy system analysis note HOMER's shortfalls. These include its limitation to intuitively select system components and technologies used in analysis [16], and a lack of transparency and flexibility in the optimization process [14, 15], which has a single objective function that is to minimize net-present cost. The reality of hybrid energy systems is that they require various considerations for each application. The limitations of available software have necessitated new simulation tools for analysis not only of emerging technologies such as RAES, but also for the diversity of applications of hybrid energy systems and their control strategies. This chapter provides the reader with the necessary background on applications for ESS along with relevant literature on optimal system sizing, and a state-of-the-art explanation on CAES and RAES technologies.

2.1 Energy Storage for Microgrids

Remote off-grid communities typically utilize DG for electricity production [17, 18]. Whereas diesel fuel in urban areas is relatively cheap, transportation of fuel to remote communities increases the cost of electricity by up to a multiple of six to ten [19]. Besides the economic tolls incurred using DG, there are several environmental and social concerns, such as: communities are susceptible to electricity blackouts, pollution from exhaust gasses, and loud noise from DG [18]. In an effort to reduce the economic, environmental, and social costs, remote communities are investing in renewable electricity generators such as wind energy converters (WEC). Figure 1 shows the nearly 300 remote off-grid communities in Canada, where green dots represent aboriginal communities and white dots represents non-aboriginal communities.

Figure 1 Map of off-grid communities in Canada [18]

DG used in remote microgrids must ramp power up and down in order to follow the variable community load. The transient and intermittent operation of DG requires them to regularly run at part-load, resulting in lower fuel efficiencies and higher greenhouse-gas (GHG) emission intensities. The addition of variable output renewable electricity generators, such as WECs, further disrupts steady DG operation, thus further lowering

DG efficiency and increasing emission intensity and mechanical wear. Energy storage may be used to overcome this problem by buffering the variability of the community load and the output of renewable energy generators, thereby allowing the DG to operate in more stable conditions for optimal efficiency. The part-load efficiency curves of three commercially available DGs shown in Figure 2 illustrate how efficiency increases with load. It should be noted that these are efficiency curves of new DGs, whereas older DGs have steeper curves and achieve a lower overall efficiency.

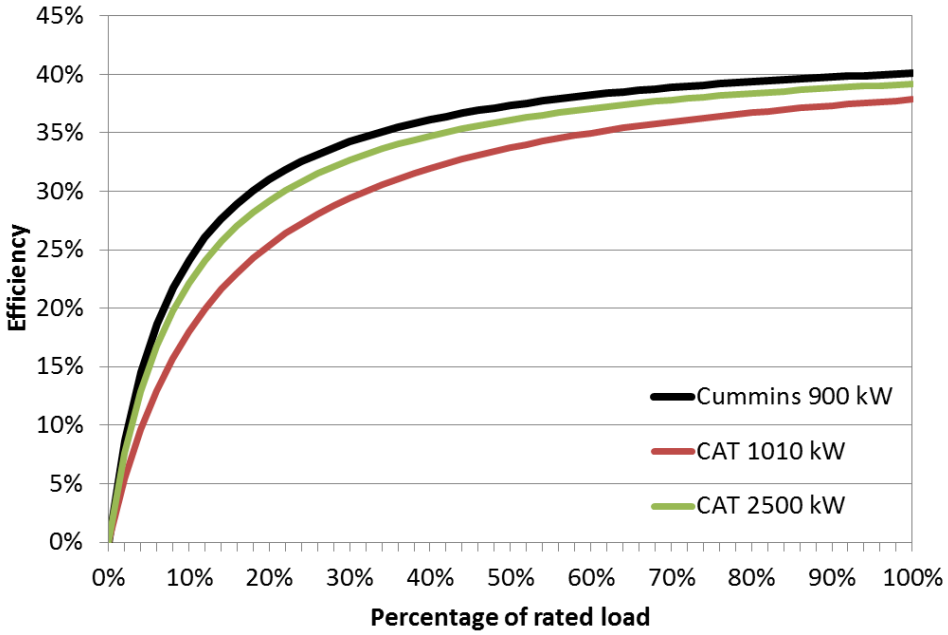

Figure 2 **Steady-state part-load efficiency curves for 3 diesel generators based on [20-22]**

When an ESS is used in combination with DG in an off-grid system, the opportunity arises to charge the storage from DG power. "Cycle charging", as it is known, involves increasing the output of a DG beyond the required load, and using the excess to charge an energy storage system, thus avoiding the low efficiency of part-load DG operation. Control strategies involving cycle charging must consider two important factors. First are the efficiency losses due to the storage system. Modeling shows that a critical load set point can be determined that dictates when cycle charging is cost effective [23]. If the load is above a critical load, the DG should follow the load; otherwise it should exceed the load and divert the excess energy to charge the storage. The second consideration is the possibility of forced curtailment of renewable energy if the storage reaches full charge during cycle charging. In low penetration rate renewable energy systems, cycle

charging is more cost effective than in high penetration systems, where renewable energy is more likely to be curtailed [23].

In the recent literature, control strategies for wind-diesel and wind-diesel-storage hybrid microgrids have focused on control for short-term variations in order to maintain adequate power quality [24-29]. There is no published study that examines the use of regenerative or near-isothermal energy storage for remote microgrid applications. Since RAES has unique operating and sizing parameters, it must be considered separately as an option for wind-diesel microgrids. Table 1 summarizes a selection of the most relevant studies into ESS for microgrids that include ESS and REC. These studies are described in detail following the table.

Table 1 Summary of studies on ESS for remote communities

Study	WEC (kW)	PV (kW)	ESS Energy (kWh)	ESS Power (kW)	DG Size (kW)	Control Strategy
Bowen et al. [30]	10	-	67 (BESS)	4.5	12	DG is back-up for WEC / ESS
Ziogou et al. [31]	3	10	30 (H_2) 6 (BESS)	1 - 2	No spec.	SOC of ESS
Ibrahim [32]	1340	-	No spec. (CAES)	-	1088	CAES supercharges DG

A study by Bowen *et al.* analyzed operational data from a wind-diesel-storage system that provided power for a farm [30]. The system includes a 10 kW WEC, 67 kWh battery, 4.5 kW inverter, a 12 kW DG, and a domestic hot water heater dump-load. The power from the battery is limited by the size of the inverter to 4.5 kW. The diesel generator acts as a back-up to the WEC and battery system. It is automatically started when the battery reaches a minimum voltage or the inverter reaches its rated capacity, and operates at 2.3 kW above the necessary load in order to charge the batteries. Results showed that the WEC provided 73% of the farm's energy, and the DG made up the remaining 27%. Most of the energy is stored in the battery for periods lasting less than 2 days; therefore there are diminishing returns from increasing the battery capacity. The authors recommend sizing the equipment to reach maximum system efficiency, suggesting that while the inverter is undersized (60% of the time the diesel generator was running was due to the

inverter reaching maximum capacity), the rest of the components are appropriately sized. Improvements could include implementing a controller that takes into account the efficiencies of each mode of operation, and also by scheduling power consumption to avoid energy deficits.

Research by Ziogou *et al.* investigates the operational control strategy of a wind-PV-diesel-storage system [31]. This system involves 10 kW of solar photovoltaic (PV) modules and 3 kW of WECs. A 6 kWh battery and a 35 kWh hydrogen energy storage system are included for short and long term energy storage, respectively. A DG with an unspecified rating provides power only during times when the energy storage is empty and there is insufficient production from the WECs or PV. The control strategy uses state of charge (SOC) bands of the battery and hydrogen storage to determine the energy flows in the system. The battery is only allowed to discharge to a SOC of 20% in order to extend the cycle life. The system is analyzed for maximum electricity load levels of 1.0, 1.5, and 2.0 kW. The control strategy seeks to avoid the consumption of diesel fuel. For a load of 1.0 kW, the system is effective and burns almost no diesel, while most of the energy stored is cycled through the battery rather than the hydrogen. As the load increases, less energy is cycled through the hydrogen and more diesel fuel is required to meet the load. At a load of 2.0 kW, the DG electricity production is greater than the energy throughput of the battery.

A study by Ibrahim involves storing excess wind energy by means of a small scale conventional CAES system [32]. The compressed air input essentially supercharges the DG, which increases the power output while lowering the fuel consumption, resulting in an overall higher efficiency. A yearlong model was developed for a village in Northern Canada using hourly wind and electrical load data, with an objective to reduce fuel consumption by storing excess wind energy using CAES. The maximum and average electrical loads are 851 kW and 606 kW, currently powered by two 544 kW DG (1088 kW maximum) and four 335 kW WEC (1340 kW maximum). The control strategy ensures that a DG never operates below 30% of its rated capacity, and diverts the excess electrical energy to the CAES. The CAES system in this study operates in conjunction

with the DG and is incapable of delivering power on its own. Compared with a baseline case of diesel only power generation, a fuel savings of 31% is achieved by incorporating the 4 WECs, but only 5% of additional fuel savings is derived from using CAES to supercharge the diesel generators.

2.2 Energy Storage for Grid Integration

At present, the majority of effort for grid integrated ESS is focused on storage for WEC because this technology is experiencing unprecedented growth rates and has the greatest installed generating capacity amongst non-dispatchable renewable energy generators worldwide [1, 33].

Boustika and Sansoto evaluate ESS sizing using many generated hourly WEC production scenarios instead of real time series data [34]. The hourly scenarios have one minute temporal resolution and are created using a probabilistic forecast based on real wind data. The role of the ESS is to minimize the imbalances in actual versus forecasted WEC production on an hourly basis. This allows WEC owners to participate in electricity markets; however the intent of the ESS is for deviation minimization, not revenue maximization. The generated hourly scenarios show strong correlation when compared to actual data. These scenarios are used to calculate the ESS size (in terms of energy and power) that is able to balance the WEC output 95% of the time. The methodology is verified by running a similar analysis using 1 minute data from a wind farm. The ESS size is calculated for WEC capacities ranging between 25 MW and 210 MW. The generated scenario predicts corresponding power requirements ranging from 5.9 MW to 38.9 MW, and energy requirements of 1.1 MWh to 7.2 MWh. The actual data results in similar values corresponding to the same range of WEC capacity, predicting power requirements of 5.1 MW to 35.5 MW, and energy requirements of 1.1 MWh to 8.0 MWh.

A paper by Korpaas *et al.* presents a method for scheduling the operation of an energy storage system coupled with a wind farm on the Nordic spot market [35]. The wind farm output is modeled as identical WECs with identical wind conditions totaling 6 MW. The non-specific energy storage technology is defined as having an energy capacity of 100

MWh, a power of 6 MW, and a round-trip efficiency (charge and discharge efficiency are both equal and constant) of 75%. The grid is modeled as a local load and an external grid that is constrained at 4 MW. Excess wind energy that is not consumed locally or exported to the external grid is either used to charge the storage or consumed by a dump load. The spot market is modeled such that WEC output commitments are made one day ahead using predicted wind conditions. A simulation is run on hourly time steps for a base case, and then the storage sizing parameters are varied to determine the effect on the economics. An ESS with larger energy capacity lowers the amount of energy lost due to grid constraints. Increasing the ESS power does not improve the performance unless the capacity is also increased. A sensitivity analysis is performed for ESS efficiency and shows that higher efficiencies increase the utility of storage.

Gill *et al.* investigate the optimal operation of an ESS for situations where WEC curtailment is regular [36]. A generic ESS is modeled based on SOC, efficiency, and power range. The ESS is used for energy arbitrage and curtailment reduction. The distribution grid is modeled based on times series data of the local demand, and a fixed import/export capacity to the transmission grid. The WEC capacity is considered to be distributed, but assumes there is perfect correlation between wind regimes. There is "firm" WEC capacity, up to a maximum of the sum of the minimum load and the export capacity to the transmission grid, and "non-firm" WEC capacity that is curtailed when the "firm" WEC capacity is met. Four cases are evaluated:

1. zero "non-firm" WECs;
2. 10 MW of "non-firm" WECs;
3. 20 MW of "non-firm" WECs;
4. 20 MW of "non-firm" WECs with no participation in energy arbitrage.

The results for each case are presented as total revenue as a function of round-trip efficiency. Case 4 is less sensitive to efficiency, and the cases with higher "non-firm" WEC production yield higher revenues. The amount of curtailed energy increases from 3% to 30% between case 2 and 3. In all cases, the ESS is determined to not be economically viable for an analysis that considers sodium sulphur batteries as the technology.

In a previous publication of the author, a RAES system is modeled and optimized for a capacity constrained grid [13]. A tidal energy converter (TEC) is to be installed on a distribution network where the MAL is equal to the installed WEC capacity (0.9 MW). The application of energy storage enables the development of TEC generating capacity by decoupling the generation from the demand, thus ensuring the 0.9 MW limit is not exceeded. A RAES system is modeled numerically to charge from the TEC output based on the modeled operation of the WEC and TEC. A curtailment analysis is conducted for various energy and power capacities to determine the optimal size ESS and its economic benefit. Avoidance of curtailment requires 6.8 MWh of storage. The ESS will operate hundreds of shallow cycles per year and tens of deep cycles per year. Economic benefit is found by reducing the storage to 2 MWh, resulting in some curtailment. RAES is a suitable storage technology for this application considering the ability to scale power and energy capacities independently.

2.3 Compressed Air Energy Storage: State of the Art

In this thesis, CAES systems are considered to be divided into three types: conventional CAES, adiabatic CAES, and regenerative or isothermal CAES. Each of these is described in the following section.

2.3.1 Conventional CAES

Conventional CAES systems use off-peak electricity to compress air and store it in underground caverns. During peak periods of demand, the compressed air is heated with natural gas and expanded through a gas turbine to generate electricity. Natural gas input is required for operation to prevent extreme temperature decrease during expansion. Using previously compressed air to run the natural gas turbine improves the efficiency by eliminating the need for auxiliary power to be drawn from the turbine to power a compressor. Only two CAES systems are fully operational worldwide: one in Huntorf, Germany, and the other in McIntosh, Alabama. A simplified system diagram of a conventional CAES plant is shown in Figure 3.

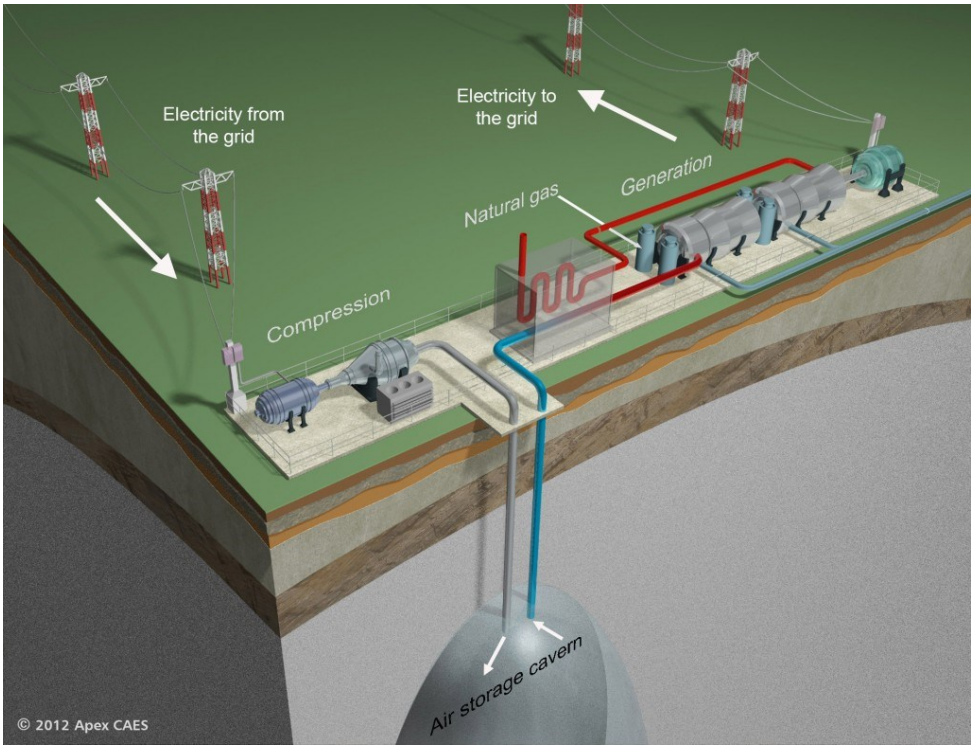

Figure 3 Conventional CAES system diagram [37]

Conventional CAES systems, such as the one in Huntorf, use the following main components:

- A double clutched motor / generator to provide power to a compressor during charging, and generate electricity during discharge;
- Multiple stages of industrial compressors to achieve the operating pressures of storage (44 -66 bar [38]);
- Intercoolers to reduce the temperature of air between compression cycles, thus reducing the power requirements of the compressors and the storage volume. Intercooling is also necessary to prevent degradation to subterranean storage formations [39];
- A storage volume (underground caverns become more economic than above ground vessels at capacities greater than 100 MWh [40]);
- High and low-pressure turbo-expanders with fuel combustors between stages;
- Control system with communication to the grid and generation sources.

Huntorf is best suited for peaking and spinning reserve duties. It achieves a heat rate of 1.61 kWh_f/kWh_e, meaning for every 1.61 units of fuel energy that are input, 1 unit of electrical energy is output . The McIntosh CAES facility uses a very similar cycle, except that heat is recuperated from the exhaust gases of the expanders and used to pre-heat air prior to expansion. The increase in efficiency from the heat recuperator reduces the heat rate to 1.2 kWh_f/kWh_e [40]. The documented round-trip efficiencies (the ratio of energy gained to the energy input of CAES) of the Huntorf and McIntosh facilities are between 29 - 46% and 34 - 54% respectively [39, 41]. McIntosh performs a wide range of operating functions including load management, ramp-rate compensation, peaking power, spinning reserve, and synchronous condenser duty [40]. Conventional CAES can respond with ramping capabilities that can reach full charge power from standby in only 4 minutes. To reach full power in discharge mode takes slightly longer at 10-12 minutes, but in a case of emergency it can be accomplished in 5-7 minutes. The switch from full charge power to full discharge power takes approximately 20 minutes [40]. The ramp rate capabilities of conventional CAES make it suitable for forecast-able ancillary services such as peak shaving, but it is not fast enough to buffer WEC output. Table 2 shows the representative costs of large and small scale conventional CAES systems.

Table 2 Representative costs of conventional CAES systems [42, 43]

Storage Medium	Size (MW)	Power-related plant components ($/kW)	Balance of power plant ($/kW)	Energy storage components ($/kWh)	Typical capacity (hrs)	Total Cost ($/kW)
Cavern	300	300	210	1.75	40	580 -900
Surface Vessel	10	300	200	40	5-12	700-980

Of the literature that exists discussing CAES, nearly all of it refers to conventional systems that require heat input during expansion. The economic case for the use of conventional CAES as grid scale energy storage has been shown to be insufficient without significant carbon taxes ($36/ton CO_2e [44] - 56/ton CO_2e [45]) or specific electricity market mechanisms [46], even when diversifying income streams with the sale of waste heat from the compression process [47]. There is limited published research on near-isothermal or “regenerative” CAES other than the author’s own publications [13,

48]. The remainder of this sub-section describes the most relevant available literature on the use of conventional CAES to integrate WEC.

Research by Mason and Archer compares coupling a large scale wind farm with natural gas combined cycle (NGCC) and conventional CAES [5]. Both systems are modeled to provide 400 MW of base load generating capacity, similar to that of a typical coal fired power plant, and transmitted via high voltage DC transmission lines. In this case, base load generation requires the system to operate at full capacity for 90% of the year, and 100% of peak load periods. The variable efficiency of the gas turbines as they ramp up and down are considered, as well as the increased efficiency required by the supporting thermal generating stations operating in spinning reserve mode. The results of the two models are compared to a conventional coal fire power plant of an equivalent base load generating capacity. Results show that the required wind capacity for the CAES far exceeds that of the NGCC, at 1110 MW and 482 MW respectively, in order to meet base load generation requirements. The CAES system cycles 20% of the total electrical output. For the NGCC system, the electricity supply is divided by 47% from wind and 53% from natural gas. While both modeled systems are found to be suitable for base load generation, the CAES has significantly lower CO_2 emissions with four times less than the NGCC case and nine times less than the conventional base load case. The capital cost of CAES is found to be twice that of NGCC, but increases in natural gas prices (up to \$10-12/GJ) and CO_2 taxes (\$90-100/t) could level the playing field.

A study by Loisel *et al.* considers the economics of a hypothetical power plant consisting of WEC and CAES [49]. Electricity can be exported from wind, CAES, or both when the grid demand is high. Within the plant, the CAES charges from wind and/or the grid when electricity export is less profitable during periods of low demand. The electricity market analyzed is in France, where grid flexibility is typically provided by on-line generators that adjust energy deliveries, and additional support is provided through the procurement of contractual reserves. This type of grid management necessitates stand-by generating capacity to balance supply and demand. Using energy storage to manage variable generation from wind power avoids the provision of additional stand-by capacities. The

wind farm capacity is 2 GW with a capacity factor of 26%. The facility uses conventional CAES rated for 1440 MW of compression and 1200 MW expansion, with a capacity of 10 hours (12 GWh). A numerical model optimizes CAES charging from wind and grid electricity in order to maximize profits of the system. The study concludes that under current pricing scheme the wind-CAES system results in negative profits. In order for the project to become cost effective, the average spread between base-load and peak electricity rates must increase.

Research by Mauch and Carvalho asks the question of whether large scale wind-CAES projects can compete in current day-ahead markets [43]. The authors model a conventional underground CAES system that stores and dispatches wind energy. Day-ahead dispatch schedules are calculated to optimize profits based on wind forecasts. Dispatch/charging algorithms are run hourly based on parameters such as efficiency, state of charge (SOC), maximum energy capacity, and maximum discharge power. Eight different price scenarios are used based on wholesale prices of electricity for balancing and day-ahead markets. The high cost of a CAES facility (at $750,000/MW) is calculated to be unjustifiable in all of the pricing scenarios considered. However, it should be noted that the market prices are based on a period of time when cheap natural gas was driving the price of electricity down. Furthermore, auxiliary grid services offered by energy storage systems are not considered. The percentage of non-dispatchable wind energy is significantly reduced (>80%) in all price scenarios, and the percentage of over-committed energy is reduced by approximately one half. With perfect wind forecasting, the economics are more favorable, but still lead to negative profits. When the CAES system operating parameters are varied annual profits are only improved modestly. The study concludes that CO_2 prices of $100/ton are necessary to justify the costs of CAES in current day-ahead markets.

The following two sections describe emerging technologies that improve upon the conventional CAES by eliminating the need for natural gas input and improving the overall efficiency.

2.3.2 Adiabatic CAES

An adiabatic CAES system has yet to be demonstrated commercially, but has the potential to surpass the efficiencies achieved by conventional CAES, and eliminate the carbon emissions associated with burning natural gas. Adiabatic CAES requires several stages of compression and expansion to achieve practical operating pressures. In conventional CAES, the thermal energy that is removed from air by the intercoolers between compression stages is simply dissipated to atmosphere. Adiabatic CAES makes use of this thermal energy by storing it and preheating the air prior to expansion, as shown in Figure 4.

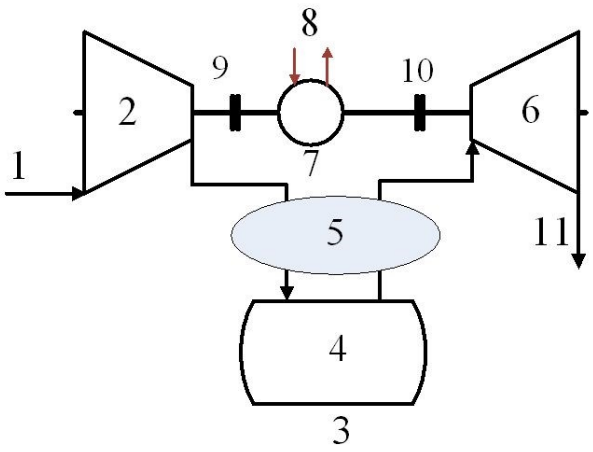

Figure 4 **Adiabatic CAES system diagram showing: 1. air input, 2. compressor, 3. air storage reservoir, 4. compressed air, 5. thermal energy storage, 6. expander, 7. motor/generator, 8. electricity, 9. and 10. clutches, 11. exhaust [50]**

The ideal case for adiabatic CAES requires isentropic compression and expansion, isobaric cooling and heating, and no heat loss during storage. In a more realistic embodiment of adiabatic CAES, those processes are polytropic. Simulations show that the maximum round-trip efficiency for the ideal case is 70%, but the more realistic case has a round-trip efficiency of 60% [39]. Adiabatic CAES requires thermal energy storage (TES) to store heat at temperatures ranging from 50 to 600 °C. The storage mediums best suited for TES in CAES applications are solid materials such as stone, ceramics, and cast-iron, or liquid mixtures of mineral oils and nitrite salts. Phase change materials on their own are not able to meet the range of temperatures required, but can be used in a hybrid system with solid materials [51]. Industrial compressors are suited for adiabatic CAES,

but development of compressor technology able to accommodate higher temperatures and therefore higher pressures will improve plant efficiency.

2.3.3 Regenerative Air Energy Storage

Recent research efforts are underway to develop a CAES system that approaches an isothermal process during compression and expansion [7]. RAES is similar to adiabatic CAES in that it stores the heat generated from compression and uses it to maintain operable temperatures during expansion, but instead of doing so between stages in inter-coolers/inter-heaters, it does so during compression/expansion. The resulting temperature change of both processes is drastically reduced to the point that it is considered quasi-isothermal. Removing heat from air reduces the amount of work required to compress it, and adding heat during expansion increases the work output. An effective method used to achieve quasi-isothermal compression is spraying liquid into the cylinder of a reciprocating compressor to absorb the thermal energy. Water and oil are suitable liquids for injection due to their specific heat capacity and density properties. The liquid is sprayed into the cylinder through nozzles that create very small (100 μm) droplets. Dividing the volume of liquid into droplets increases the surface area for heat transfer, allowing it to take place at very high speeds. This increases the achievable compression ratio up to 30 [52]. Compression can take place without the injection of water simply by allowing the cylinder walls to absorb the heat generated during compression, but the rate at which the heat transfer takes place severely diminishes the power density of such a system. Systems using hydraulic compressors are capable of approaching isothermal compression, but operating at high speeds incurs additional fluid friction losses. Reciprocating compressor/expanders are used because they offer sufficiently robust, reliable, rapid, and efficient power delivery [7].

The energy transfer in the system is defined by the fundamental thermodynamic equation. Eqs. 1 - 7 are based on the theory described in [7]:

$$T \times dS = dH - V \times dp \tag{1}$$

The change in enthalpy (dH) is:

$$dH = C_{\mathrm{p,a}} \times dT + m_{\mathrm{w}} \times C_{\mathrm{p,w}} \times dT \tag{2}$$

Where $C_{\mathrm{p,a}}$ and $C_{\mathrm{p,w}}$ are the heat capacities of air and water respectively, and m_{w} is the percent mass of water per unit mass of air. dT is the change in temperature resulting from compression. Air is considered on a per unit mass basis as an ideal gas, therefore:

$$V = \frac{R \times T}{p} \tag{3}$$

Adding Eqs. (2-3) to Eq. (1) yields:

$$dS = \left(C_{\mathrm{p,a}} + m_{\mathrm{w}} \times C_{\mathrm{p,w}}\right) \frac{dT}{T} - \frac{R \times dp}{p} \tag{4}$$

Since the process is considered reversible, the change in entropy dS from the combined system of water and air is zero. Therefore:

$$\left(C_{\mathrm{p,a}} + m_{\mathrm{w}} \times C_{\mathrm{p,w}}\right) \frac{dT}{T} = \frac{R \times dp}{p} \tag{5}$$

Integrating Eq. (5) yields:

$$\frac{T_2}{T_1} = \left(\frac{p_2}{p_1}\right)^{\frac{n-1}{n}} \tag{6}$$

Where T_1, P_1 and T_2, P_2 are the properties before and after compression, respectively. The integration of Eq. (5) also yields the exponential ratio containing n, calculated as:

$$n = \left(1 - \frac{R}{C_{\mathrm{p,a}} + m_{\mathrm{w}} \times C_{\mathrm{p,w}}}\right)^{-1} \tag{7}$$

As the amount of water injected into the compression cylinder increases (m_{w} increases), the term n approaches 1, and as a result T_2/T_1 in Eq. (6) also approaches 1. However, this is the ideal case: a completely reversible, isothermal process. In the practical case, a thermodynamic efficiency term can be introduced, η_{therm}, which can be thought of as how isothermal the process is.

$$\frac{T_2}{T_1} = \frac{1}{\eta_{\mathrm{therm}}} \left(\frac{p_2}{p_1}\right)^{\frac{n-1}{n}} \tag{8}$$

As the compression process becomes less isothermal, a temperature increase occurs. During expansion, the equation simply changes to:

$$\frac{T_3}{T_2} = \eta_{\mathrm{therm}} \times \left(\frac{p_3}{p_2}\right)^{\frac{n-1}{n}} \tag{9}$$

Where T_3, P_3 are the properties after expansion. The specific work during compression (w_{chg}) and expansion is a function of the temperature difference and the heat capacity of

air and water. Since the term η_{therm} does not account for a loss of work (simply a temperature increase), a separate efficiency term is introduced as $\eta_{\text{RAES, chg}}$.

$$w_{\text{chg}} = (C_{\text{p,a}} + m_{\text{w}} * C_{\text{p,w}}) * (T_2 - T_1) \times \eta_{\text{RAES, chg}} \quad (10)$$

The work for expansion (w_{dschg}) is similar:

$$w_{\text{dschg}} = (C_{\text{p,a}} + m_{\text{w}} * C_{\text{p,w}}) * (T_3 - T_2) \times \eta_{\text{RAES, dschg}} \quad (11)$$

The energy density of RAES depends on the thermodynamic efficiency (η_{therm}) which is a function of the amount of water injected during compression. Figure 5 shows the relationship between thermodynamic efficiency and the volumetric fraction of water injected during compression.

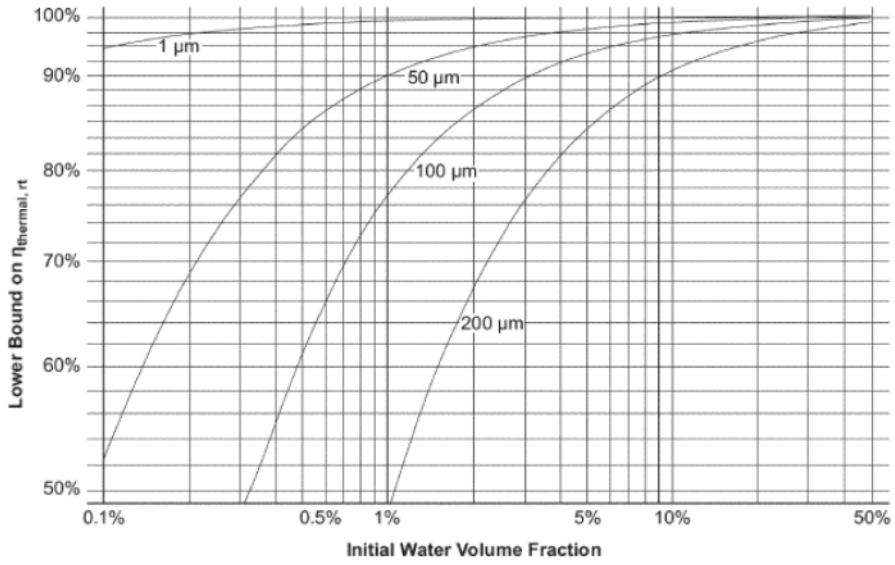

Figure 5 **Thermodynamic efficiency versus water injection volumes for various droplet sizes [7]**

In order to achieve an energy density practical for use, an ideal thermodynamic efficiency is set by balancing the temperature increase and energy density. For example, a high energy density can be achieved with a low thermodynamic efficiency, but storing high temperature fluids and gasses adds technical complexity. According to the patent filed by LightSail Energy the ideal thermodynamic efficiency is 90%, which is achieved by spraying 2.5% by volume water as 100 µm droplets into a cylinder running a compression ratio of 14.1 at 20 Hz, resulting in a temperature increase of approximately

20 K [7]. The rate of heat transfer is significantly faster than the compression process, at approximately 0.001 seconds (1000 Hz equivalent). The operating speed of 20 Hz (1200 rpm) is chosen because the highest mechanical efficiencies are achievable in the machine and its auxiliary systems.

RAES technology under development is modular and therefore offers flexibility in siting and sizing. It can achieve a high round trip efficiency of 70% compared to conventional CAES (29 – 54%) [48]. If waste heat is captured the discharge efficiency of RAES can be further increased by preheating the water entering the cylinder. Where cold climates are a concern, the cycle life of RAES is longer than other ESS such as lead acid batteries, which degrade quickly in the cold. Many of the technologies CAES uses (such as reciprocating compressors, variable frequency drives, pumps, hydraulic motors, etc.) are adopted from existing industries and are therefore mature, reliable, available, and cheap. Compressors and expanders are already available and highly modular, enabling multiple operating configurations. The geophysical expertise needed to develop underground storage caverns exists due to widespread use in the fossil fuel industry, and above ground pressure vessels are widely manufactured for countless industrial purposes. TES systems and heat transfer media are widely available to handle all ranges of temperatures.

A simplified RAES system consists of three main components, listed below and shown in Figure 6. A further description of RAES can be found in a patent filed by one of several companies developing this technology [7].

1. compressor/expander (CE) power unit rated in 500 kW increments;
2. air storage tank rated in 1000 kWh increments;
3. water tank for thermal energy storage (TES).

Other components in the system such as pumps, valves and variable frequency drives are omitted from Figure 6 because they are not directly modeled for this research.

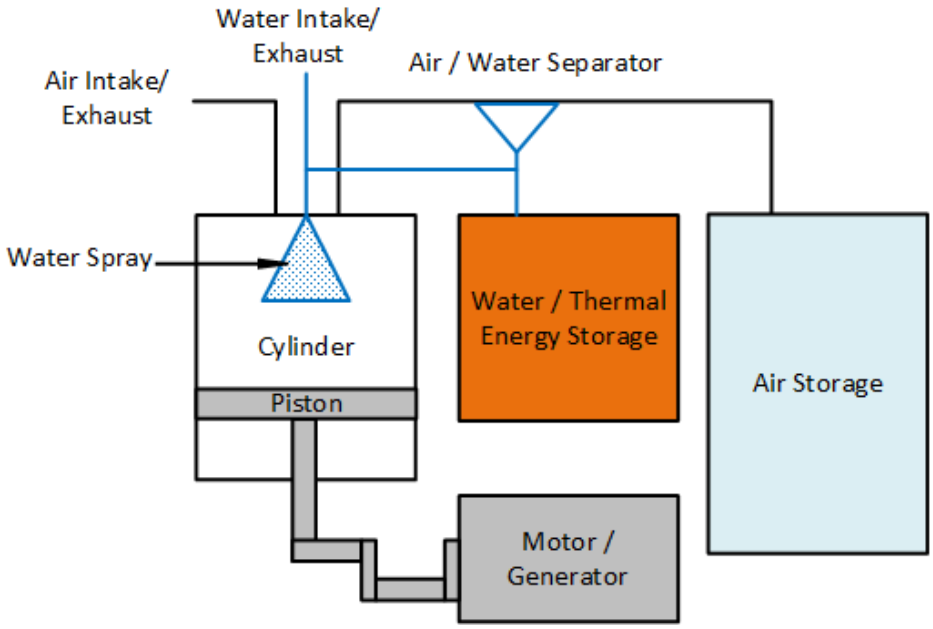

Figure 6 A simplified RAES system showing major components based on [53]

These components are modular, allowing for discrete sizes to fit an application. For example, 2 power units and 3 storage units would give an overall rating of 1000 kW and 3000 kWh.

As this section has shown, RAES shows a number of advantages over other CAES technologies. These are highlighted in Table 3. A disadvantage of RAES is the high cost, which represents the projected costs of the first deployed systems; economy of scale is expected.

Table 3 Comparison of CAES technologies

CAES Type	Flexible Sizing	Efficiency (%)	Fossil Fuel Input	Maturity	Power Cost ($/kW)	Energy Costs ($/kWh)
Conventional	No	29 - 54	Yes	Commercial	500	2-40
Adiabatic	Yes	60	No	Theoretical	-	-
Regenerative	Yes	70	No	Development	2000	100

CHAPTER 3 METHODOLOGY

The objective of this research is the creation and development of a modeling and analysis tool that can be applied to simulate RAES operation and performance for diverse RE integration scenarios. In order to provide flexibility in its analysis capabilities, the simulation tool includes models for many aspects of grid-connected and off-grid energy systems, and application specific control strategies. For the purposes of this research, a hybrid energy system can be divided into three sections: the electricity grid (or microgrid), the generation, and the energy storage. The model is built in MATLAB and uses time step analysis to simulate operation and interactions within the energy system based on collected data. The application specific control strategy dictates energy flows. A parametric sweep optimization scheme delivers results that enable the selection of RAES system sizing to achieve various goals. The model is applied to two case studies. The following section describes the theory used in modeling each component of the hybrid energy systems, and the analysis methodology used to evaluate ESS.

3.1 Electricity Grid

The model for an electricity grid will vary depending on the energy system being analyzed. For microgrid system analysis, it is necessary to simulate the load profile on the grid. For grid connected systems, the load is not necessarily required, but there are often constraints placed on the grid that need to be modeled, such as RE electricity export limits.

3.1.1 Load Profile

The load on an electricity grid is the instantaneous power requirement that needs to be supplied by electricity generators and energy storage. Typical aggregated grid loads follow a diurnal profile that peaks during daytime and troughs overnight. The diurnal profile is consistent throughout the year, but in cold climates it is generally highest in the winter months, and lowest in the late summer months. The daytime peak is typically a result of residential end uses in the morning and evening in addition to commercial and industrial end uses throughout the day. Figure 7 shows the annual average, minimum, and

maximum hourly aggregated loads for conventional grids and microgrids. The conventional grid data is the aggregated Nova Scotia load [54], and the microgrid data is from Ramea, a microgrid community in Newfoundland & Labrador [53]. In showing the annual average, minimum, and maximum hourly loads, the variation throughout the year is highlighted in addition to the variation throughout the day. For example, the profile of annual minimums likely occurs for hours on the same (or similar) date (*i.e.* a weekend in late summer) and the same can be said about annual maximums (*i.e.* the coldest weekday of the year).

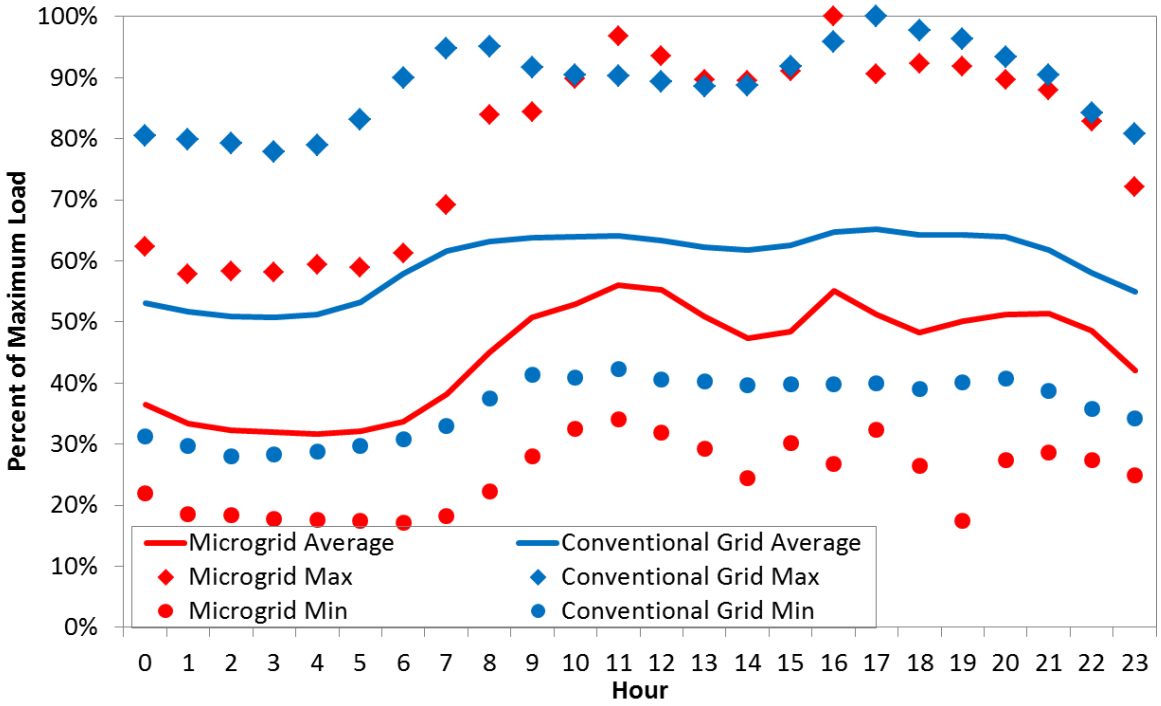

Figure 7 Average aggregated hourly grid and microgrid load profiles [53, 54]

A microgrid daily load profile is more stochastic because of the fewer distinct loads, while a conventional grid is smoother because of its extensive aggregation. Modeling the load in energy system analyses for microgrids is necessary due to their innate isolation; the ability to export and import electricity is not possible so the grid cannot be assumed to act as an infinite sink or source. Control strategies use the instantaneous grid load to dispatch electrical power from generators and storage. In this model, the grid load is represented by measured time series data that is imported for the simulation.

3.1.2 Grid Constraints

When modeling conventional electricity grids, the immediate load profile is of less significance because the electricity supply from RE and ESS does not need to match the instantaneous load. This is because the deficit from RE and ESS can be supplemented by generation or importing/exporting electricity from elsewhere on the grid. This is especially common on low voltage distribution grids, the circuits that distribute electricity from transmission lines to feed low and medium voltage electrical loads, as shown in Figure 8.

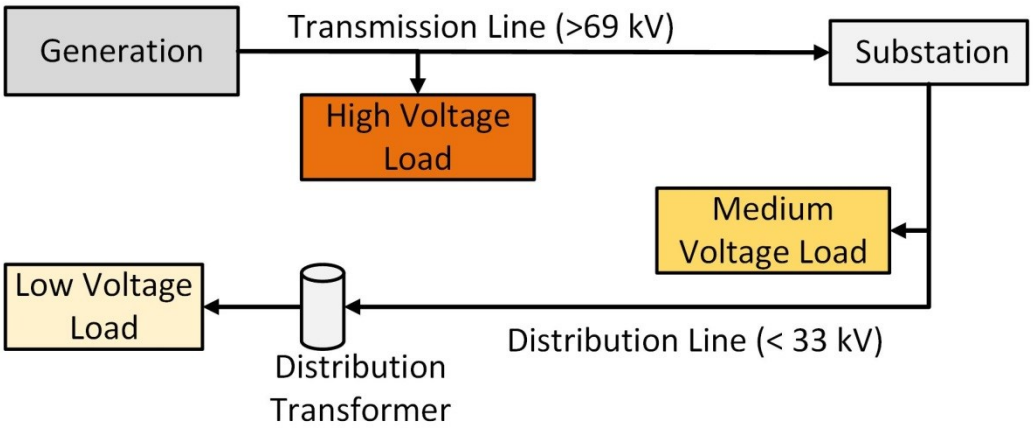

Figure 8 Conventional electricity grid configuration

Most distribution grids were built with the intention of serving the load. When electricity generation is fed directly onto a distribution grid, voltage fluctuation issues can arise. This may impose that for RE fed into distribution grids, the power output cannot exceed the load on that grid's feeder (in order to prevent back-feeding). As per utility regulations [55], this problem can be avoided by limiting the installed non-dispatchable RE generating capacity on distribution grids to the minimum annual load (MAL) at the sub-station. The MAL is measured or estimated through an interconnection study, which also provides other information on the transformer feeding the distribution circuit of interest. A portion of a sample interconnection study is shown in Figure 9, including the MAL.

Supply Sub-station Data	
Sub-station Name	MILTON
Sub-station ID	50W
Transformer ID	50W-T53
Transformer HV (kV)	69
Transformer LV (kV)	26.4
Transformer Rated MVA	7.5/10/12.5

Supply Sub-station Load Data	
Peak Load (MVA)	13.5
Est. Min Load (MVA)	3.6

Figure 9 Example distribution interconnection data [56]

Figure 9 shows a MAL of 3.6 MVA, which means the RE generating capacity limit is 3.6 MW. This scenario is modeled by adding a constraint to the output from RE (P_{WEC}) and ESS ($P_{\mathrm{RAES,\,dschg}}$).

$$P_{\mathrm{RAES,\,dschg}} + P_{\mathrm{WEC}} <= \mathrm{MAL} \tag{12}$$

If the MAL is exceeded, the energy must be curtailed. It should be noted the MAL constraint is a policy limitation rather than a technical one. In some jurisdictions the load on distribution sub-station feeders is measured using real-time communication. This enables a higher capacity for variable REC, and prevents back-feeding by only curtailing energy if the output exceeds the real-time load (rather than the annual minimum).

3.2 Generation

All of the electrical load (real load or load from storage) on the grid must be supplied by a generator of some type. Each type of generator is modelled based on technology performance characteristics. The modelled generators used in this research include DG, WEC, and CHP.

3.2.1 Diesel Generator

A DG is modelled for use in the case study of a wind-diesel microgrid. Communities powered by DG typically have several units for redundancy, but it is common for only one to run at a time. The others are rotated on a weekly or monthly basis to verify functionality. For analysis, the DG is modelled based on a CAT 1010 kW unit [20]. This nominally sized (1010 kW) DG has a comparatively lower efficiency than other new DGs (Δ = -2% to -5% depending on output, see Figure 2). This was selected as it is appropriately sized for most microgrids and represents both new and high-quality old DG.

The DG model is scaled based on the existing DG infrastructure in the community of interest by maintaining the part-load efficiency curve and adjusting the maximum power output to match the size of the community. This ensures that the part load operation of the DG is accurately modeled in order to track fuel consumption. A typical control strategy for DG in microgrid is shown in Figure 10. As long as the load (P_L) is less than the individual DG capacity, a single DG will operate ($P_{DG,1}$). If the load exceeds the DG capacity ($P_{DG,max}$), the load is split evenly between two DGs ($P_{DG,1}$ and $P_{DG,2}$). When the load is split between two DGs, the overall efficiency drops because, for example, each is operating at 50% part load rather than a single DG operating at 100% (see efficiency curve of Figure 2).

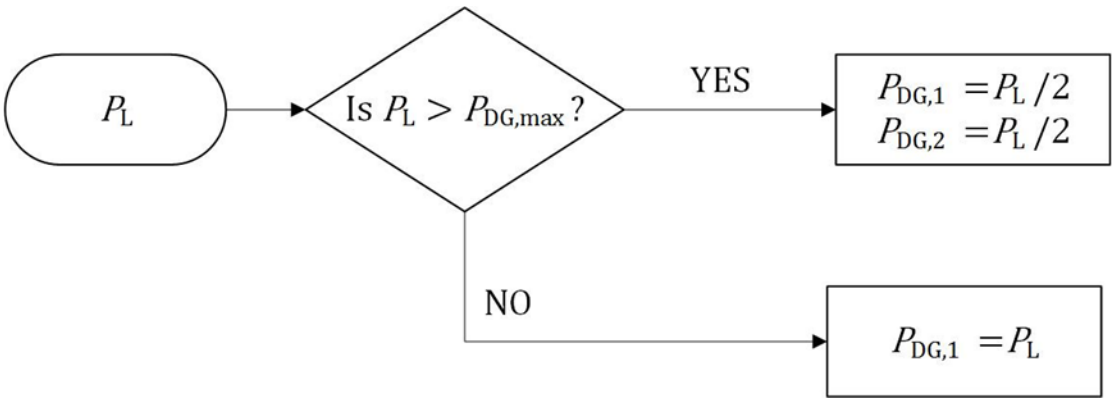

Figure 10 Typical DG operating control strategy

The fuel consumption of the DG is calculated as a function of the power output. The manufacturer supplied fuel consumption data at steady-state is typically given in units of

L/h at 50%, 75%, and 100% of the DG rated output. Figure 11 shows the fuel consumption rate in blue ($\dot{F}_{DG}$) as a function of partial load for a CAT 1010 kW DG. The perfect linearity may indicate these are estimate values based on rudimentary operating assumptions. Although fuel consumption rate is expected to vary from this line during actual operation, these values are the best available information from the specifications and will be utilized. The linear relationship between partial load and fuel consumption makes it possible to extrapolate to lower loads (represented by the dotted lines in Figure 11). The manufacturer data can then be used to calculate the efficiency of the DG (η_{DG}) using the following equation:

$$\eta_{DG} = \frac{P_{DG} \times 1 \text{ hr}}{\dot{F}_{DG} \times 10 \frac{\text{kWh}}{\text{L}}} \tag{13}$$

The conversion factor between energy in kWh and litres of diesel is assumed to be 10 kWh/L [57]. The part-load fuel consumption line is interpolated to calculate the efficiency of the DG for every percentage point of part-load operation, resulting in the efficiency curve shown as a red line in Figure 11.

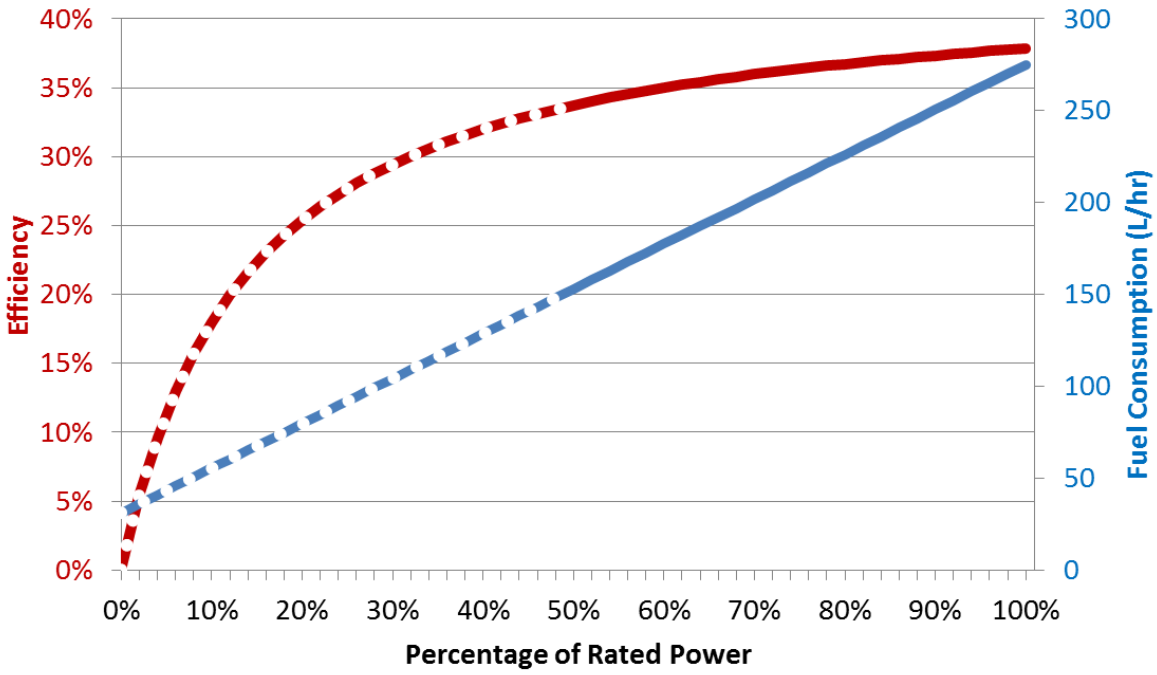

Figure 11 **Part-load fuel consumption for a CAT 1010 kW diesel generator, the dotted lines represent extrapolated values [20]**

The fuel consumption rate ($\dot{F}_{\mathrm{DG}}$) is interpolated from the blue line for the CAT 1010 kW machine shown in Figure 11, based on the DG output power (P_{DG}) in kW. The diesel fuel consumed (F_{DG}) during a time step (Δt) is calculated in units of kWh.

$$F_{\mathrm{DG}} = \dot{F}_{\mathrm{DG}} \times \Delta t \times 10 \ \frac{\mathrm{kWh}}{\mathrm{L}} \tag{14}$$

Frequent starting and stopping of a DG has negative effects on efficiency because it may not be running at its optimal operating temperature. DG start-up energy costs have been shown to be equivalent to 1 – 4 minutes of continuous high load operation [58]. When cycle charging, starting and stopping the DG is more frequent and the engine is less likely to completely cool off, so it is assumed that each start-up fuel penalty is the equivalent of 1 minute of full load operation, ($P_{\mathrm{DG,\,max}}$).

$$F_{\mathrm{DG,\,start}} = \frac{P_{\mathrm{DG,\,max}} \times \frac{1}{60}\,\mathrm{h}}{\eta_{\mathrm{DG}}} \tag{15}$$

Beyond the reasons of improved efficiency and lower emissions, operation of DG at part-load below 60% [24] and frequent starting and stopping of the engine [59] should be avoided in order to prevent damage and prolong the life of the system. Damage resulting from low load operation manifests itself in the form of deposits in the cylinders and exhaust due to incomplete combustion [60]. In this model if the DG is started it remains in service for a minimum of one hour as recommended in [23, 30]. The total fuel consumed by the DG during the length of each time step (Δt) is recorded and can be used to calculate the total diesel consumption for a period of interest.

DG require a cooling jacket during operation to prevent overheating, typically using a water-glycol mixture. They also expel large volumes of high temperature gasses in the exhaust. The distribution of waste heat is approximately 50 % in flue gas heat, and 50% in cooling jacket heat, and both heat sources present an opportunity for the recovery of thermal energy [61]. Typical DG waste heat temperatures range from 350 – 400 °C in the exhaust gasses, and 80 – 90 °C in the water jacket [61]. Using the modern heat recovery equipment, approximately 50% of the total waste heat can be recovered [62]. For example, a DG that is 33% efficient for an output electrical power of 100 kW results in 100 kW of recoverable waste heat and 100 kW of lost heat. In this model, the recoverable heat, Q_{DG}, is calculated as follows:

$$Q_{\mathrm{DG}} = F_{\mathrm{DG}} \times (1 - \eta_{\mathrm{DG}}) \times HR \quad (16)$$

Where *HR* is the heat recovery system effectiveness coefficient, and is assumed to be 50% [62].

When an ESS is co-located with DG, a control strategy that uses cycle-charging can improve the overall fuel efficiency by allowing the DG to run at higher part-loads. Consider a DG with a load being increased incrementally. For each incremental increase in load, the incremental gain in efficiency diminishes due to asymptotic behavior. For example, in Figure 11 the efficiency gain from increasing the part-load from 0% to 20% is Δ = 25%, substantially higher than the Δ = 8% incremental efficiency gain from increasing the part-load from 20% to 40%. Using this logic, and a fixed storage system efficiency, it is possible to determine a critical set-point for any DG where increasing the output beyond that point is no longer advantageous. The cycle charging set-point depends on the round-trip efficiency of the storage and the part-load efficiency curve of the DG.

Assuming a storage system round-trip efficiency of 60%, and a CAT 1010 DG, the set-point is determined by calculating the efficiency gained for each incremental increase of 2% of the DG's rated power. The point at which the incremental change in efficiency becomes negative is the cycle charging set-point, beyond which cycle charging has a net-negative effect. The set-point for the CAT 1010, shown in Figure 12, is approximately 21%, or 212 kW, where the gray curve crosses the x-axis.

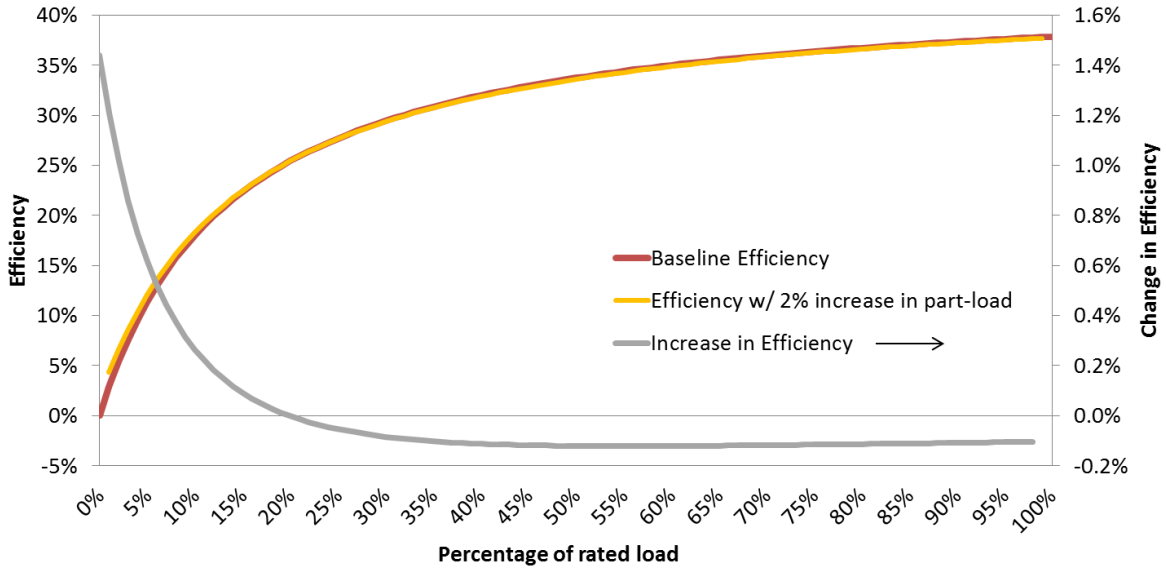

Figure 12 Effect of incrementally increasing diesel generator output for cycle charging

This means that cycle charging is only advantageous if the DG would otherwise be operating below a part-load of 21%. The critical set-point is constant for a given DG and storage round-trip efficiency, regardless of how much the load is increased for cycle charging, as shown in Figure 13.

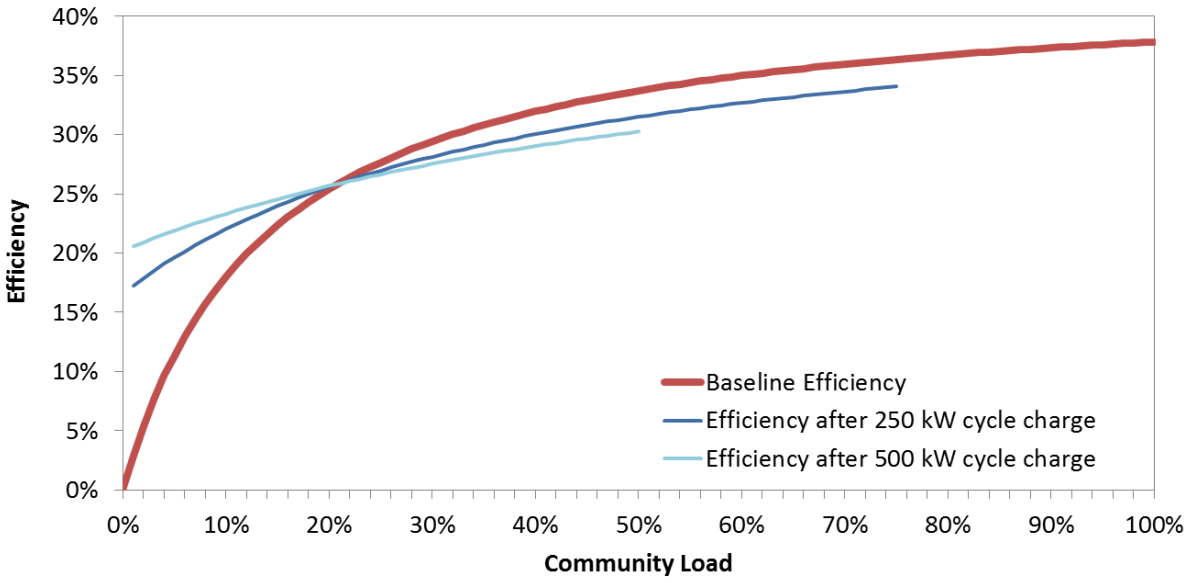

Figure 13 Effective diesel generator efficiency using cycle charging at various power rates

In Figure 13, the horizontal axis represents the community load required for the DG to feasibly be used for cycle charging. For example, cycle charging with 250 kW means

running the DG at 250 kW higher than the community load, and using the extra power to charge ESS. At a community load of 10% with 250 kW of cycle charging, the DG runs at 351 kW (35% rated load). Instead of a baseline efficiency of 15% to meet the load, the DG runs with an efficiency of approximately 30%, however, after the efficiency losses in the storage, the equivalent DG efficiency is approximately 20%. In this particular case, cycle charging resulted in an overall efficiency increase of 5%. As Figure 13 implies, the highest overall efficiency is attained by cycle charging with 500 kW (to 70% part-load) at any time when the DG would otherwise be operating below a part load of 21%.

The round-trip efficiency of the storage dictates how effective cycle charging is for any given part-load. As the round-trip efficiency increases, the cycle charging critical load set point also increases because the small incremental gains in DG efficiency are less burdened by the losses in the storage. Figure 14 was created using the logic described in Figure 12 and Figure 13 to show how the optimal cycle charging critical set point varies according to round-trip efficiency of an ESS.

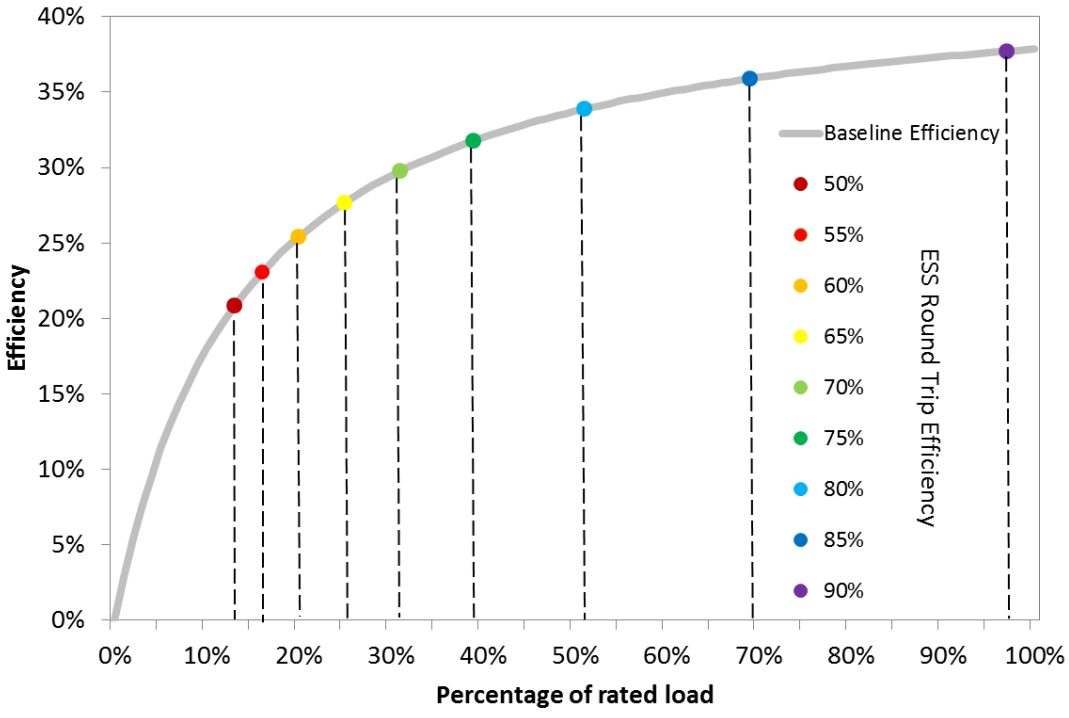

Figure 14 **Diesel generator cycle charging set-points for a range of storage round-trip efficiencies**

Cycle charging will only occur when the DG drops below the critical set-point, which is a percentage of its rated load. Figure 14 shows that an ESS with a round-trip efficiency of 50% rarely has the opportunity to cycle charge because the critical cycle charging set point is only 14% of the DG rated load. An ESS with 90% round-trip efficiency used for cycle charging will almost always result in higher overall efficiencies because the critical set-point is 97% of the rated DG load. Thus, the round-trip efficiency of the storage is crucial for dispatching beneficial cycle charging.

The RAES round-trip efficiency is assumed to be a function of RAES power and SOC, so the critical set-point for cycle charging will vary depending on different operating conditions. As the control strategy does not employ predictive logic, an average round-trip RAES efficiency of 60% is assumed for determining the cycle charging set-point. The benefits of cycle charging increase when DG and RAES are operating at higher loads. In this model the cycle charging set-point is at 21% of the rated load (210 kW), based on Figure 14. For any load below 21% of the DG rated power, cycle charging occurs and places an additional 500 kW of load on the DG to charge the RAES. For example, if the load was 150 kW, the DG would run at 650 kW, using 500 kW to charge the RAES and supplying the remaining 150 kW to the grid.

3.2.2 Wind Energy Converter

WEC power is calculated based on measured wind speed data, imported as a time series of average speeds for the duration of the time step. The wind speed data must be correlated to the proper height of the WEC being modeled. This is accomplished using the wind shear power law:

$$U_{\text{hub}} = U_{\text{anem}} \left(\frac{Z_{\text{hub}}}{Z_{\text{anem}}}\right)^{\alpha} \tag{17}$$

Where U_{hub} and U_{anem} are the wind speeds at the WEC hub height (Z_{hub}) and the data collection height (Z_{anem}), and α is the wind shear coefficient specific to the WEC site. The values of α used in the case studies are: 0.2 for the microgrid case study (assumed based on the coastal terrain), and 0.325 for the constrained case study [63]. The extractable power from the wind is a function of air density, ρ_{a}, its stream-speed, U, the turbine area, A_{WEC}, and power coefficient, C_{WEC}.

$$P_{\mathrm{WEC}} = \frac{1}{2} C_{\mathrm{WEC}} \rho_a A_{\mathrm{WEC}} U^3 \tag{18}$$

The WEC power coefficient is the ratio of produced electrical power, P_{WEC}, to the power available in the wind over the swept area of the turbine. The relationship between the wind speed and power coefficient is primarily an aerodynamic characteristic and is determined in controlled test environments and provided by the manufacturer for each specific turbine. Given the power curve and time series wind speed data, power output can be modeled for any WEC. Several WECs are modeled for the analyses contained in this document:

1. GE 82.5, rated 1.62 MW, hub height 82.5 m [64];
2. Windmatic 65, rated 65 kW, hub height 25 m [65];
3. Enercon E-33, rated 335 kW, hub height 50 m [66].

Figure 15 shows the power curves for the modeled WECs.

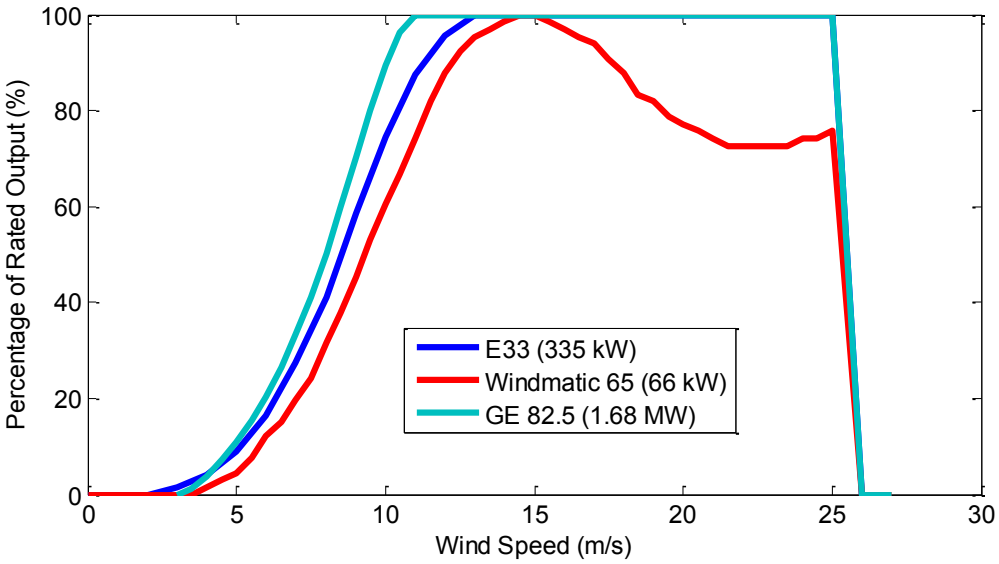

Figure 15 Modeled WEC power curves

Throughout the simulation, the wind speed at the WEC hub height is used to calculate average power (P_{WEC}) using cubic interpolation between points on the corresponding WEC power curve from Figure 15.

In actual power output, a hysteresis is observed as WEC follows swings in the wind speed, as well as turning on and off during storm control operation. This is due to the

inertia of the rotor and in most modern WEC, the blade pitch controls. In this model these effects are neglected because the power output is calculated based on the averaged wind speeds over increments no shorter than 10 minutes. For higher temporal resolution models, the hysteresis effects should be considered. Another aspect of WEC operation that should be considered is downtime due to maintenance or faults. This is known as the WEC availability, which is the percentage of time the WEC is fully operational. The industry standard of acceptable WEC availability is 97%, although many modern WEC farms achieve higher availabilities [67]. Because of this, availability does not have a significant effect on yearlong simulations of WEC operation. Availability is not modeled for this reason, and also because doing so may conceal important operational events that must be captured. For example, modeling WEC availability less than 100% may incur a random instance of downtime that occurs during a period of high sustained wind speeds. This would disguise the amount of energy that requires storage during that event by breaking a single high energy event into two smaller events.

The result of WEC simulation is a time series of electrical power output values for a single WEC. Depending on the control strategy, P_{WEC} is either exported directly to the grid, used to charge the RAES system ($P_{\mathrm{RAES,\,chg}}$), or curtailed ($P_{\mathrm{WEC,\,curt}}$). In the microgrid case, where installed WEC capacity is varied in a parametric sweep optimization, the P_{WEC} time-series is scaled for varying penetration rates. The penetration rate (PR), which will be used frequently in subsequent discussion, is the ratio of installed WEC capacity ($P_{\mathrm{WEC,\,max}}$) to the community maximum load ($P_{\mathrm{L,max}}$):

$$PR = \frac{P_{\mathrm{WEC,\,max}}}{P_{\mathrm{L,max}}} \tag{19}$$

In the microgrid case, the P_{WEC} time series scaling is accomplished by multiplying the time series of a single WEC output by the penetration rate and the ratio of the maximum load to the WEC name-plate capacity ($P_{\mathrm{WEC,\,NP}}$):

$$P_{\mathrm{WEC\ (scaled)}} = P_{\mathrm{WEC}} \times PR \times \frac{P_{\mathrm{L,\,max}}}{P_{\mathrm{WEC,\,NP}}} \tag{20}$$

In the conventional grid case, the P_{WEC} time series is fixed for all simulations. A single WEC is modeled and scaled according to the number of installed WECs:

$$P_{\mathrm{WEC\ (scaled)}} = P_{\mathrm{WEC}} \times N_{\mathrm{WEC}} \tag{21}$$

WEC layout is optimized to minimize the effect of wind shading that WECs have on each other. For this reason, (and because the exact layout is not known for either case study site) WEC wind shading is neglected.

3.2.3 Combined Heat and Power Plant

In the constrained grid case study, a CHP plant is co-located near the proposed RAES installation site, with infrastructure already in place to transmit steam. The electrical output of the CHP plant is exported directly to the transmission grid, and does not interfere with energy generation or storage taking place on the distribution grid. In this model, heat is the only output of the CHP plant that is considered. The heat (steam) from the CHP plant is used by RAES for the following purposes:

- Increase the expansion efficiency;
- Mitigate thermal losses incurred during time between charge and discharge modes;
- Ensure thermal stability during periods of cold weather (below freezing).

The availability of steam is a function of the CHP plant efficiency (η_{CHP}) and electrical power output (P_{CHP}). The rate of heat produced by the CHP plant ($\dot{Q}_{\mathrm{CHP}}$) is calculated as follows:

$$\dot{Q}_{\mathrm{CHP}} = P_{\mathrm{CHP}} \times \left(\frac{1}{\eta_{\mathrm{CHP}}} - 1\right) \times HR_{CHP} \tag{22}$$

Where HR_{CHP} is the heat recovery effectiveness coefficient. Not all of the heat produced at the CHP plant is recoverable, and not all of it is transmittable for other uses. The CHP plant of interest feeds steam to an industrial facility that was previously a paper mill, so a pipeline currently exists to transmit steam for many other end-uses besides RAES (heating, industrial processes, etc.). The temperature and pressure of the steam in the pipeline are kept constant while the CHP plant is operational. The total enthalpy (h_{steam}) of the steam is calculated using the known temperature and pressure. The amount of energy available in the steam pipeline is calculated as follows:

$$\dot{Q}_{\mathrm{steam}} = \dot{m}_{\mathrm{steam}} \times h_{\mathrm{steam}} \tag{23}$$

Where $\dot{m}_{\text{steam}}$ is the mass flow rate of steam through the pipeline. The CHP plant modeled for this research generates a steam resource that is orders of magnitude larger than what a RAES system can utilize. While the CHP plant is operational, the energy from the steam line is only used to heat water from the TES directly prior to expansion. This accomplishes an increase in efficiency and in doing so mitigates the losses incurred between charge and discharge modes. The use of waste heat to ensure the thermal stability of the system is discussed in Section 3.3.2.

3.3 Regenerative Air Energy Storage

As previously described, RAES systems can be broken down into two mains systems, each with subsystem components:

- Power Unit:
  - Compressor/expander (CE);
  - Motor Generator;
- Energy Unit:
  - Air storage;
  - Water storage (TES).

Each of these systems requires individual considerations; these are described in the following subsections. The general operational parameters of a RAES system are described in Table 4.

Table 4 Operational parameters of RAES

Parameter	Value
Compression Ratio	200
Max Pressure (bar)	200
Minimum Pressure (bar)	40
Power module rating (kW)	500
Energy module rating (MWh)	1
Thermodynamic Efficiency	90%
Temperature increase during compression (K)	32

3.3.1 Power Unit

The power unit is a specialized CE with three modes: charging, discharging, and standby. Although it is a variable power output machine, there is a limited charging and

discharging power band between $P_{\text{RAES, min}} = 250\,\text{kW}$ and $P_{\text{RAES, max}} = 500\,\text{kW}$. The lower limit ($P_{\text{RAES, min}}$) is imposed because of the low efficiency that results from such low part-load operation. The charge efficiency is a function of the SOC ($\eta_{\text{RAES, SOC}}$) and the power ($\eta_{\text{RAES, Power}}$). The discharge efficiency is a function of both SOC and power as well, but is also related to TES temperature. The charge and discharge efficiencies that are dependent on SOC and power are calculated by linear interpolation between the minimum and maximum efficiency, shown in Figure 16. These baseline efficiency values are assumed based on round trip efficiencies values between 55% and 65% for the range of operable SOC and power. The efficiencies used in this analysis are estimates for early stage RAES technology and are expected to increase as RAES matures [7].

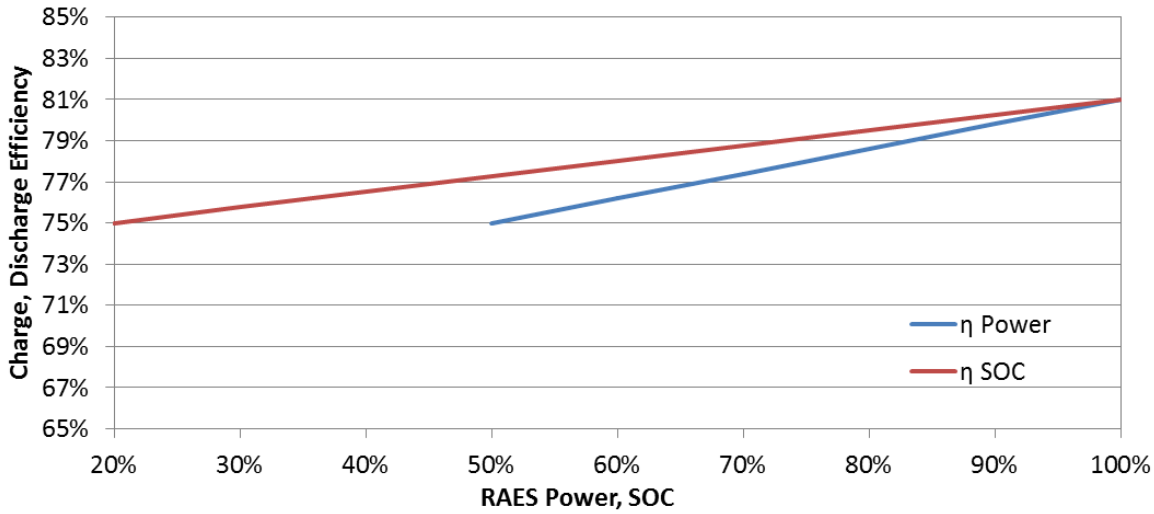

Figure 16 Range of one-way charge and discharge efficiencies

The one-way charging efficiency ($\eta_{\text{RAES, chg}}$) is determined by calculating the average of the separate efficiencies.

$$\eta_{\text{RAES, chg}} = \frac{\eta_{\text{RAES,SOC}} + \eta_{\text{RAES,Power}}}{2} \tag{24}$$

The one way discharging efficiency ($\eta_{\text{RAES, dschg}}$) is determined by calculating the average of the separate efficiencies and then adjusting it based upon the temperature of the TES (T_{TES}).

$$\eta_{\text{RAES, dschg}} = \left(\frac{\eta_{\text{RAES,SOC}} + \eta_{\text{RAES,Power}}}{2}\right) \times \left(\frac{T_{\text{TES}}}{T_{\text{amb}} + \Delta T_{\text{comp}}}\right) \tag{25}$$

Where T_{TES} is the temperature of the TES, T_{amb} is the ambient temperature, and ΔT_{comp} is the temperature increase through compression. If T_{TES} is higher than $T_{\text{amb}} + \Delta T_{\text{comp}}$ (achievable through the addition of waste heat), and the efficiency during discharge is higher than normal because of the added heat [68]. The ΔT_{comp} is assumed to be 32 K, based on a compression ratio of 200 and a thermodynamic efficiency of 90%.

3.3.2 Energy Unit

The air storage tank pressurizes with air and the TES (water tank) heats up as the system charges. For each simulation, the storage unit has a defined storage capacity (E_{RAES}) in units of kWh. E_{RAES} represents the energy stored in both the air pressure vessel and the TES, which are mutually dependent except when waste heat is added to the system. During each time step, the charge power ($P_{\text{RAES, chg}}$) or the discharge power ($P_{\text{RAES, dschg}}$) affects the energy stored in the system. If RAES is in standby, then the energy remains the same. It should be noted that the system will never charge and discharge in the same time step. The pressure drop due to the temperature decrease in the stored air is accounted for in the round-trip efficiency.

$$E_{\text{RAES},i} = E_{\text{RAES},i-1} + \Delta t \left(P_{\text{RAES, chg}} \times \eta_{\text{RAES, chg}} - \frac{P_{\text{RAES, dschg}}}{\eta_{\text{RAES, dschg}}} \right) \quad (26)$$

The RAES system only discharges when the pressure of the air tank is above a threshold of 40 bar. The SOC of the system is based on the air storage pressure, which is calculated such that for SOC = 100% the pressure is 200 bar, and for SOC = 20% the pressure is 40 bar. Since E_{RAES} represents the usable energy in the system, when E_{RAES}= 0, the SOC = 20%. It is assumed that at the beginning of each simulation, the system is initiated with SOC = 20%. Statistically, at the end of a simulation the SOC will also be 20%, so multi-year analyses with the same resource data would have duplicate results.

Q_{TES} and E_{RAES} are calculated separately in order to track the TES temperature. While E_{RAES} represents all the stored energy available to do work, Q_{TES} only represents the heat in the TES. If $E_{\text{RAES}} = 0$ the system cannot discharge, no matter how much heat is available in Q_{TES}. The TES uses liquid water that is subject to sensible heating and cooling during compression and expansion. Most of the thermal energy generated during

compression transfers to the water due to its large surface area (atomized liquid), high specific heat capacity, and high density. The heat in the water is added to the energy stored in the TES, Q_{TES}. Any available waste heat (Q_{WH}) can also be stored in the TES.

$$Q_{\mathrm{TES},\,i} = Q_{\mathrm{TES},\,i-1} + Q_{\mathrm{WH}} + \Delta t\left(P_{\mathrm{RAES,\,chg}} \times \eta_{\mathrm{RAES,\,chg}} \times \frac{q_{\mathrm{w}}}{q_{\mathrm{w+a}}} - \frac{P_{\mathrm{RAES,\,dschg}}}{\eta_{\mathrm{RAES,\,dschg}}} \times \frac{q_{\mathrm{w}}}{q_{\mathrm{w+a}}} - \dot{Q}_{\mathrm{Loss}}\right) \quad (27)$$

The ratio $\frac{q_{\mathrm{w}}}{q_{\mathrm{w+a}}}$ represents the proportion of specific sensible heat stored in the water compared the total specific sensible heat generated during compression or expansion:

$$\frac{q_{\mathrm{w}}}{q_{\mathrm{w+a}}} = \frac{(m_{\mathrm{w}} \times C_{\mathrm{p,w}})}{(C_{\mathrm{p,a}} + m_{\mathrm{w}} * C_{\mathrm{p,w}})} \frac{\Delta T}{\Delta T} \quad (28)$$

Where ΔT is the temperature change during compression ($T_2 - T_1$ in Eq. 8) or expansion ($T_3 - T_2$ in Eq. 9), which is dependent on the thermodynamic efficiency as discussed in Section 2.3.3. Since thermodynamic efficiency and the water to air volume ratio are assumed to be constant throughout operation, $\frac{q_{\mathrm{w}}}{q_{\mathrm{w+a}}}$ is also a constant value (0.986).

$\dot{Q}_{\mathrm{Loss}}$ is the rate of thermal loss, which is calculated based on the ambient temperature, T_{amb}, the temperature of the TES, and an assumed heat loss coefficient, $\dot{q}_{\mathrm{L}}$, for the TES. The value of $\dot{q}_{\mathrm{L}}$ varies depending on the energy capacity of the RAES system (0.1 kW/K for each 1 MWh module) [68].

$$\dot{Q}_{\mathrm{Loss}} = \dot{q}_{\mathrm{L}} \times (T_{\mathrm{TES}} - T_{\mathrm{amb}}) \quad (29)$$

The water used during compression/expansion is taken from the TES, and its temperature has an effect on the efficiency due to the heating/cooling effects of compression/ expansion processes. It is ideal to have colder water sprayed into the cylinder during RAES charging, and warmer water during expansion. To prevent any adverse effects on the charge efficiency, it is assumed that the water taken from the TES is always cooled by a heat exchanger to ambient temperatures (*e.g.* heat dump) prior to compression. Pre-compression cooling is not required when the thermal storage is at an appropriate temperature for system charging ($T_{\mathrm{TES}} = T_{\mathrm{amb}}$). The temperature of the TES system is regulated such that the temperature does not exceed an upper limit, $T_{\mathrm{TES,\,max}}$, which varies depending on the application, as shown in Table 5. In both cases, the lower limit for temperature is 278 K, which prevents the water from freezing.

Table 5 TES operational temperature limits

Application	$T_{\text{TES, max}}$ (K)	Limit	$T_{\text{TES, min}}$ (K)	Limit
Integrated with DG	343	Must maintain DG cooling below 348 K	278	Avoid freezing
Integrated with CHP	363	Must not allow water to boil	278	Avoid freezing

The TES temperature is calculated based on the TES mass, M_{TES}, and specific heat $(C_{p,\text{TES}})$.

$$T_{\text{TES}} = \frac{Q_{\text{TES}}}{M_{\text{TES}} \times C_{p,\text{TES}}} \tag{30}$$

The mass of the TES depends upon the capacity. For each MWh of storage capacity, there is assumed to be approximately 33000 kg of water, based on a 2.5% by volume water/air ratio before compression [7].The mass of water required for each MWh storage module is based on the specific work (w) done in Eqs. (10-11), which is calculated on a per unit mass of air basis. The amount of air (M_{a}) required to meet a specific storage capacity is calculated using the following equation:

$$M_{\text{a}} = \frac{1\text{MWh}}{w} \tag{31}$$

The corresponding amount of water (M_{w}) is therefore:

$$M_{\text{w}} = m_{\text{w}} \times M_{\text{a}} \tag{32}$$

When waste heat is available from an intermittent source such as a DG, then it is used to heat the TES directly. When waste heat is available from a continuous supply of high temperature steam, it heats the water being used in RAES immediately prior to discharge to the maximum allowable temperature $T_{\text{TES, max}}$. This is more efficient than maintaining the whole TES at $T_{\text{TES, max}}$.

3.4 Analysis Methodology

A combination of the above models is created using an application specific rule-based control strategy for the hybrid energy system under investigation. The control strategies used in this research are based on a single energy storage service RAES system: the main objective is to minimize WEC curtailment. Each case study has its own control strategy, which are described in detail and given in logic flow diagrams in Chapters 4 and 5. Yearlong simulations are run as a time step analysis, with the control strategy dictating

energy flows within the system. In order to optimize RAES sizing, an application specific parametric sweep is performed. For the microgrid case study, the parametric sweep varies RAES energy capacity and installed WEC capacity. For the conventional grid case study, the parametric sweep varies RAES power and RAES energy capacity. For each set of parameters, a yearlong simulation of system operation is carried out in which all variables are logged in time series values, allowing in-depth analysis of many aspects of the system including fuel consumption, WEC curtailment, RAES power and energy level, RAES efficiency, and more. Specific details of the analysis methodology are given for each case study in Chapters 4 and 5. The results of individual simulations are presented graphically as operational profiles for each component of the hybrid energy system. These are used to analyze trends throughout the varying operating conditions that occur within the yearlong simulation period. The results of the parametric sweep are presented in three dimensional contour plots. These illustrate the effectiveness of varying system sizes to accomplish various goals including but not limited to fuel savings, curtailment avoidance, and simple payback period.

CHAPTER 4 MICROGRID CASE STUDY

The following section describes a case study in which the previously described modeling methodology is applied to a remote microgrid community.

4.1 Background

In this case study, RAES is used in a remote microgrid community to buffer the variations in community electricity load, buffer the intermittency of WEC, and operate DG at its optimal efficiency. Quality data collection of energy production and use in remote microgrids has only recently become a priority due to concerns around diesel fuel costs and GHG emissions, so data is difficult to obtain. This case study is based upon Ramea, a remote island on North West Island, part of the Ramea archipelago off the southern coast of Newfoundland, as shown in Figure 17. A general climate and energy description of Ramea is given in Table 6.

Figure 17 Map of Atlantic Canada showing Ramea

Table 6 Description of Ramea

Population (2011)	715		
Temperature (°C)	Min	Average	Max
	-15.9	6.4	25.2
Electrical Load (kW)	Min	Average	Max
	186	484	1091
Diesel Generator Size	3 x 925 kW		
Installed WEC Capacity	6 x 65 kW		

Ramea is the pilot site for a wind, diesel, and hydrogen energy storage research and development system. The hydrogen storage system consists of an electrolyzer, storage tank, and a combustion generator. As one of the first isolated wind-diesel-hydrogen systems in the world, reliable data exists and two data sets were made available for analysis. Both include Ramea electricity load, as well as WEC generation or local wind speed. Data from year 2005 predates the storage system, and data from year 2010 does not include any storage related data. These datasets are detailed in Table 7.

Table 7 Description of Ramea measured datasets

Data Period	Temporal Resolution	Wind Data
January through August 2005	15 minute	WEC Production
January through December 2010	1 hour	14 m height Wind Speed

4.1.1 Community Electricity Demand

In the following analysis, the higher resolution 15 minute data from 2005 is used to model community load. Although missing four months of data is less than ideal, the 2005 data captures a significant portion of the seasonal variations in load. Since a full year of data is available from 2010, it is possible to extrapolate the results from 8 months of simulation in 2005 to a full year. Ramea's average monthly and annual load for both years is shown in Figure 18. The average diurnal load profile for each month is shown in Figure 19.

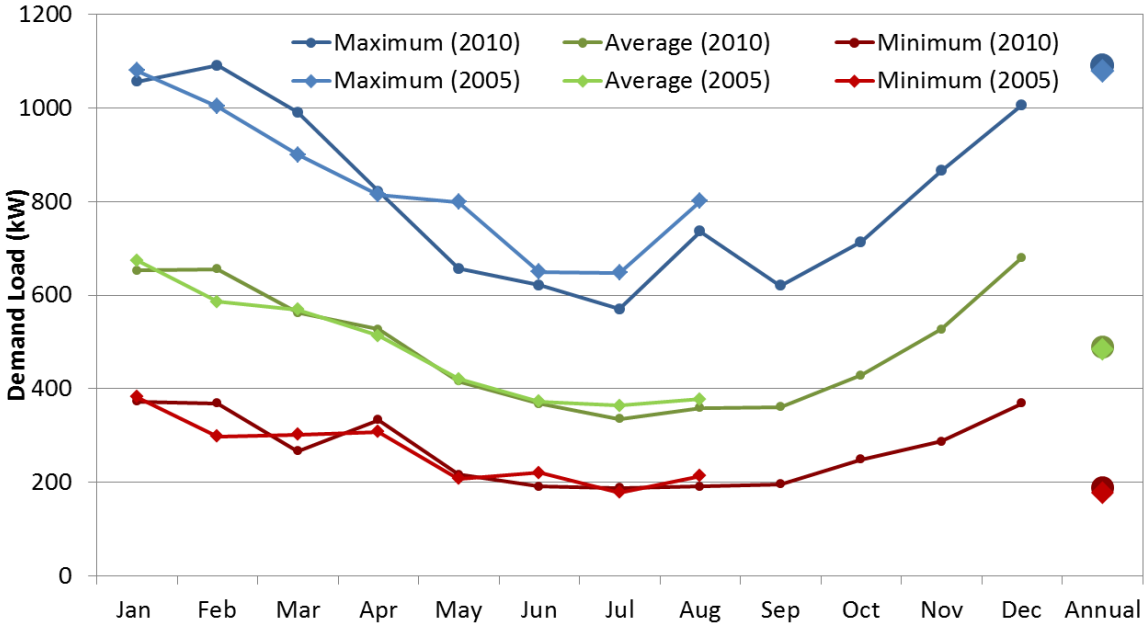

Figure 18 Average monthly and annual electricity load in Ramea

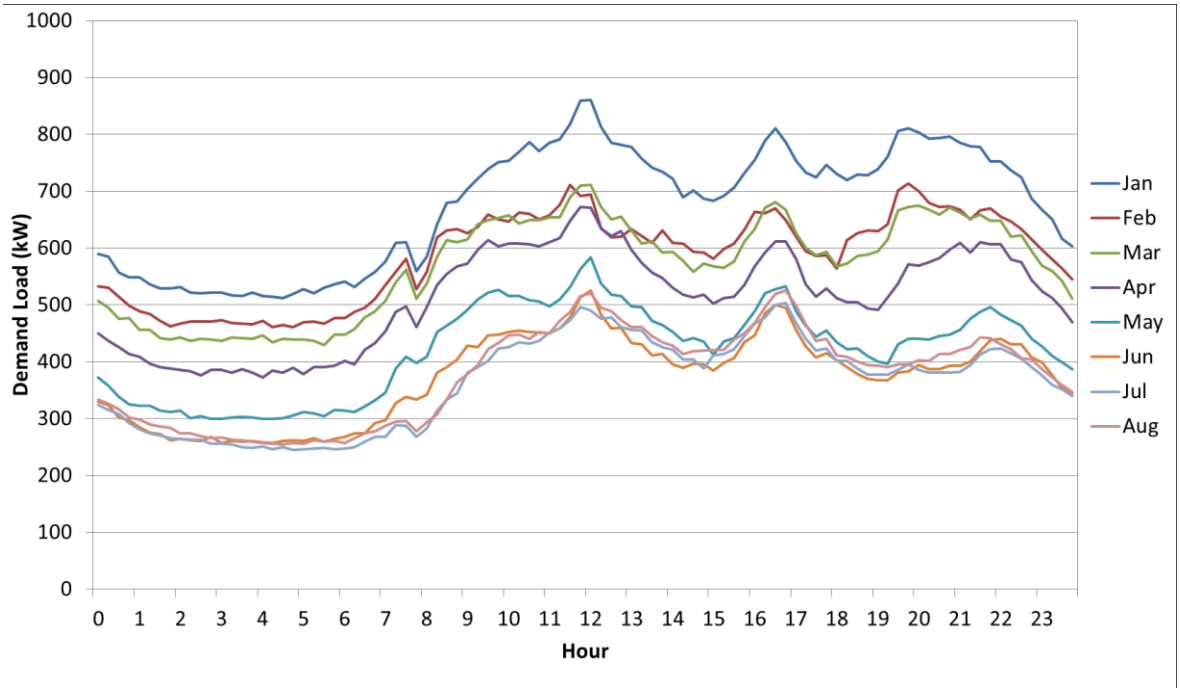

Figure 19 Average diurnal load profile by month for Ramea (2005 data)

Figure 18 and Figure 19 show a high degree of variability across long and short timescales, especially considering that the diurnal profile is averaged over a month. In Figure 18, the average load nearly doubles between July and January. The load data from year 2005 closely resembles the data from year 2010. The 15 minute time series data in Figure 19 captures short term variations such as a brief demand valley at hour 8.

4.1.2 Wind Energy Production

Wind energy at Ramea is generated by six Windmatic 65 kW WECs. The WEC production data from 2005 implies a capacity factor of 12%. This low value was due to ongoing commissioning during that year. According to Natural Resources of Canada (NRCan), the capacity factor of Ramea WECs is 33%, resulting in approximately 1100 MWh of energy annually [69]. Using the 2010 wind resource data and the Windmatic 65 kW power curve, the presently developed research model estimates annual energy production of the WEC system to be 956 MWh, equal to a capacity factor of 28%. This value assumes an availability of 100% and does not take into account turbine wind shading. The 2010 wind resource data is used for simulation purposes and results in the higher capacity factor similar to NRCan statements. The Windmatic 65 WEC is modeled

for the baseline analysis, but the Enercon E33 WEC is modeled for system optimization as it is a current production turbine that is rated for remote northern operation. A WEC availability of 100% is assumed in operational simulations in order to ensure that all potential energy curtailment/storage events are accurately accounted for, as discussed in Section 3.2.2.

4.1.3 Diesel Consumption

According to NRCan and others, the diesel fuel consumption in Ramea prior to the installation of the energy storage system was approximately 1 million liters annually [70, 71]. The annual electricity production of the DGs in 2010 was 3324 MWh. The capacity factors of an individual DG (925 kW) and the total DG capacity (2775 kW) are 41% and 13.6% respectively. This means that under typical operation only a single DG is running, and averages 41% of its rated capacity. Dividing the DG electricity production by diesel fuel consumption gives an annual operating efficiency of 35%.

4.2 Objective

The objective of this study is to demonstrate the operation of RAES in a microgrid using the numerical model described in Chapter 3. The model is used to determine the optimal energy storage characteristics of energy, power, and cycling profile. Co-locating a RAES system with a DG provides access to waste heat. The thermal energy captured from the DG cooling systems and exhaust system allows the RAES system to avoid thermal losses during standby operation, and also boost the efficiency of the expansion process by increasing the temperature of the water in the thermal energy storage (TES). The one-line diagram in Figure 20 shows the flows of energy within a wind-diesel-storage system that includes RAES.

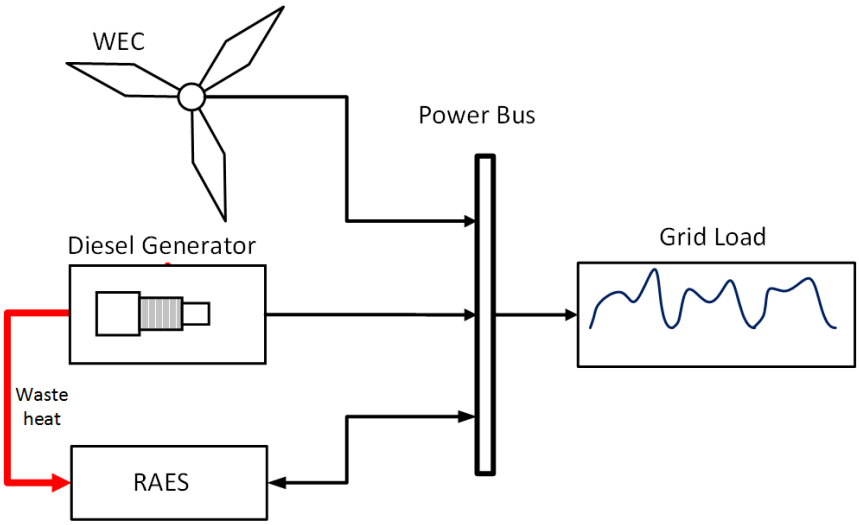

Figure 20 One-line diagram of a wind-diesel-RAES microgrid

The WEC penetration rate and the RAES energy capacity are varied in order to determine their effect on fuel consumption. The parametric sweep optimization scheme uses the following incremental variations of WEC penetration rate and RAES storage capacity:

- E-33 WEC penetration from 0% to 300% of load in 25% increments;
- RAES storage capacity from 1 MWh to 10 MWh in 1 MWh increments.

Each variation of the system results in a unique operational profile throughout the 8 month simulation period. The total diesel fuel consumption is calculated for each system variation and compared to the baseline fuel consumption (0% WEC penetration) to determine the fuel savings. The simple payback period is then calculated based on the ratio of the system cost to the value of fuel savings. RAES power is not varied because of similarity between the minimum size power module (500 kW) and the average community load (484 kW). A larger RAES power capability would require substantial capital expenditure for a small increase in relative utility (see results in section 4.4.3). Table 8 shows the assumed system costs used to analyze the economic benefit of each variation of the system. The optimal size RAES and WEC penetration level can be determined by the evaluating the fuel savings or the simple payback period. A valuation of environmental and GHG emissions reductions is not included in this project as there remains considerable range and implementation of such carbon-credit systems.

Table 8 Assumed microgrid system costs

Component	Cost
RAES Power Module	$2000/kW
RAES Energy Module	$200/kWh
Installed Wind Capacity	$4500/kW
Bulk Diesel Fuel	$1.5/L

The pricing of RAES technology is based on targets provided by LightSail's engineering team. The price of installed wind capacity is based on the projected costs for installation in remote communities described in [72]. The price of diesel is highly dependent on the mode of transportation used to ship it to the community. The average monthly bulk price of diesel fuel across Canada is shown in Figure 21. Fly-in communities have the highest prices for diesel, while islands accessible by barge have the lowest fuel costs. The assumed bulk price of $1.5/L is based on the average additional transportation costs (fuel, personnel, logistics, etc.) to remote communities, which are likely to be higher in certain remote communities and also likely to increase over time.

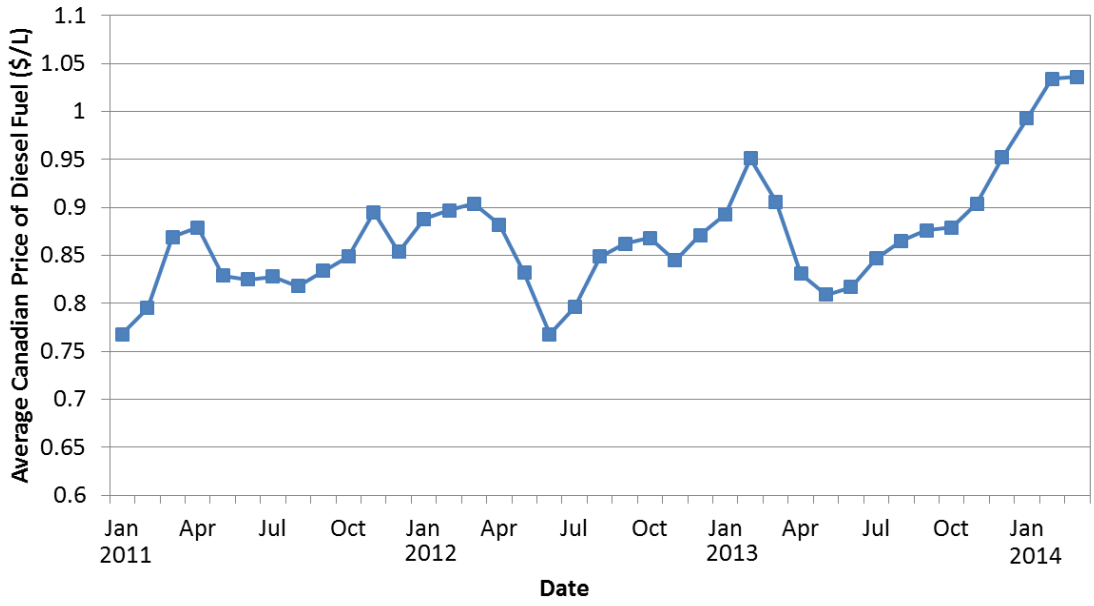

Figure 21 Average price of bulk diesel fuel throughout Canada (2011 – 2014) [73]

4.3 Control Strategy

The control strategy for these analyses has a single primary objective, which is to take maximum advantage of WEC electricity when it is available. This will export wind

power, P_{WEC}, directly to the grid if there is electricity demand, P_L, and store it otherwise. If wind is unavailable, then stored energy takes priority to meet the load. The DG is only started if both the WEC and RAES are unable to provide the necessary power, and if the required DG output is below 21% of its rated load, then cycle charging is initiated. Figure 22 and the following section describe the process through which the model dispatches the WEC, DG, and RAES.

RAES Charging

The use of the remainder of WEC power that exceeds the load ($P_{WEC} - P_L$) is dictated by its value and the SOC of the RAES. If the RAES is already fully charged (SOC = 1), or if the excess power is outside of the operable RAES bandwidth [$(P_{WEC} - P_L) \leq P_{RAES,\,min}$ or $(P_{WEC} - P_L) \geq P_{RAES,\,max}$], then some WEC power must be curtailed. Otherwise, all excess power is used to charge the RAES system.

If the WEC output is less than the load, then P_{WEC} is completely exported to the grid. The remainder of the load has to be powered by discharging the RAES system and/or powering with the DG.

RAES Discharging

RAES can fully supplement WEC power if it is in an operable SOC range [$0.2 \leq SOC \leq 1$] and if the required RAES discharge rate ($P_L - P_{WEC}$) is within the operable RAES power bandwidth [$P_{RAES,\,min} \leq (P_L - P_{WEC}) \leq P_{RAES,\,max}$]. Otherwise, the DG is necessary to meet the load.

Diesel Generator

If the DG is operating below the cycle charging set point ($P_{DG,\,CC}$), the DG increases its output to charge the RAES system (as long as there is storage capacity available). As recommended in [23, 30], frequent starting and stopping of the DG should be avoided. As such, if the DG is started for cycle charging, the control system ensures that it cycle charges for at least 1 hour prior to shutting down.

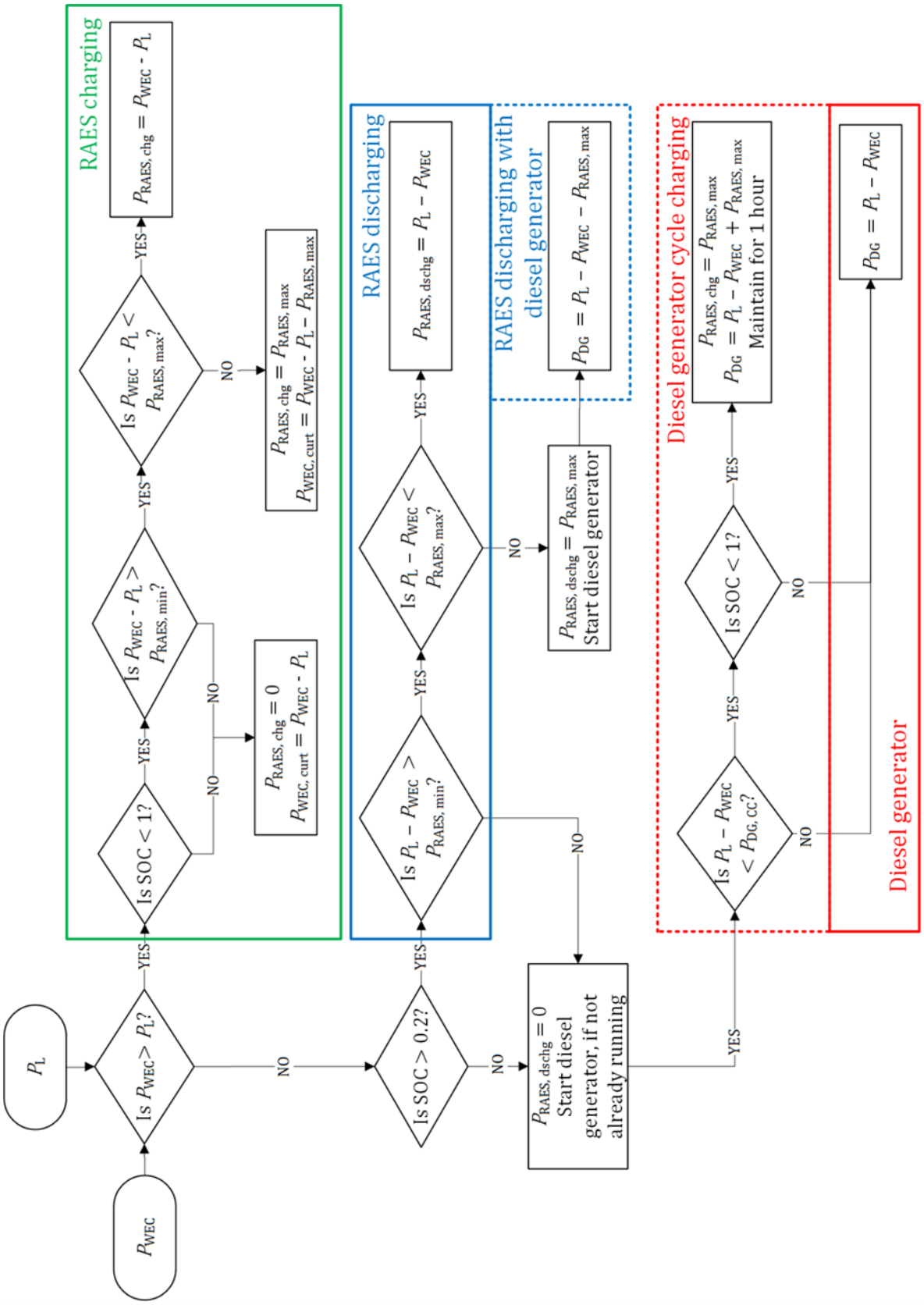

Figure 22 Microgrid case study control strategy flow chart

4.4 Case Study Results

The following subsections describe the results of the microgrid case study, beginning with a demonstration of the modeled system in operation, followed by a baseline analysis, a system optimization, and an investigation of the effectiveness of waste heat recovery.

4.4.1 WEC-DG-RAES System Operation

Figure 23 shows the modeled operation of a WEC-DG-RAES system. For demonstration purposes, a system with 4 MWh of storage and 100% wind penetration is simulated. The minimum and maximum RAES powers are 250 and 500 kW respectively. Figure 23 shows five plots for the operation of the system in varying conditions during 3 days in May:

a) community load,
b) WEC output,
c) DG output,
d) RAES power,
e) RAES energy.

The demonstration begins with a period of low wind speed where the load is met almost entirely by the DG. Towards the middle of day 0 the WEC output increases and lowers the demand on the DG. When the DG generation nears 210 kW the cycle charging set-point is met and output is increased by 500 kW and directed to the RAES for charging. This is followed by a further increase in WEC output causing the shut-down of the DG. At day 1 the WEC output is sufficient to meet the load and charge the RAES. The excess is used to charge the RAES overnight, but when the system reaches 100% SOC (4000 kWh), the excess WEC output is curtailed. The reader should note that the incidences of cycle charging during the middle of day 0 have produced negative effects in terms of fuel consumption. This is because the earlier charging of the RAES from the DG has resulted in curtailed WEC energy (due to SOC = 100%) that could otherwise been used to charge the RAES. These types of incidences are unavoidable without a more sophisticated control strategy that includes predictive logic.

As the wind dies down late in day 1, the DG is started even though there is ample stored energy. This is because the required power to meet the load is too low for RAES discharge (less than 250 kW). As the WEC generation further decreases the RAES enters the operable power band, and it discharges for the duration of day 1 and into day 2. When the RAES is fully discharged in early day 2, the DG is started again to meet the load, and it operates above the cycle charging critical set point. Throughout the operation, the temperature of the TES remains relatively constant at the upper limit as waste heat from the DG counteracts heat loss from the TES. The temperature decreases approximately 30 degrees (slightly less than assumed due to added heat from the DG when discharge briefly stops) during discharge, but rises again when the DG starts.

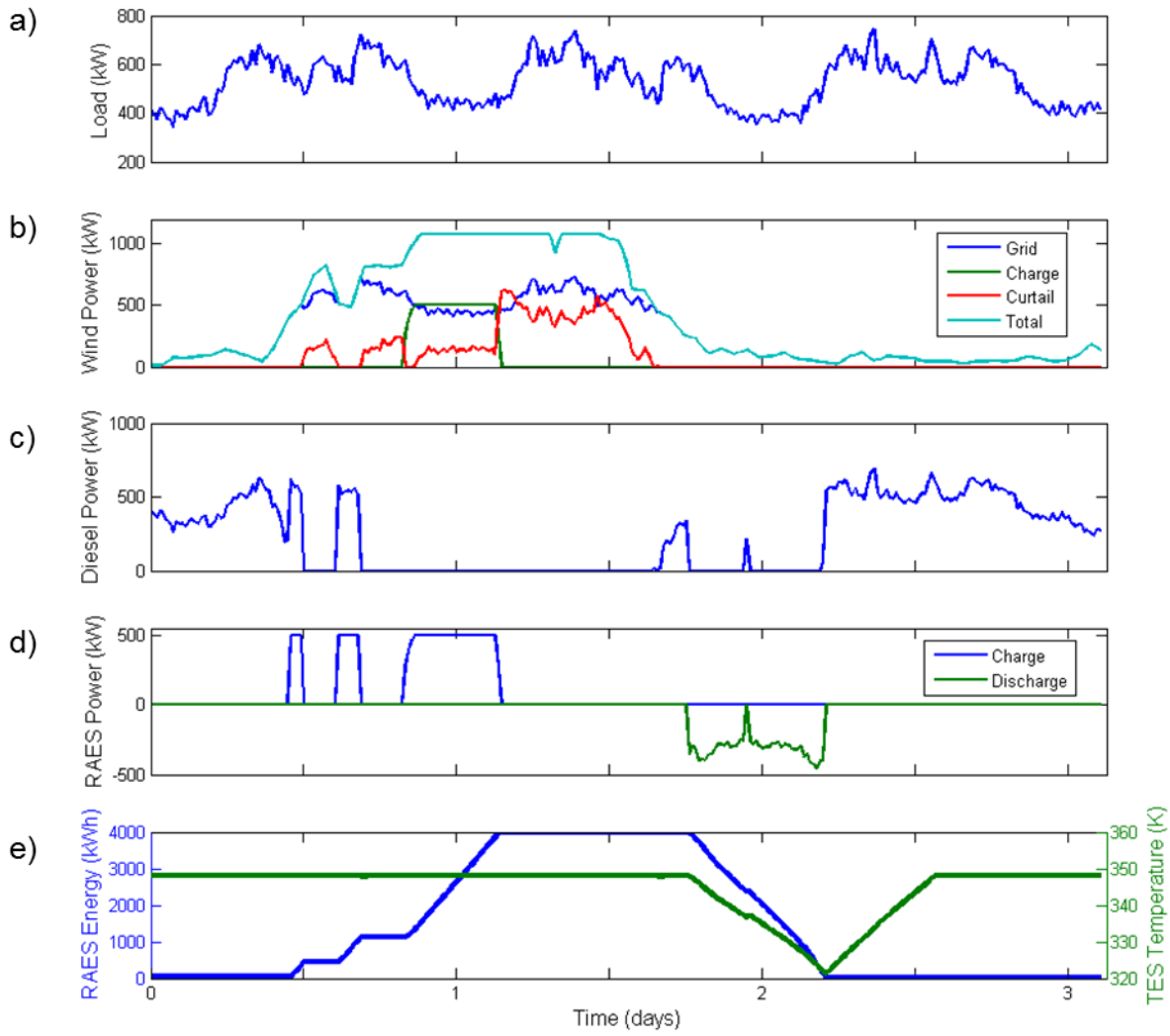

Figure 23 **Simulation period for a 4 MWh system with 100% WEC penetration showing a) community load, b) WEC output, c) DG output, d) RAES power, e) RAES energy.**

4.4.2 Baseline Analysis Results

Two baseline analyses were conducted for each of the datasets that was available from the community. Base case 1 considers the community to be powered only by DG. Base case 2 considers the community as a wind-diesel hybrid grid without energy storage at the present installed WEC capacity (6 x Windmatic 65 kW). The results of the baseline analyses are shown in Table 9. In order to compare the 2005 (incomplete) and 2010

(complete) data sets, the 2010 results are shown for both the full year and for the period of January through August.

Table 9 Results of baseline analyses for the community

Period		Jan–Dec 2010	Jan–Aug 2010	Jan–Aug 2005
Total Energy Demand (MWh)		4282	2816	2822
Base Case 1 – Diesel Only	Diesel Production (MWh)	4282	2816	2822
	Diesel Consumption (L)	1256300	828230	829240
Base Case 2 – Wind and Diesel	Diesel Production (MWh)	3324	2255	2261
	Diesel Consumption (L)	1030900	697080	698620
	WEC Production (MWh)	956	560	560
	WEC Curtailment (MWh)	3	1	1
	Fuel Savings (L)	225400	131150	130620
	Fuel Savings (%)	18	16	16

The simulation for base case 2 predicts 1.03 million liters of diesel fuel consumption, which agrees with the community's measured fuel consumption. This validates the DG and WEC models created for this project.

4.4.3 System Optimization

To determine an optimal RAES system for fuel savings in a wind-diesel microgrid, multiple simulations were performed to determine what combination of installed WEC generating capacity and RAES energy capacity conserves the most fuel. Fuel savings are calculated for each simulation by comparison to the baseline system consisting of just a DG. Figure 24 shows the variation in annual fuel consumption according to the RAES capacity and the WEC penetration rate. For levels of penetration rates less than 100%, energy storage does not lower the overall fuel consumption by a significant amount. This is because the WEC output rarely exceeds the community load to a level necessary of minimum charging power. The use of cycle charging does not have a significant impact on fuel savings because the DG is not frequently required to operate below the set-point threshold (21% of rated DG load). For WEC penetration rates between 100% and 200%, the high wind periods are short enough so that most can be accommodated by RAES capacities of 3 MWh or less. Additional capacity is infrequently used and thus does not lower fuel consumption. Beyond WEC penetration rates of 200% the fuel consumption strongly decreases with increased RAES capacity. However, the RAES power capability of 500 kW limits the capture-able WEC energy in such high penetration rate cases. It

should be noted from Table 8 that because of incremental sizing, increasing the RAES power capability by adding another CE (500 kW) nearly doubles the price of the storage system.

The annual fuel savings are determined by comparing the fuel consumption shown in Figure 24 (A) to the base case 1 fuel consumption from Table 9. The ratio of the total cost of WEC and RAES over the value of fuel savings is equivalent to the simple payback period for these incremental systems. The simple payback period is shown in Figure 24 (B). The lowest simple payback systems are low penetration WEC only systems. In WEC penetration levels below 75%, a RAES system is not economically viable as the WEC rarely requires storage, so there is justification for the capital cost. It follows logically that extending the energy capacity at low wind penetration levels does not improve the economics of RAES.

The most cost effective WEC + RAES system is a 1 MWh storage system with 75% WEC penetration rate, which has a simple payback period under 6 years. Beyond WEC penetration rates of 75%, significant fuel savings are accessible by adding RAES, but the additional capital costs of WEC+RAES lengthen the simple payback period in comparison with a 75% penetration, 1 MWh system. For a system with a wind penetration level of 175%, the lowest simple payback period comes with a RAES system of 2 MWh. The simple payback with RAES is approximately half of a year longer than a system with no RAES. It may seem unlikely that a developer could justify spending the additional capital for RAES without improvements in their simple payback. However, when the systems are evaluated on a both a simple payback and environmental consideration, the advantage shifts towards the RAES system. Including RAES with 175% WEC penetration saves over 40,000 litres of diesel fuel annually compared with a WEC + DG system alone. While this only represents approximately 9% relative increase in fuel savings compared to a system without RAES, it translates into GHG emission reductions of approximately 112 tons of CO_{2e}. A valuation of such environmental and GHG emissions reductions is not included in this project as there remains considerable range and implementation of such carbon-credit systems. For example, the carbon tax in

British Columbia is applied at the sale point for fossil fuels. The carbon tax for diesel fuel is $0.0767/L [74], a value that would only have minor changes on the simple payback period.

A northern community whose mandate includes aggressively reducing diesel fuel consumption will find that a WEC+RAES solution offers significant fuel savings over a WEC only system. For example, a WEC penetration rate of 175% with a RAES of 500 kW, 2 MWh increases the simple payback to 7.8 years from 7.3 years, but saves an additional 40,000 liters (9% additional savings) of diesel fuel annually compared to a system without RAES. The same penetration rate with a RAES of 500 kW, 5 MWh system increases the simple payback back to 8 years, but saves an additional 30,000 liters of diesel fuel annually. These are considerable additional diesel fuel savings with less than a year more payback period, but do require additional capital investment. The RAES system nearly pays for itself, and such a high level of WEC penetration necessitates RAES (or another ESS).

Assuming a conservative operation lifecycle of 20 years, this system will continue to lower fuel consumption for 12 years after the payback period has ended. With a 175% penetration WEC and 5 MWh RAES system, over the 12 years following payback the RAES system will result in 840,000 L of additional fuel savings. At the assumed cost of diesel fuel, and without taking into account fuel price escalation, the RAES system saves $1,260,000 for the remote community. The 12 years of WEC operation result in $7,200,000 of fuel savings, a large portion of which is only possible due to the inclusion RAES. Compared to the $2,000,000 capital cost of the RAES system, the additional revenues make it a worthwhile investment.

The model was also used to perform a sensitivity analysis examining the effect of increased diesel fuel costs. For a diesel price of $2.50/L, the shapes of the contours are very similar to the results from the analysis using a price of $1.50/L shown in Figure 24 (B). However, the values for simple payback are generally shorter by approximately

30%. This means that while the economics improve for all RAES and WEC systems, the optimal sizing remains similar.

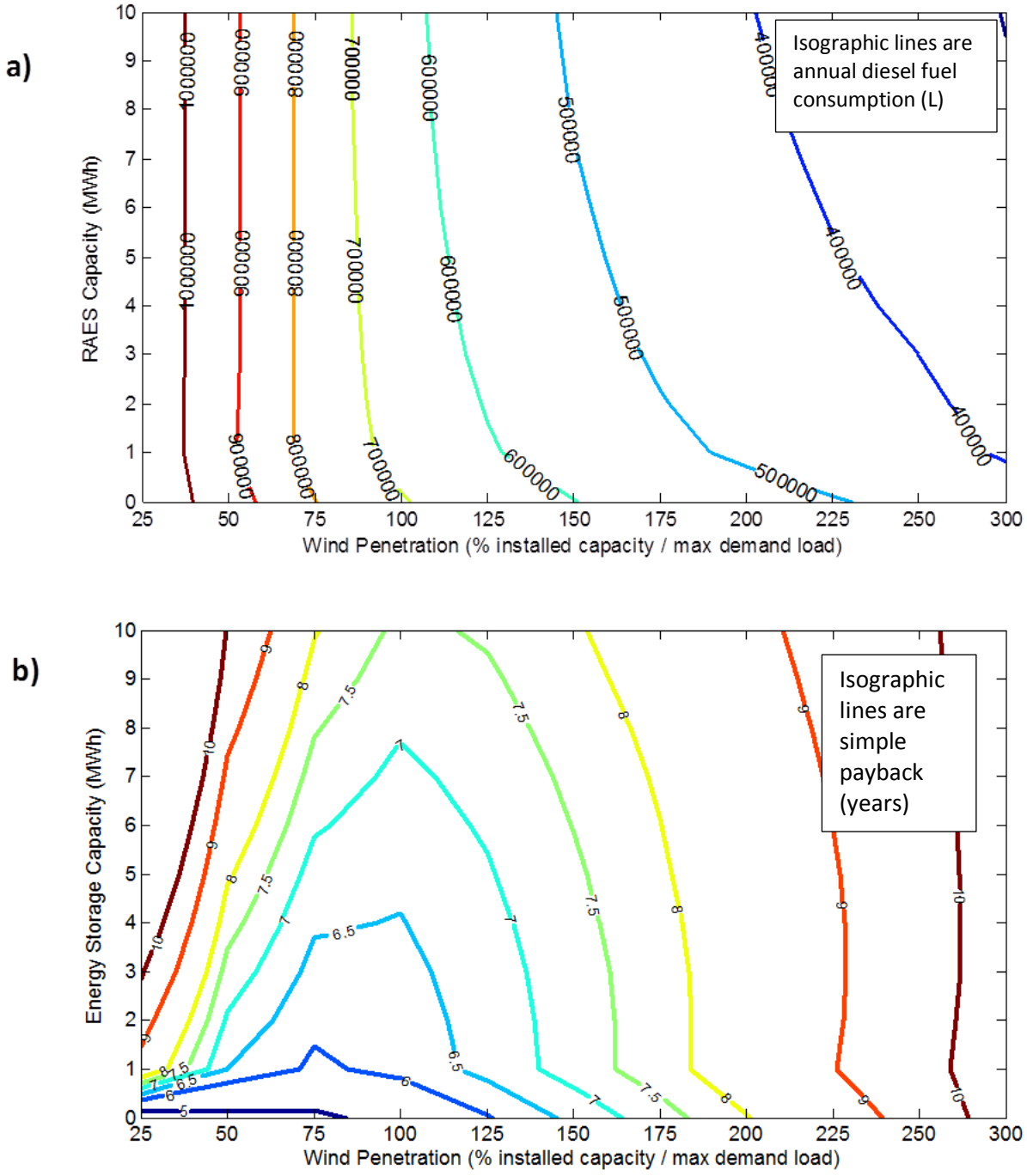

Figure 24 **Contour plots showing a) annual diesel consumption (L) and b) simple payback period (years) for varying storage capacities and wind penetration levels**

4.4.4 Waste Heat Recovery Effectiveness

In all the previous analyses, the use of WHR from the DG has been included in the model. WHR achieves two benefits for RAES: it helps to minimize thermal heat losses during standby operation of the RAES system, and boosts the discharge efficiency (and in turn the round-trip efficiency of the system). The final analysis for this case study quantifies how effectively WHR improves RAES system performance. Three variations of the same system are compared:

- No WHR
- WHR included at 75°C
- WHR included with a higher operable TES temperature range, 95°C

The analysis is performed for a 0.5 MW RAES system with 5 MWh of energy capacity, and a WEC penetration rate of 175%, based on the optimal system sizing discussion from the previous section.

Table 10 Effects of WHR for a 0.5 MW, 5 MWh RAES system with 175 % WEC penetration

RAES System	Energy throughput (MWh)	Average discharge efficiency	Average round-trip efficiency	Additional fuel savings from WHR (L)
No WHR	234.1	72.4 %	55.6 %	-
WHR, $T_{\mathrm{TES,max}}$ = 75 °C	264.8	84.4 %	64.8 %	9456
WHR, $T_{\mathrm{TES,max}}$ = 95 °C	270.8	86.6 %	66.5 %	11102

Table 10 shows that by capturing waste heat from the DG, the round-trip efficiency of the RAES system is increased by Δ = 9%. The limiting factor of how much the efficiency can be boosted is the upper limit for temperature in the TES, since expansion efficiency is a function of TES temperature. In this study, it is assumed that the TES is recovering waste heat by cooling the DG, and is subject to a limit of $T_{\mathrm{TES,max}}$ = 75 °C to maintain the DG cooling system. Once the TES reaches this limit, thermal energy either from the DG or the WEC dump load needs to be shed. By boosting $T_{\mathrm{TES,max}}$, the average round-trip efficiency can be increased farther, but as Table 10 shows, there are diminishing returns. If $T_{\mathrm{TES,max}}$ was raised to 95 °C by using heat from the high temperature exhaust gasses, the round-trip efficiency only increases by approximately Δ = 2%, which is likely not worth the added technical complexities.

CHAPTER 5 CONSTRAINED GRID CASE STUDY

The following section describes an alternative case study in which the previously described modeling methodology is applied to hybrid energy system connected to a capacity constrained electricity grid.

5.1 Background

This case study involves using RAES to increase the amount of WEC that can be developed on a distribution grid in Brooklyn, a small town in Southern NS. The proposed project is being developed under Nova Scotia's Community Feed-in Tariff (COMFIT) program, which offers a subsidized electricity tariff for community-based renewable energy projects interconnected on medium voltage distribution grids [75]. According to COMFIT regulations, the installed capacity of non-dispatchable renewable energy generators (such as WEC) must be lower than the estimated minimum annual load (MAL) at the sub-station of the distribution grid to which they are interconnected. The sub-station in question has an estimated MAL of 3.6 MW [56], but by involving an ESS the WEC capacity allowance has been increased to 4.8 MW. The RAES will ensure the output of the WEC does not exceed the minimum annual load of 3.6 MW by storing and/or curtailing it, thus avoiding a reversal in electricity flow through the distribution sub-station feeder. The WEC-RAES system will be co-located alongside a 29 MW CHP plant in order to have access to waste heat.

5.1.1 Wind Resource

Site specific data is not available for this analysis; however a full year of data is available from a nearby meteorological tower located in Barrington, NS. Although the distance separating the point of data collection and the proposed WEC sites is approximately 100 km, the two locations share similar elevation, land cover, terrain, and proximity to the Atlantic coast. Such similarities allow confident use of the Barrington data to model WEC operation in Brooklyn [63]. Figure 25 shows the locations of Brooklyn and Barrington on a map of Southern Nova Scotia.

Figure 25 Map of Southern NS detailing Brooklyn and Barrington locations

Table 11 highlights the characteristics of the meteorological tower and the data that was collected.

Table 11 Barrington wind resource metadata

Tower location (lat. long.)	N 43.00 E 65.00
Elevation	20 m above sea level
Time step length	10 minutes
Data collection duration	2012/07/31 - 2013/08/01
Anemometer heights	40 m, 50 m, 58 m
Shear factor	0.325
Mean wind speed (80 m)	7.02 m/s

The shear factor was provided by the engineers responsible for the WEC development [63]. Figure 26 shows the distribution of wind speeds at the Barrington site, extrapolated to 80 m above ground level using the power law from Eq. 16.

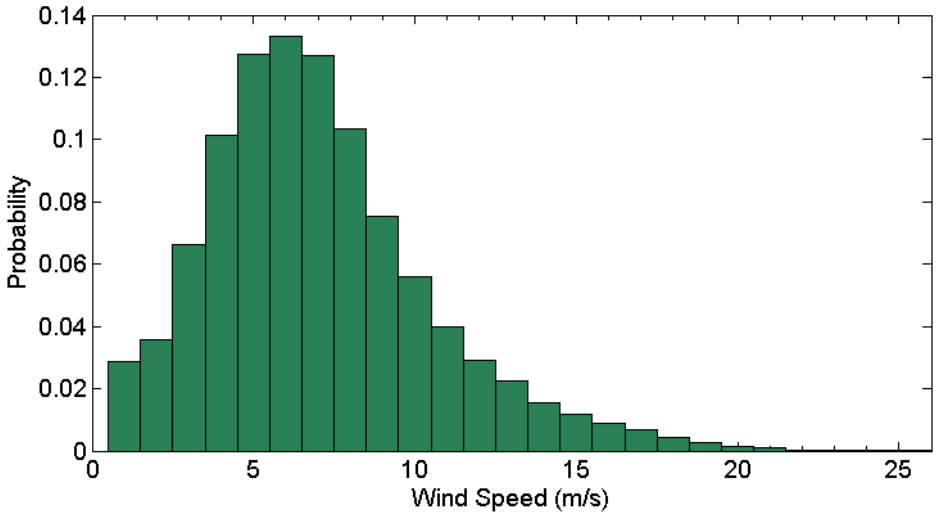

Figure 26 80 m wind speed distribution at Barrington met tower site

The Barrington data will be used to model WEC production at the chosen development site in Brooklyn, which has been allotted up to 4.8 MW of capacity for WEC development. The WEC configuration is three GE 82.5 units, each rated 1.62 MW. As with the previous case study, an availability of 100% is assumed for the WEC in operational simulations in order to ensure that all potential energy curtailment/storage events are accurately accounted for, as discussed in Section 3.2.2.

5.1.2 System Interconnection

The 4.8 MW of WEC capacity in Brooklyn will feed into the 26.4 kV distribution grid that is supplied by the Milton sub-station (ID: 50W). Milton is a step down sub-station for transmission (138 kV to 69 kV) and distribution (69 kV to 26.4 kV) circuits. The MAL on the distribution feeder is 3.6 MW. The combined output of the WEC and RAES will be measured on a meter as it feeds into the 26.4 kV distribution grid, and the amount of electricity that flows through the meter will determine revenue from the wind and storage (the WEC and RAES will share the same tariff of $131/MWh). The Brooklyn CHP plant is interconnected to the Milton sub-station via a 138 kV transmission line. Its output either feeds the 26.4 kV distribution grid, the 69 kV transmission lines, or bypasses Milton and continues down another 138 kV transmission line. Figure 27 shows a map of the area, highlighting the locations of the WEC site, CHP plant, RAES site, Milton sub-station, as well as the transmission and distribution lines.

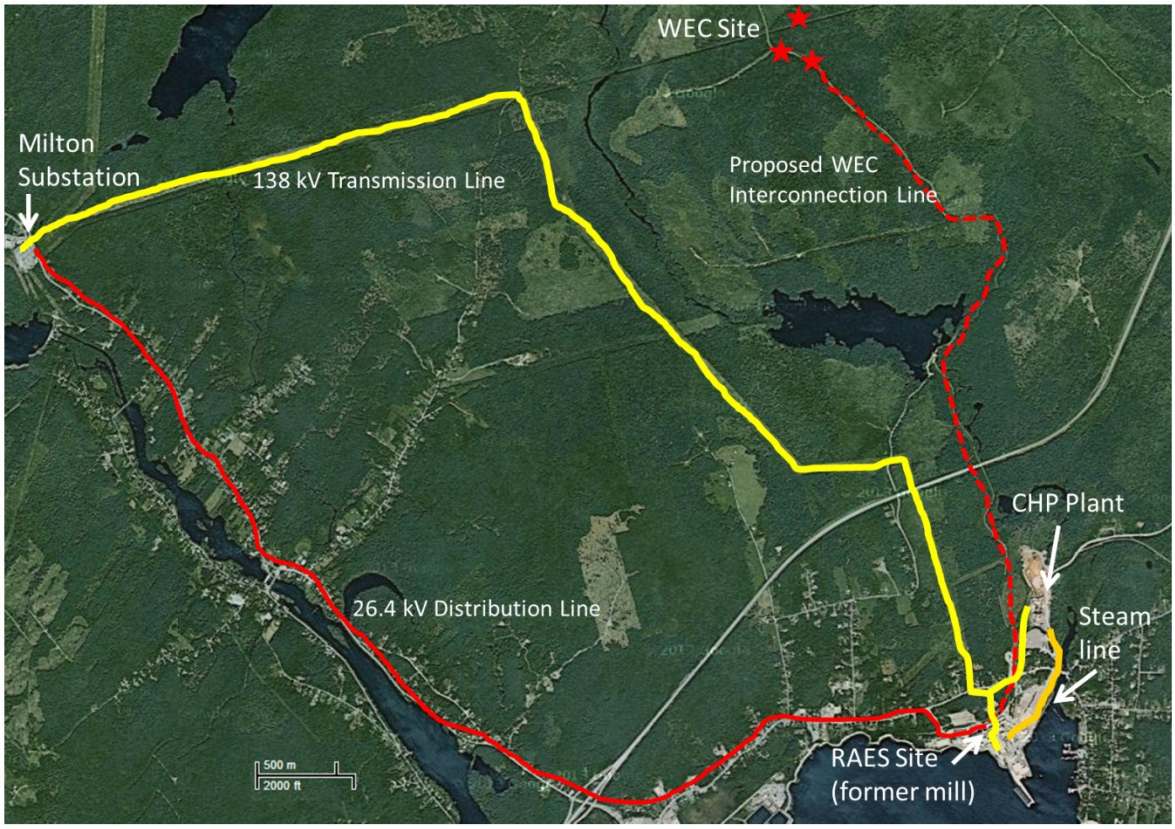

Figure 27 Map of the Brooklyn Wind and Energy Storage project layout

5.1.3 Brooklyn CHP

The Brooklyn CHP plant was designed primarily to provide steam to a paper mill, and electricity generation was considered secondary. Now, after the closure of the mill, electricity is the primary product and steam is secondary. The name plate electricity capacity of the generator is 29 MW, and 100 MW of steam is generated from a bubbling fluidized bed that burns chipped biomass fuel. Presently, the plant only operates for 6 months of the year, from mid-October to mid-April. Each day the plant receives a generation schedule that typically has the plant running at 50% capacity overnight (off-peak) and at 100% (on-peak) during the day, with an hour-long transitional period of 75% operation in between. Steam is transferred to the mill site via an 18" pipe and has a condensate return line. At present, the low volume of steam being transferred makes an open-loop system favorable, which means the condensate does not return to the boiler.

The properties of the saturated steam before and after the mill closure are shown in Table 12.

Table 12 Steam properties at the Brooklyn CHP plant

Steam Property	Prior to mill closure	After mill closure
Steam State	Superheated	Saturated
Temperature (˚C)	260	155
Flow rate (kg/s)	31.9	0.63
Pressure (Bar)	13.1	13.1
Enthalpy of Steam (kJ/kg)	2954	2786
Rate of Heat (kW)	94 MW	1.8 MW

The CHP plant is capable of sending more steam than it currently does to the site, should additional demand appear. All the excess steam at the CHP plant is condensed in cooling towers. For this reason, the steam available at mill site is considered independent of the power output of the CHP plant, as long as the CHP plant is running. The power purchase agreement (PPA) between NSPI and Brooklyn Power (the operators of the plant) expires in 2028. It is unknown whether or not the plant will continue to operate after the PPA expires.

5.2 Objective

The objective of this research is to model and analyze RAES technology operating as a means to extend the WEC generating capacity on a constrained grid. The RAES will also be thermally interconnected with the Brooklyn CHP plant. The RAES will leverage the surplus of heat outputs from the plant by using it to boost efficiency and power. The modeling and simulation of this system serves to optimally size the RAES system in order achieve the aforementioned objectives. Figure 28 shows the main components of the system and how they are interconnected.

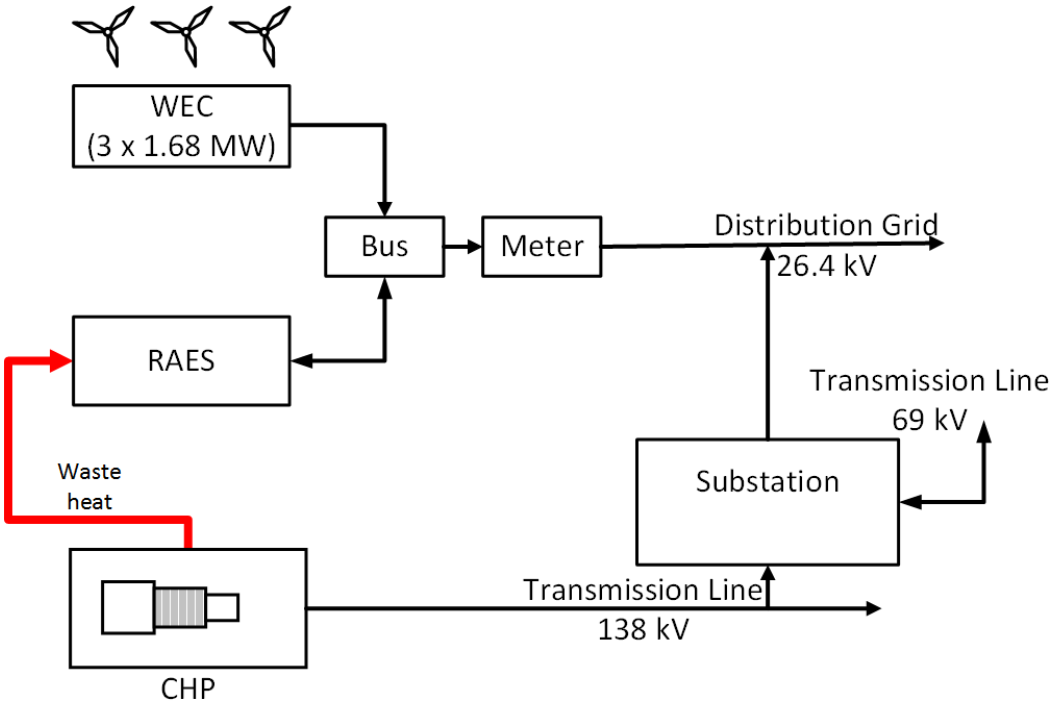

Figure 28 One-line diagram of the Brooklyn Wind and Energy Storage project interconnection

In this case, RAES power and energy capacity are varied as follows:

- RAES energy capacity: 1 MWh to 20 MWh in 2 MWh increments;
- RAES power: 0.5 MW to 2 MW in 0.5 MW increments.

Each variation of the system results in a unique operational profile throughout the year-long modeled period. In each simulation, all of the variables are recorded on a time step basis, allowing in-depth analysis of many aspects of the system. Some of the main analysis criteria are WEC curtailment, RAES throughput, RAES efficiency, system costs, and revenue from electricity sales. Table 8 shows the assumed system component costs used to analyze the economic benefit of each variation of the system.

Table 13 Assumed constrained grid system costs

Component	Cost
RAES Power Module	$2000/kW
RAES Energy Module	$200/kWh
Installed Wind Capacity	$2275/kW
RAES + WEC Tariff	$0.131/kWh

The pricing of RAES technology is based on the same assumed price as the microgrid case study. The price of installed wind capacity is based on forecasted procurement, development, and construction costs in the region [76].

5.3 Control Strategy

The control strategy for these analyses has a single primary objective, which is to maximize curtailment avoidance. This will export wind power, P_{WEC}, directly to the grid if there is available capacity within the MAL, and store it otherwise. If wind is unavailable, then stored energy discharges up to the rate allowable by the MAL in preparation for the next curtailment avoidance (*i.e.* charging). Figure 29 and the following section describe the process through which the model dispatches the WEC and RAES.

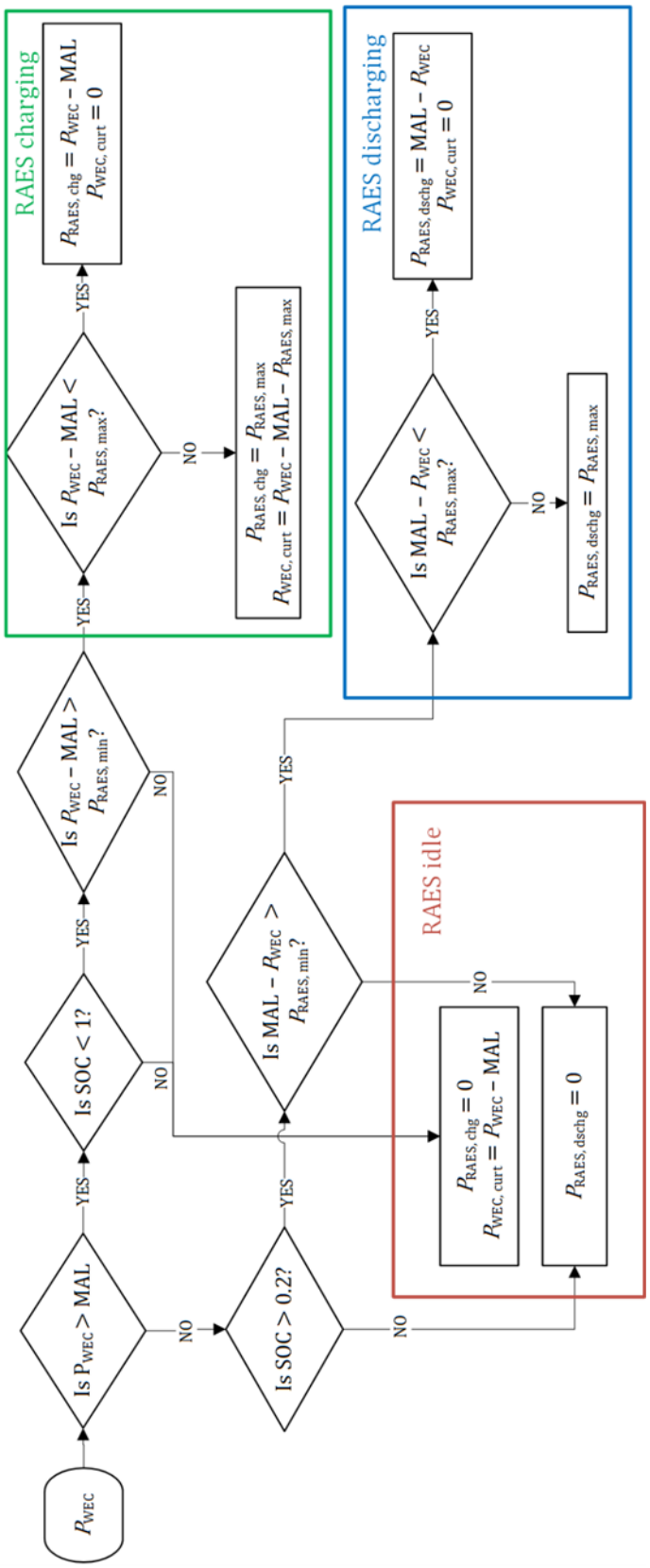

Figure 29 Constrained grid case study control strategy flow chart

As previously stated, if the WEC output, P_{WEC}, is greater than the MAL, then the RAES system enters charge mode operation.

RAES Charging

The use of the remainder of WEC power that exceeds the MAL ($P_{\mathrm{WEC}} - \mathrm{MAL}$) is dictated by the SOC of the RAES, and by the amount of excess power available. If the RAES is already fully charged (SOC = 1), or if the excess power is outside of the operable RAES bandwidth $[(P_{\mathrm{WEC}} - \mathrm{MAL}) \leq P_{\mathrm{RAES,\,min}}]$ or $[(P_{\mathrm{WEC}} - \mathrm{MAL}) \geq P_{\mathrm{RAES,\,max}}]$, then some WEC power must be curtailed. Otherwise, all excess power is used to charge the RAES system. If the WEC output is less than the MAL, then P_{WEC} is completely exported to the grid. The remaining capacity available under the MAL can be met by discharging the RAES system.

RAES Discharging

RAES can discharge if it is in an operable SOC range ($0.2 \leq \mathrm{SOC} \leq 1$) and if the required RAES discharge rate ($\mathrm{MAL} - P_{\mathrm{WEC}}$) is within the operable RAES power bandwidth $[P_{\mathrm{RAES,\,min}} \leq (\mathrm{MAL} - P_{\mathrm{WEC}}) \leq P_{\mathrm{RAES,\,max}}]$. If there is no WEC output, the RAES can discharge at full power.

If the RAES is neither charging nor discharging, it idles in standby operation.

5.4 Case Study Results

The following subsections describe the results of the constrained grid case study, beginning with a demonstration of the modeled system in operation, followed by an analysis of WEC production and curtailment, a system optimization, and an investigation of the effectiveness of waste heat recovery.

5.4.1 WEC-RAES System Operation

For demonstration purposes, a RAES system with 0.5 MW and 4 MWh is simulated. The period lasts 3 days during the summer season when waste heat from the CHP plant is not available. Figure 30 shows three plots for the operation of the system:

a) WEC output,
b) RAES power,

c) RAES energy and temperature.

It should be noted that the teal line representing total WEC output occasionally conceals the blue line representing WEC output exported to grid in Figure 30 (A). The period begins with WEC output just below the MAL. A few hours into the first day (day 0) the WEC output exceeds the MAL and the RAES begins to charge. The charging is intermittent because at certain times the excess WEC output is not enough to power the RAES system. When the wind drops sufficiently below the MAL, the RAES discharges slightly and then continues to charge. Over the course of charging, the TES temperature rises approximately 30 degrees but incurs some losses during idling and discharge. At the end of the first day the RAES reaches a full SOC, but the WEC output remains at full capacity, requiring heavy curtailment. While the RAES system is in standby operation, thermal losses are incurred in the TES, shown by the slight sloping line during day 1. After idling for nearly a day, the RAES system discharges continuously over several hours. The WEC output remains low and the RAES idles for the rest of the period except for a short charge and discharge cycle.

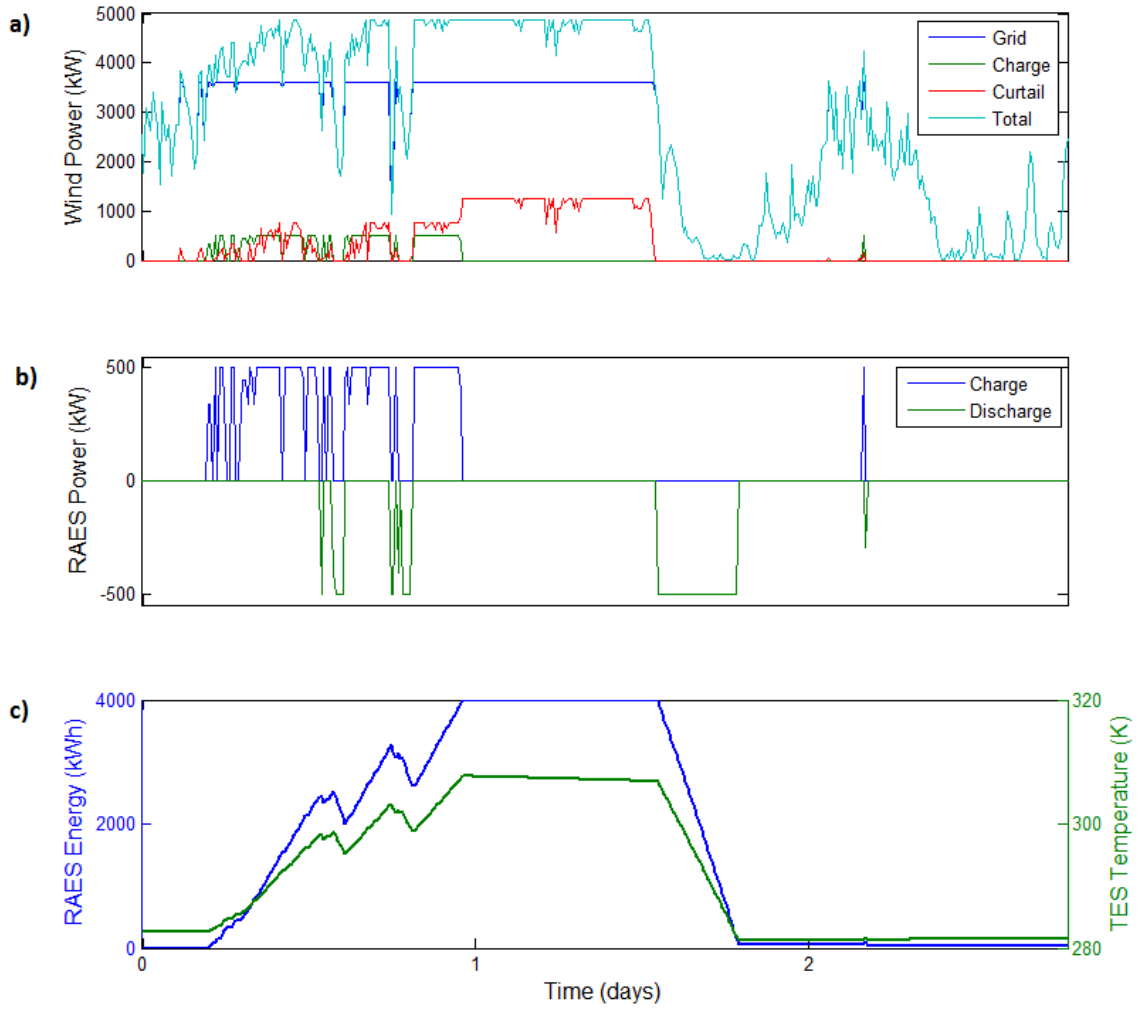

Figure 30 **Simulation period for a 0.5 MW, 4 MWh system showing a) WEC output, b) RAES power, c) RAES energy and temperature when waste heat is not available**

Figure 31 shows a similar operational plot, but during this period waste heat is available from the CHP plant. Since the steam supply is continuous, it does not directly heat the TES but it heats water from the TES directly prior to expansion during discharge operation. The temperature of the water used during discharge is represented by the dotted green line, and appears constant at the maximum TES temperature because it receives continuous heat from the steam source. Since continually heating the TES to its maximum temperature it not practical, the TES temperature (solid green line) fluctuates with charging and discharging.

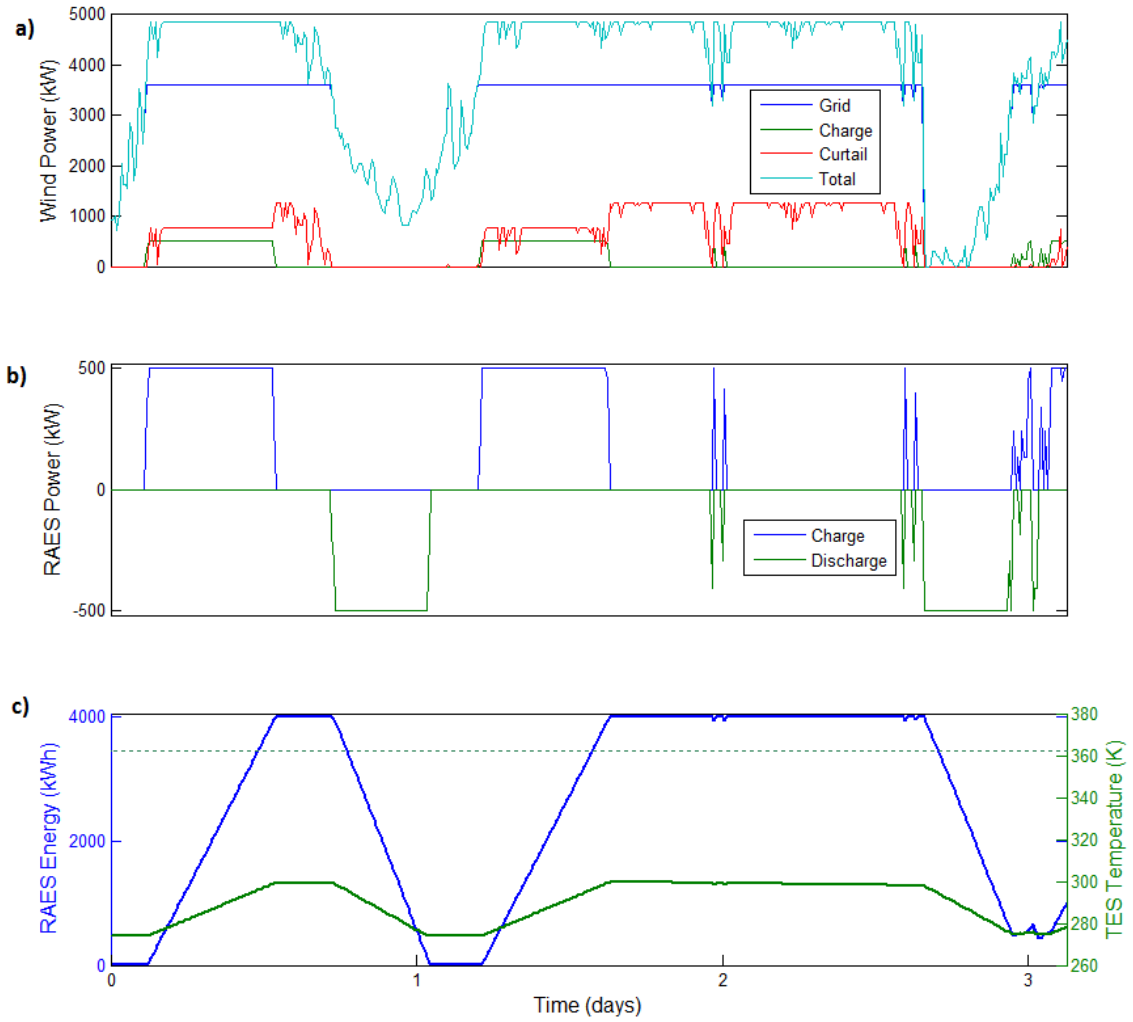

Figure 31 **Simulation period for a 0.5 MW, 4 MWh system showing a) WEC output, b) RAES power, c) RAES energy and temperature when waste heat is available**

In this period, the high sustained wind speeds lead to a more consistent RAES operational profile. As expected, the RAES charges when there is sufficient WEC output, and discharges when the WEC output drops well below the MAL. Observant readers will note that the time required for a full discharge cycle in Figure 31 (end of day 0) lasts slightly longer than in Figure 30 (end of day 1) due to an increased discharge efficiency resulting from the high temperature of the TES.

5.4.2 WEC Production and Curtailment

The following analysis shows how much of the WEC production is fed into the grid and how much is required to be curtailed for a system without energy storage. This provides a

basic understanding of the storage requirements for increasing the installed WEC capacity beyond the MAL. Table 14 shows the results of the annual WEC production and necessary curtailment without any form of ESS for 4.86 MW of installed WEC. It also shows the WEC production from a system that conforms to the 3.6 MW capacity limit. The 3.6 MW WEC results assume that a 3.6 MW WEC configuration with an identical power curve is possible (WEC output is scaled linearly).

Table 14 Results of WEC production and curtailment

Case		Energy (MWh)	Revenue	Percentage of Total (%)
4.86 MW WEC	Total WEC Production	17026	$2,230,406	100.0
	WEC Curtailment	1966	($257,546)	11.6
	Total WEC export	15060	$1,972,860	88.4
3.6 MW WEC	Total WEC Production	12611	$1,652,041	74.1

The required curtailment rate when the WEC is operating at nameplate capacity is nearly 26 %. However, Table 14 shows that cumulatively throughout the year, only 11.6 % of the WEC production is curtailed, resulting in a loss of revenue of over $250,000. However, the additional WEC capacity over the MAL limit results in over $300,000 of additional revenue annually from electricity sales, even before a RAES system is considered. Figure 32 shows how the WEC production and curtailment varies by month throughout the year for a 4.8 MW WEC system.

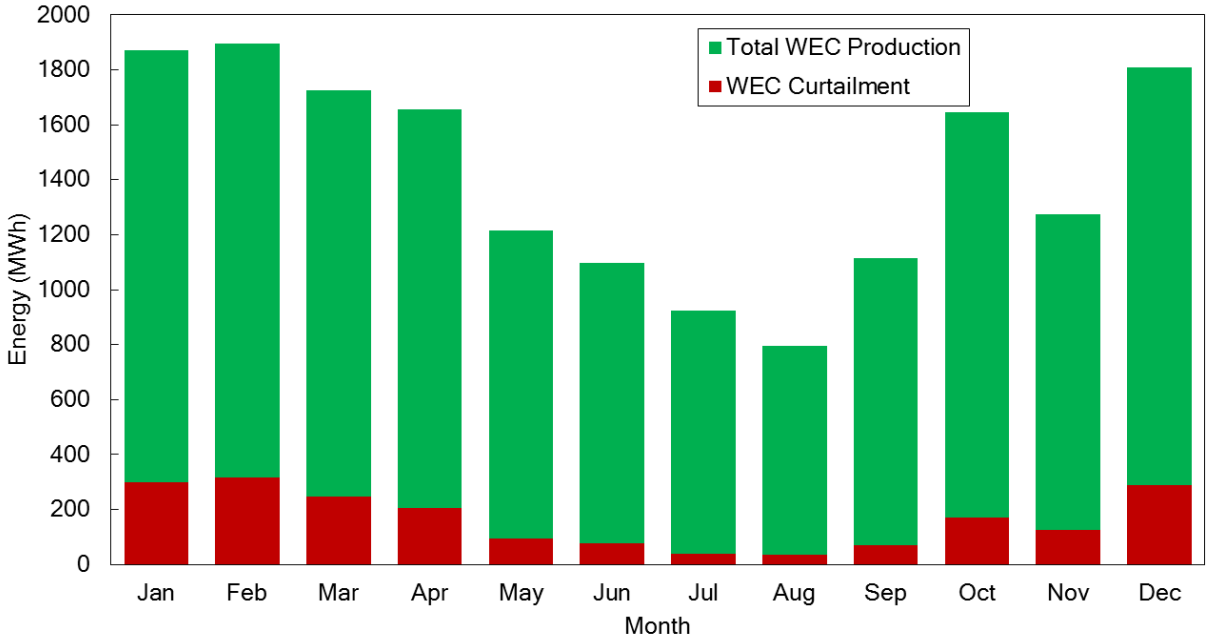

Figure 32 WEC production and curtailment by month for 4.8 MW of installed WEC

WEC production decreases during the summer months and increases during the winter months, which is representative of seasonal wind speed variation in NS. Figure 32 shows that WEC curtailment follows a similar trend, but the lower wind speeds in the summer also result in a significantly lower amount of curtailment relative to WEC production. This is important because it means the RAES spends more time in standby operation during the summer. For the purposes of ESS design, it is also useful to understand how much energy is curtailed during individual periods of curtailment. A period of curtailment is the duration between when the WEC begins and ends curtailing its output. The amount of energy curtailed during this period is defined as the curtailment event energy. Figure 33 shows the total curtailment throughout the year for varying curtailment event energy levels (teal bars), and also the cumulative curtailment for each energy level, including the energy curtailed in lower energy levels (blue bars). For example, the first teal and first blue bars are equal, and the first two teal bars add up to the second blue bar. The values above the bars represent the number of occurrences for each energy level.

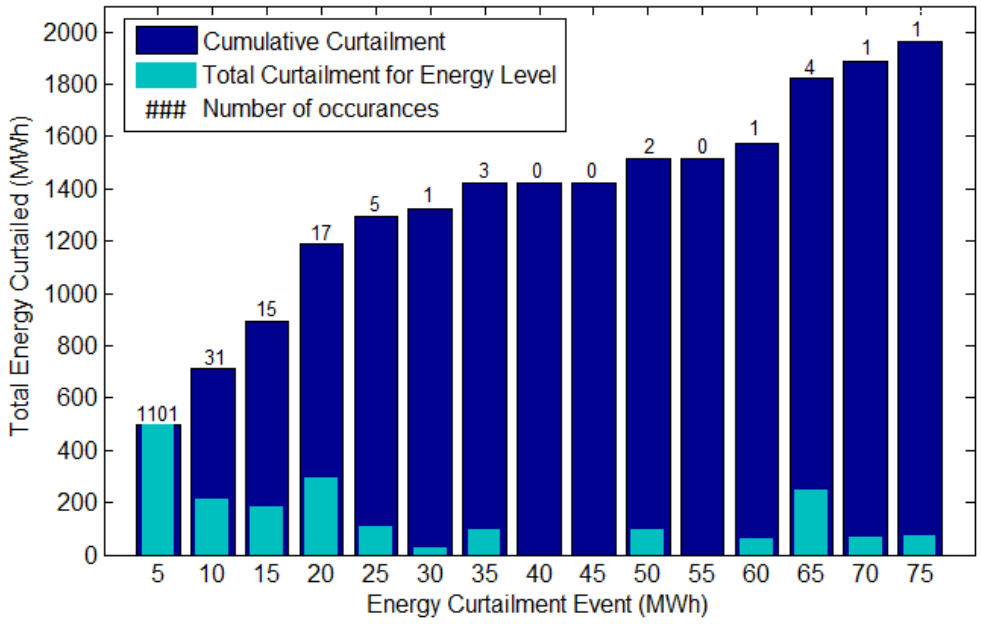

Figure 33 **Cumulative and total curtailment and number of occurrences for varying curtailment event energy levels**

Events in which 5 MWh or less is curtailed accumulate to the most energy throughout the year for any single energy level because they occur so frequently (on average only 0.45 MWh is stored during these events). The longest period of curtailment results in the loss of nearly 75 MWh and only occurs once (hence the ordinate value). Of the energy that requires curtailment, 25% occurs in events requiring 5 MWh or less, and 60% occurs in events requiring 20 MWh or less (as shown in the blue cumulative curtailment bars). The slope of cumulative curtailment bars is steep until the 20 MWh of energy event, and begins to flatten out for higher energy levels. This means the most practical curtailment avoidance can made in the 0 to 20 MWh, since curtailment events above this level are infrequent. The utility of varying ESS energy capacities can be evaluated using Figure 33. However, the following limitations should be noted: it does not consider the power capability of a RAES system (the curtailment rate will occasionally fall outside the power bandwidth of a RAES system), and it does not show that portions of the larger curtailment events can be captured using a smaller capacity system (for example the first 5 MWh of a 70 MWh curtailment event can be captured with a 5 MWh RAES capacity). In order to fully prevent curtailment, 75 MWh of storage is required. A 75 MWh ESS would be very costly and would operate at a low SOC and utilization for most of the year

(it only once fully cycles to SOC = 1). Such a large system is not practical for this particular application. As such, in the following optimization analysis, the maximum energy capacity considered is 20 MWh, which will require some curtailment. The results address the limitations and considerations of this type of curtailment analysis by analyzing the operation of varying sizes of RAES system.

5.4.3 System Optimization

Multiple year-long simulations were performed in a parametric sweep to determine what combination of installed RAES power and energy capacity most effectively minimizes curtailment. Figure 34 shows the results of these simulations on a contour plot that represents the amount of curtailed energy (in MWh) that is avoided for varying RAES system sizes. The reader should note that avoided curtailment represents only the energy that is used to charge the RAES, not the total RAES energy throughput (due to round-trip efficiency).

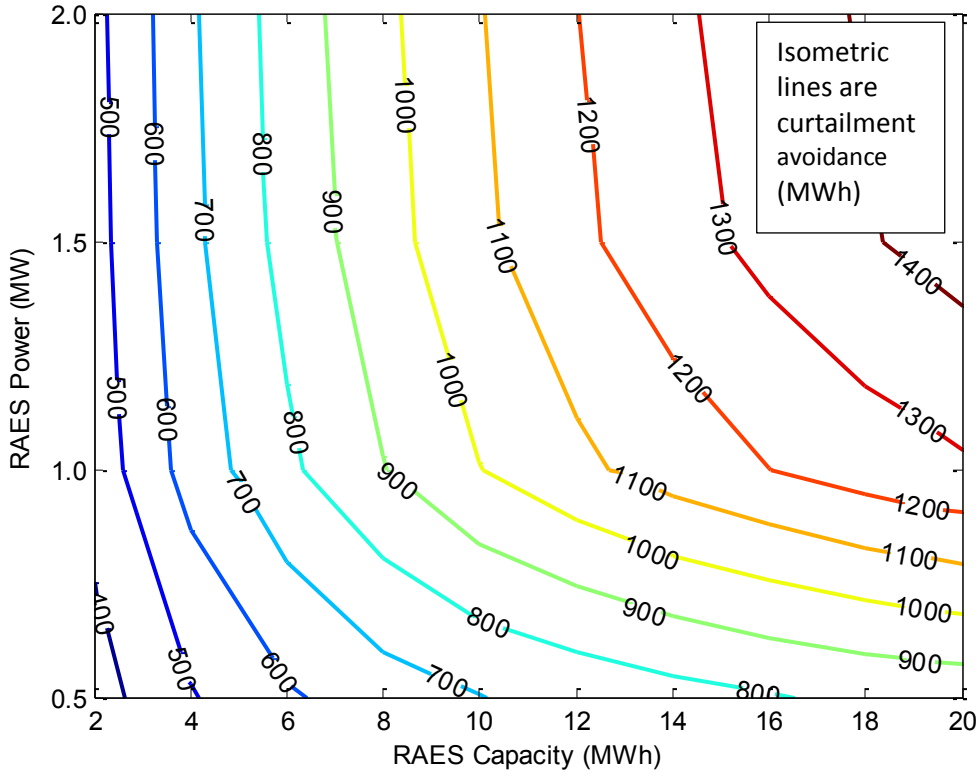

Figure 34 Avoided curtailment (MWh) as a function of RAES power and capacity

The amount of WEC output curtailed in the baseline case described in Table 14 is 1966 MWh. The smallest system simulated (0.5 MW, 2 MWh) stores 400 MWh annually, meaning over 1500 MWh is still curtailed. The largest system (2 MW, 20 MWh) stores approximately 1500 MWh, meaning nearly 500 MWh is curtailed. For RAES capacities below 4 MWh, increasing power above 0.5 MW does not significantly improve curtailment avoidance. This is because curtailment events are long enough that the system can reach a full SOC even if $P_{\mathrm{WEC,\,curt}}$ is greater than $P_{\mathrm{RAES,max}}$, and similarly, the time between curtailment events is long enough that the system can fully discharge at lower RAES power rates. For the same reason, power capabilities above 1 MW for capacities 6 – 12 MWh and above 1.5 MW for capacities 12 – 20 MWh do not significantly decrease curtailment. The biggest gains in avoiding curtailment are made through adding energy capacity up to 8 MWh, and increasing RAES power between 0.5 and 1.0 MW.

While Figure 34 is useful for evaluating the effect RAES has on WEC curtailment, it does not portray the actual energy output of the RAES system. The round-trip efficiency of the RAES system results in losses. The value of the additional saleable energy enabled by RAES is based on the energy it discharges and the tariff for electricity ($131/MWh in this case). Figure 35 shows the additional revenue in dollars that RAES generates for varying system sizes.

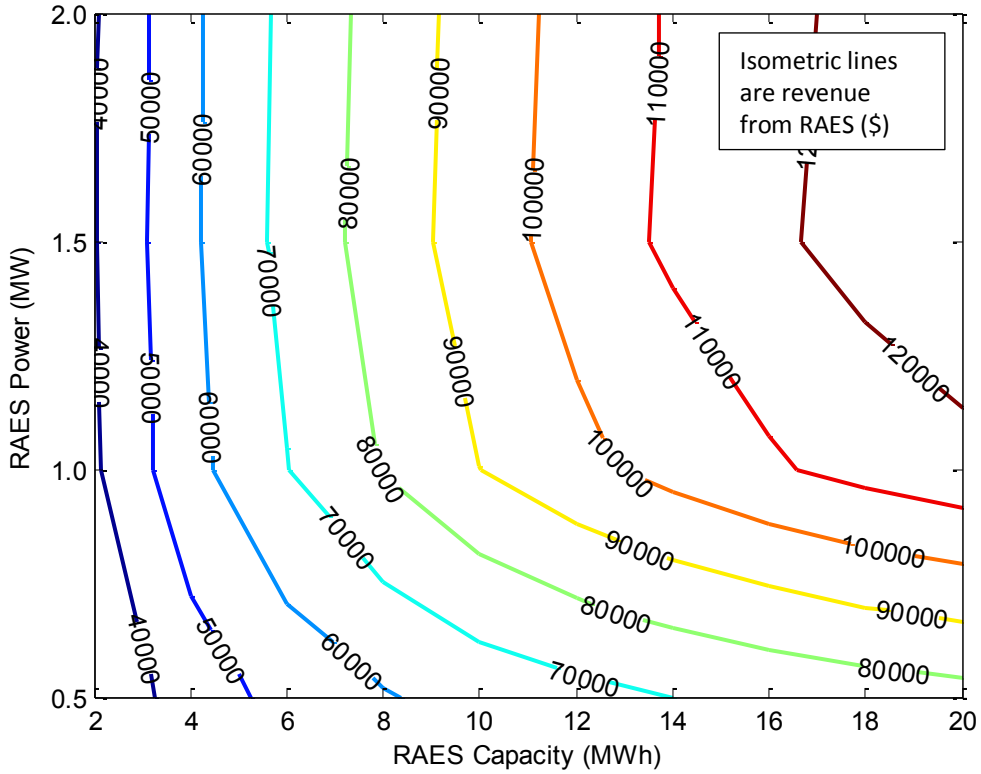

Figure 35 **Revenue generated ($) by RAES systems of varying power and energy capacities**

Using RAES to avoid curtailment enhances revenue by tens of thousands of dollars annually. For example, a 0.5 MW, 8 MWh system yields $60,000 annually, but such a system would cost $2,600,000 based on the assumed costs in Table 13. The simple payback on the RAES system is over 43 years. However, in order to fully appreciate the value of RAES, one must also consider the additional WEC revenue that RAES enables by extending the allowable installed WEC capacity. The benefits of adding power and energy capabilities to a RAES system can be intuitively evaluated by examining how the simple payback period of the RAES system changes. Figure 36 shows the simple payback period of RAES and the 1.2 MW of additional installed WEC capacity (4.8 MW – MAL = 1.2 MW). It is calculated as the ratio of the summed costs and annual revenues of RAES and the additional 1.2 MW of installed WEC. The additional WEC revenue is based on the difference between revenues shown in Table 14.

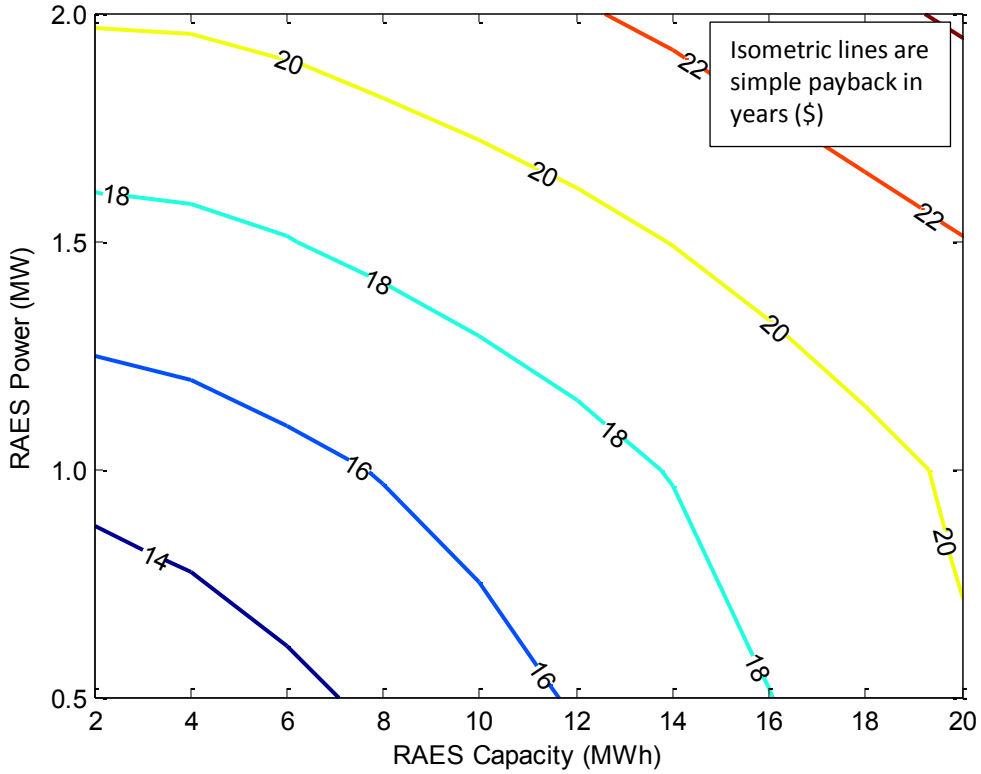

Figure 36 **Simple payback period (years) of RAES and additional installed WEC capacity**

Figure 36 shows that there are economic disadvantages in increasing the scale of both power and energy of a RAES system because of the assumed fixed capital cost rates. With economy of scale considered in the capital cost of RAES, the simple payback will shorten, but such scaling for pricing is unknown. While a significant amount of WEC electricity will require curtailment, developers will tend towards smaller RAES systems, such as a 0.5 MW, 4 MWh configuration, which has a 13 year simple payback period. This is because at its present capital cost, most of the value that RAES provides is not in the extra electricity it cycles, but in its enablement of 1.2 MW of additional installed WEC capacity (which generates over $320,000 worth of electricity annually).

Assuming the same operational life of 20 years, a 0.5 MW, 4 MWh system will continue to lower WEC curtailment for 7 years after the payback period has ended. During this period the RAES will generate an additional $315,000 on its own, but also enables $2,250,000 of additional revenue from the extended installed WEC capacity. The capital

cost is assumed to be $1,800,000 for the RAES system, and $2,730,000 for the additional WEC capacity. The return of the extended WEC capacity and the RAES system over the 20 year lifetime is approximately 57%.

A limitation of these results is that in this analysis RAES is only providing a single service (curtailment mitigation), while a RAES system offering other ancillary services could add revenue streams. The ability of a RAES system to perform other services in this scenario depends on how much time it is fully dispatchable (in standby operation) or partially dispatchable (at reduced power), and not needed for curtailment avoidance. Figure 37 shows a probability plot of the SOC of a 0.5 MW RAES system that has 4 MWh of storage.

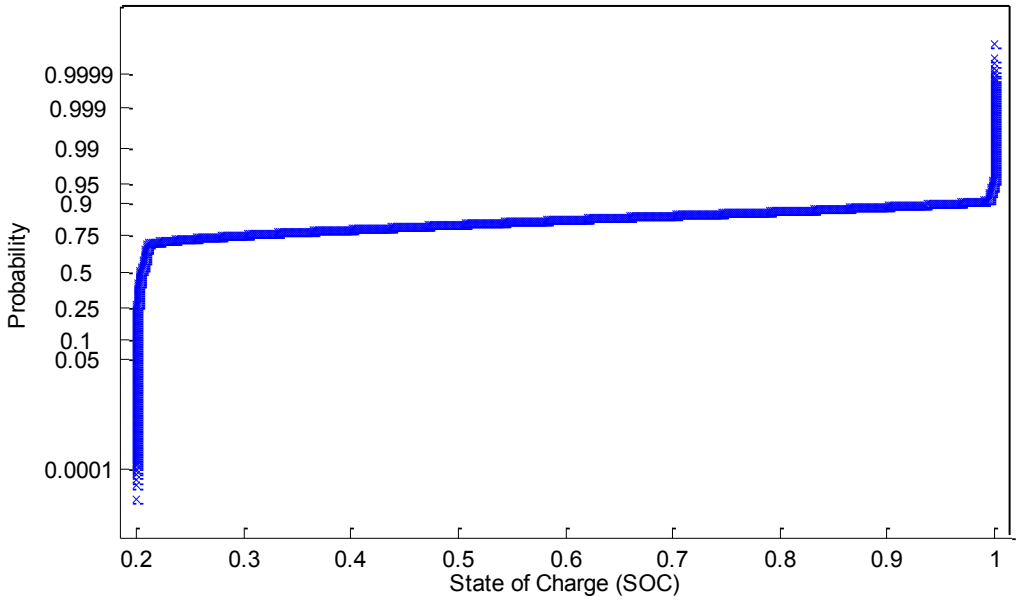

Figure 37 Probability plot for the SOC of a 0.5 MW, 4 MWh RAES system

For nearly 75% of the year, the RAES is fully discharged at SOC = 20% and thus fully dispatchable. The RAES is operating between SOC = 20% and SOC = 100% for 10% of the year, and at SOC = 100% for the remaining 15% of the year. This means there is ample availability for the system to perform other valuable ancillary services. The modeling and analysis of a RAES system capable of multiple ESS services is beyond the scope of this research.

5.4.4 Waste Heat Recovery Effectiveness

In this case study, it was assumed the RAES system used WHR of the CHP plant steam for the 6 months of the year that it was available. This section shows how effective WHR was to mitigate thermal losses in the TES, and boost RAES discharge efficiency. Because it has already been established that smaller RAES systems are more economically feasible in this application, the WHR effectiveness is analyzed for a 0.5 MW, 4 MWh RAES configuration. Table 15 shows the effect WHR has on RAES efficiency, energy output, and the additional revenue that it generates for availabilities of 6 months and a hypothetical 12 months, compared to a system without WHR.

Table 15 Effects of WHR for a 0.5 MW, 4 MWh RAES system

RAES System	Energy throughput (MWh)	Average discharge efficiency	Average round-trip efficiency	Additional revenue from WHR
No WHR	290.6	73.0%	57.6 %	-
6 months WHR	339.3	87.9 %	69.4 %	$6386
12 months WHR	358.8	92.5 %	73.1 %	$8944

The results in Table 15 suggest that the use of WHR is valuable from an efficiency perspective. Even when steam is only available for 6 months during the winter, it increases the average round-trip efficiency of RAES by Δ = 12 %. The additional 6 months of steam availability in the 12 month case only marginally improves the efficiency. This is because the RAES system is less active in the summer months when WEC production is lower, as seen in Figure 32. The financial benefit of using WHR for this application provides $6000 - $9000 of additional revenue for the 6 and 12 months steam availabilities. This is simply a result of the low capacity factor that the RAES system has – it sits idle for nearly 75% of the year. Were it more active, the efficiency increase that WHR provides would result in higher revenues from RAES because it would increase the energy throughput.

CHAPTER 6 CONCLUSIONS AND RECOMMENDATIONS

This research creates a new modeling methodology for the emergent regenerative air energy storage (RAES) technology, and through various performance analyses it investigates RAES as an enabler to accommodate high penetration rates of renewable energy on electricity grids. RAES is a novel energy storage technology soon to be adopted for grid integration purposes. Several unique characteristics significantly differentiate it from other energy storage systems (ESS) such as: a limited power band, an efficiency that varies with power, state of charge (SOC), and operational mode (charge, discharge, and standby), and the ability to decouple power and energy capacity in system sizing. **The objective to design and build a numerical model and simulation tool to analyze and optimize RAES for varying renewable energy integration scenarios is met.** The model simulates electricity grid systems including loads, generation, and storage. The model uses time series data, user defined constraints, and operational parameters to create year-long simulations of hybrid energy systems. A parametric sweep enables the user to intuitively optimize the size of RAES and renewable energy systems to achieve different goals by examining trends and apex points. The model simulates the operation of each main subsystem of RAES:

- The compressor/expander power module, which has an operable power band and whose efficiency is dependent on SOC and rate of charging or discharging;
- The air storage module, which is the critical determinant of SOC;
- The TES, which affects efficiency of the compressor/expander during discharge, and can be supplemented by waste heat to boost efficiency and prevent thermal heat loss.

The model was applied to two case studies: a remote community in Northern Canada powered by diesel generators (DG), and a capacity constrained distribution grid. The results from these case studies are valid for a range of economic and technical scenarios. RAES may be applied to a remote community for diesel fuel reductions of hundreds of liters (and cost) by storing wind energy converter (WEC) electricity that is otherwise curtailed, and/or by increasing the DG operating efficiency using cycle charging. For

such northern communities, low WEC penetration rates render RAES ineffective and uneconomical because the storage is rarely utilized. Using assumed cost values, a remote community employing only DG will achieve the shortest simple payback of 6 years by installing WEC up to a penetration rate of 75% and a 0.5 MW, 1 MWh RAES system. It should be recognized that any further installation of WEC+RAES will increase payback period because its capital expense will be larger than WEC alone (on both a per kW and per kWh basis), but that this comes with significant advantages of reduced environmental impact from the further reduction in diesel fuel consumption.

RAES may be deployed to conventional distribution grids in order to extend the allowable installed WEC capacity by buffering WEC output. In this case, RAES is not economical in its prevention of WEC curtailment alone, but by enabling a higher installed WEC capacity, which results in more WEC output during times when the RAES is not required. The biggest gains from a RAES system are made by minimizing capital costs on the power module, and sizing the energy modules to accommodate roughly 30 % of the WEC output that requires curtailment. A 0.5 MW, 4 MWh RAES system generates $45,000 of additional revenue annually, but by allowing an additional 1.2 MW of installed WEC, another $300,000 is attainable each year. The RAES system is only required for curtailment avoidance for 25% of the year. The remainder of the year it can be made available for performing other ancillary services for the grid to improve its economic benefits.

One of the most unique features of RAES is its ability to use low grade waste heat to boost efficiency during discharge. In both cases analyzed, the use of waste heat improved the average round-trip efficiency of RAES from 60% to approximately 70%. This finding encourages future developers of RAES technology to leverage the energy in “waste” heat whenever and wherever it is available.

The model developed for this research has limitations. Foremost is the fact that the control strategies for RAES are limited to perform the single ESS service of WEC curtailment avoidance in the conventional grid case study, as well as cycle charging in

the microgrid case study. In order to perform multiple services, such as ramp-rate compensation, peak shaving, and energy arbitrage, a predictive control strategy is required. It is recommended that future embodiments of this model incorporate weather forecasting in order to be able to dispatch the ESS to perform multiple value-added ESS services. Another limitation is the several assumptions made with regards to RAES operational parameters and costs. As the technology matures, higher fidelity assumptions of RAES (*e.g.* efficiency variation as a function of SOC, power, temperature, cost economy of scale) can be included in the model. Similarly, assumptions regarding the use of RAES with DG (*e.g.* true efficiency map; start-up time efficiency; minimum run-time, etc.) may be advanced. Such advancements would enable confident high-resolution system performance assessment to study dynamic effects of the RAES and evaluate opportunities to further increase the penetration rate of renewable energy. Finally, the case studies presented herein are meant only to demonstrate the functionality of the model. The results should not be interpreted as universally applicable to ESS sizing. All applications of ESS for RE integration require site specific considerations and data collection to accurately model and optimize the system.

BIBLIOGRAPHY

[1] J. DeCesaro, K. Porter and M. Milligan. Wind Energy and Power System Operations: A Review of Wind Integration Studies to Date. The Electricity Journal (22), pp. 34-43. 2009.

[2] F. Díaz-González, A. Sumper, O. Gomis-Bellmunt and R. Villafáfila-Robles. A review of energy storage technologies for wind power applications. Renewable and Sustainable Energy Reviews 16(4), pp. 2154-2171. 2012.

[3] G. Brinkman, D. Lew, P. Denholm. Impacts of renewable generation on fossil fuel unit cycling: Costs and emissions. NREL, Tech. Rep. PR6A2055828. May 20, 2012.

[4] A. Cavallo. Controllable and affordable utility-scale electricity from intermittent wind resources and compressed air energy storage (CAES). Energy 32(2), pp. 120-127. 2007.

[5] J. E. Mason and C. L. Archer. Baseload electricity from wind via compressed air energy storage (CAES). Renewable and Sustainable Energy Reviews 16(2), pp. 1099-1109. 2012.

[6] M. Hessami and D. R. Bowly. Economic feasibility and optimisation of an energy storage system for Portland Wind Farm (Victoria, Australia). Appl. Energy 88(8), pp. 2755-63. 2011.

[7] D. A. Fong, S. E. Crane, E. P. Berlin, A. P. Abkenar, K. Mahalaktar, Y. Hou and T. Bowers, "Compressed Air Energy Storage System Utilizing Two-Phase Flow To Facilitate Heat Exchange," US 8196395 B2, June 12, 2012.

[8] A. Evans, V. Strezov and T. J. Evans. Assessment of utility energy storage options for increased renewable energy penetration. Renewable and Sustainable Energy Reviews 16(6), pp. 4141-4147. 2012.

[9] S. Koohi-Kamali, V. V. Tyagi, N. A. Rahim, N. L. Panwar and H. Mokhlis. Emergence of energy storage technologies as the solution for reliable operation of smart power systems: A review. Renewable and Sustainable Energy Reviews 25, pp. 135-165. 2013.

[10] T. U. Daim, X. Li, J. Kim and S. Simms. Evaluation of energy storage technologies for integration with renewable electricity: Quantifying expert opinions. Environmental Innovation and Societal Transitions 3, pp. 29-49. 2012.

[11] J. K. Kaldellis, D. Zafirakis and K. Kavadias. Techno-economic comparison of energy storage systems for island autonomous electrical networks. Renewable and Sustainable Energy Reviews 13(2), pp. 378-392. 2009.

[12] C. Rae and F. Bradley. Energy autonomy in sustainable communities—A review of key issues. Renewable and Sustainable Energy Reviews 16(9), pp. 6497-6506. 2012.

[13] S. Manchester, L. Swan and D. Groulx, "Compressed air energy storage for in-stream tidal generation on a limited capacity electricity grid," at European Wave and Tidal Energy Conference 2013, Aalborg, DK, 8 p. 2013.

[14] O. Erdinc and M. Uzunoglu. Optimum design of hybrid renewable energy systems: Overview of different approaches. Renewable and Sustainable Energy Reviews 16(3), pp. 1412-1425. 2012.

[15] S. Sinha and S. S. Chandel. Review of software tools for hybrid renewable energy systems. Renewable and Sustainable Energy Reviews 32, pp. 192-205. 2014.

[16] W. Zhou, C. Lou, Z. Li, L. Lu and H. Yang. Current status of research on optimum sizing of stand-alone hybrid solar–wind power generation systems. Appl. Energy 87(2), pp. 380-389. 2010.

[17] T. M. Weis, A. Ilinca and J. Pinard. Stakeholders' perspectives on barriers to remote wind–diesel power plants in Canada. Energy Policy 36(5), pp. 1611-1621. 2008.

[18] Natural Resources Canada. Status of remote/off-grid communities in Canada. Technical Report. Government of Canada, Ottawa, 2011.

[19] Qulliq Energy Corporation. "Electricity rate schedules" Nunavut, Canada, 2011.

[20] Caterpillar. "Diesel Generator Set Continuous 1010 ekW Datasheet", USA, 2011.

[21] Caterpillar. "Diesel Generator Set Continuous 2500 ekW Datasheet", USA, 2011.

[22] Cummins. "DFD 900 Prime Generator Set Datasheet", USA, 2008.

[23] C. Dennis Barley and C. Byron Winn. Optimal dispatch strategy in remote hybrid power systems. Solar Energy 58(4–6), pp. 165-179. 1996.

[24] B. Sedaghat, A. Jalilvand and R. Noroozian. Design of a multilevel control strategy for integration of stand-alone wind/diesel system. International Journal of Electrical Power & Energy Systems 35(1), pp. 123-137. 2012.

[25] A. M. Howlader, Y. Izumi, A. Uehara, N. Urasaki, T. Senjyu, A. Yona and A. Y. Saber. A minimal order observer based frequency control strategy for an integrated wind-battery-diesel power system. Energy 46(1), pp. 168-178. 2012.

[26] L. Leclercq, B. Robyns and J. Grave. Control based on fuzzy logic of a flywheel energy storage system associated with wind and diesel generators. Math. Comput. Simul. 63(3–5), pp. 271-280. 2003.

[27] P. Sivakumar, S. Thirukkovai, K. Yogeshraj and A. Abdullah. Reactive power regulation of wind-diesel hybrid system. Procedia Engineering 38, pp. 3152-3165. 2012.

[28] S. Vachirasricirikul, I. Ngamroo and S. Kaitwanidvilai. Coordinated SVC and AVR for robust voltage control in a hybrid wind-diesel system. Energy Conversion and Management 51(12), pp. 2383-2393. 2010.

[29] R. Sebastián and R. P. Alzola. Effective active power control of a high penetration wind diesel system with a Ni–Cd battery energy storage. Renewable Energy 35(5), pp. 952-965. 2010.

[30] A. J. Bowen, M. Cowie and N. Zakay. The performance of a remote wind–diesel power system. Renewable Energy 22(4), pp. 429-445. 2001.

[31] C. Ziogou, D. Ipsakis, C. Elmasides, F. Stergiopoulos, S. Papadopoulou, P. Seferlis and S. Voutetakis. Automation infrastructure and operation control strategy in a stand-alone power system based on renewable energy sources. J. Power Sources 196(22), pp. 9488-9499. 2011.

[32] H. Ibrahim, R. Younès, A. Ilinca, D. Ramdenee, M. Dimitrova, J. Perron, M. Adegnon, D. Boulay and C. Arbez. Potential of a hybrid wind-diesel-compressed air system for nordic remote canadian areas. Energy Procedia 6, pp. 795-804. 2011.

[33] J. K. Kaldellis and D. Zafirakis. The wind energy (r)evolution: A short review of a long history. Renewable Energy 36(7), pp. 1887-1901. 2011.

[34] T. Boustika and S. Sansoto. “Sizing an energy storage system to minimize windpower imbalances from the hourly average” at Power & Energy Society General Meeting 2012. IEEE, 2012.

[35] M. Korpaas, A. T. Holen and R. Hildrum. Operation and sizing of energy storage for wind power plants in a market system. International Journal of Electrical Power & Energy Systems 25(8), pp. 599-606. 2003.

[36] S. Gill, G. W. Ault and I. Kockar. “The optimal operation of energy storage in a wind power curtailment scheme” at IEEE Power and Energy Society General Meeting 2012. San Diego, CA, 22 - 26 July 2012.

[37] Apex CAES. CAES Overview. Available: http://www.apexcaes.com/caes. Accessed Feb 26, 2014.

[38] M. Raju and S. Kumar Khaitan. Modeling and simulation of compressed air storage in caverns: A case study of the Huntorf plant. Appl. Energy 89(1), pp. 474-481. 2012.

[39] N. Hartmann, O. Vöhringer, C. Kruck and L. Eltrop. Simulation and analysis of different adiabatic compressed air energy storage plant configurations. Appl. Energy 93, pp. 541-548. 2012.

[40] EPRI-DOE. Handbook of energy storage for transmission and distribution applications. Tech. Rep. 1001834. EPRI, Palo Alto, CA. 2003.

[41] B. Elmegaard and W. Brix. "Efficiency of compressed air energy storage" at International Conference on Efficiency, Cost, Optimization, Simulation and Environmental Impact of Energy Systems. Novi Sad, Serbia, 2011.

[42] EPRI-DOE. Handbook supplement of energy storage for grid connected wind generation applications. Tech. Rep. 1008703. EPRI, Palo Alto, CA, 2004.

[43] B. Mauch, P. M. S. Carvalho and J. Apt. Can a wind farm with CAES survive in the day-ahead market? Energy Policy 48, pp. 584-593. 2012.

[44] J. B. Greenblatt, S. Succar, D. C. Denkenberger, R. H. Williams and R. H. Socolow. Baseload wind energy: Modeling the competition between gas turbines and compressed air energy storage for supplemental generation. Energy Policy 35(3), pp. 1474-1492. 2007.

[45] E. Fertig and J. Apt. Economics of compressed air energy storage to integrate wind power: A case study in ERCOT. Energy Policy 39(5), pp. 2330-2342. 2011.

[46] R. Madlener and J. Latz. Economics of centralized and decentralized compressed air energy storage for enhanced grid integration of wind power. Appl. Energy 101, pp. 299-309. 2013.

[47] H. Safaei, D. W. Keith and R. J. Hugo. Compressed air energy storage (CAES) with compressors distributed at heat loads to enable waste heat utilization. Appl. Energy 103, pp. 165-179. 2013.

[48] S. Manchester and L. Swan. Compressed air storage and wind energy for time-of-day electricity markets. Procedia Computer Science 19(0), pp. 720-727. 2013.

[49] R. Loisel, A. Mercier, C. Gatzen and N. Elms. Market evaluation of hybrid wind-storage power systems in case of balancing responsibilities. Renewable and Sustainable Energy Reviews 15(9), pp. 5003-5012. 2011.

[50] H. Chen, X. Zhang, J. Liu and C. Tan. Compressed air energy storage. *Energy Storage - Technologies and Applications*. A.F. Zobaa, Ed. InTech, Croatia, 2013.

[51] C. Bullough, C. Gatzen, C. Jakiel, M. Koller, A. Nowi and S. Zunft. "Advanced adiabatic compressed air energy storage for the integration of wind energy" at Proceedings of the European Wind Energy Conference. London, UK, 2004.

[52] M. W. Coney, P. Stephenson, A. Malmgren, C. Linnemann and R. E. Morgan. “Development of a reciprocating compressor using water injection to achieve quasi-isothermal compression” at International Compressor Engineering Conference. Indiana, USA, 2002.

[53] E. Vaz. “Storage-Enabled Microgrids: from Remote Communities to Smart Grids”, at the Renewable Energy Conference, Halifax, NS, 2013.

[54] Nova Scotia Power. Open access same-time information (OASIS) - transmission hourly total net Nova Scotia load. Halifax, 2011.

[55] NERC. "2012 Special Assessment: Interconnection requirements for variable generation", NERC, Atlanta, USA, 2012.

[56] Nova Scotia Power. IR#459 preliminary assessment. Halifax, NS, 2013.

[57] C. Song. *Chemistry of Diesel Fuels* CRC Press, 2000. Boca Raton, USA.

[58] J. A. M. Bleijs, C. J. E. Nightingale and D. G. Infield. Wear implications of intermittent diesel operation in wind/diesel systems. Wind Engineering, vol. 17, pp. 206, 1993.

[59] H. G. Beyer and T. Degner. Assessing the maximum fuel savings obtainable in simple wind-diesel systems. Solar Energy 61(1), pp. 5-10. 1997.

[60] L. Mike. "Generator Capacity Forum Discussion" Retrieved from http://caterpillar.lithium.com/t5/Power-Generation-Site-Design/Generator-Capacity, Aug. 14, 2012.

[61] S. L. Liu, W. Chen, Z. Cai and C. Zheng. "Study on the application of high temperature heat pump to recover waste heat of marine diesel engine" at International Conference on Energy and Environment Technology, Guilin, 2009.

[62] A. Fetters. "Diesel efficiency overview" at Alaska Rural Energy Conference, Juneau, USA, 2011.

[63] D. G. Swan, Eon Wind Inc. "Liverpool Project" E-mail communication, Jan 2, 2014.

[64] GE. 1.6 - 82.5 Data Sheet. Technical Report, GEA18755B. General Electric, USA, 2012.

[65] Windmatic. Windmatic 65 Power Curve. Idaho National Laboratory. Retrieved from www.inl.gov/wind/software/powercurves/pc_windmatic.xls, May 9, 2013.

[66] Enercon. Wind energy converters product overview. Enercon. Aurich, DE, 2010.

[67] A. M. Graves, K. Harman, M. Wilkinson and R. Walker. "Understanding availability trends of operating wind farms" in AWEA WINDPOWER Conference, Houston, TX, 2008.

[68] D. Fong, LightSail Energy. "Waste heat recovery" Personal Communications, May 10, 2013 & September 20, 2013.

[69] M. Oprisan. "Introduction of hydrogen technologies to ramea island" in IEA Wind – KWEA Joint Workshop on Wind Energy, Jeju-Do, Korea, 2007.

[70] RETScreen International. "Ramea island case study". RETScreen. Canada, 2009.

[71] T. Iqbal. "Feasibility study of pumped hydro energy storage for Ramea wind-diesel hybrid power system" Memorial University, St. John's, 2009.

[72] T. M. Weis and A. Ilinca. The utility of energy storage to improve the economics of wind–diesel power plants in Canada. Renewable Energy 33(7), pp. 1544-1557. 2008.

[73] Natural Resources Canada. Monthly Average Wholesale (Rack) Prices for Diesel in 2014 - Canada. Available: http://www2.nrcan.gc.ca/eneene/sources/pripri Accessed March 8, 2014.

[74] BC Ministry of Finance. How the Carbon Tax Works. Available: www.fin.gov.bc.ca/tbs/tp/climate/carbon_tax.htm Accessed March 10, 2014.

[75] NS Department of Energy. "Community feed-in tariff program facts" DOE, Halifax, NS, 2011.

[76] PWC. "Advanced energy deployment group project plan" Report. Halifax, NS, 2014.

APPENDIX A MATLAB Code for Microgrid Case Study

Main Code

```
% RAES for Wind / Diesel Hybrid Systems
% Sebastian Manchester (sebmanchester@gmail.com)
% Copyright 2014 as part of the Renewable Energy Storage Lab
% Please direct inquiries to Dr. Lukas Swan

clc, clear;
tic;
%% Inputs
% In this section you must define input data sets that describe the
community
% load, wind resource, and temperature. They should be equivalent in
time step and overall
% length.
data1 = load('-mat','Ramea_15_min');
vars = fieldnames(data1);
for i = 1:length(vars)
    assignin('base', vars{i}, data1.(vars{i}));
end

data3 = load('-mat','Ramea_temp_15min');
vars = fieldnames(data3);
for i = 1:length(vars)
    assignin('base', vars{i}, data3.(vars{i}));
end

Load = Load_15min;          %assign variable names
wind = Wind_15min;
x = size(Load,1);           %checks number of time steps
T_amb = Temp_15min(1:x,1);
dt = 0.25;                  %time step (hrs)
%% Operating Parameters

%Diesel generator
maxload = max(Load);
P_d_max = 925;                  %rated power (kW) NEW
P_d_eff = 0.21*P_d_max;         %point where cycle charging benefit ends
(0 = no cycle charging)
cycleP = 500;
%Choose cycle charging control strategy
cycle = 1; %1 (cycle charges to P_d_eff) or 2 (cycle charges @ maxP)
%Choose how long diesel should run for if turned on for cycle charging
runTime = 1; %hrs
startup  =  P_d_max*(1/60)/CAT_1010(P_d_max,P_d_max);  %Startup  costs  (2
min of full load operation)
fuel_startup = 0; %initiate counter at 0
diesel_price = 1.5; % ($)

%RAES system
maxcap = 10; %MWh
cap                                                                    =
[0.0000000000001;0.1;0.2;0.3;0.4;0.5;0.6;0.7;0.8;0.9;1]*maxcap*1000;
```

```
I = size(cap,1);
maxP = 500;                          %rated maximum power (kW)
minP = 250;                          %rated minimum power
eff_chg_b = 0.8;
eff_dschg_b = 0.8;
eff_range_P = [0.67 0.81];             %efficiency range from 0 to 100%
for POWER
eff_range_SOC = [0.75 0.81];           %efficiency range from 0 to 100%
for SOC
eff_chg_P_b = eff_range_P;           %baseline charge eff for maxP
eff_chg_SOC_b = eff_range_SOC;       %baseline charge eff for SOC = 1
eff_dschg_P_b = eff_range_P;         %baseline discharge eff for maxP
eff_dschg_SOC_b = eff_range_SOC;      %baseline discharge eff for SOC =
1
dT = 32.6;                                %(K) temperature rise during
compression

%TES system
HRS = 1;                    %1 = on, 0 = off
HR = 0.5;                   %heat recovery effectiveness
Cp_TES = 4.18;              %heat capacity (kJ/kg/k)
HX = 1 ;                    %heat exchanger efficiency
heatloss = 0.1;             %heat loss rate (kW/K)
maxTemp = 368;              %TES temp limit (normally 348 K)

%WEC
pen = [25; 50; 75; 100; 125; 150; 175; 200; 225; 250; 300]; % (% of max
load)
J = size(pen,1);
maxwind = max(wind);

%System Costs
capcost = 200;        %$/kWh
powcost = 2000;       %$/kW
WECcost = 4500;       %$/kW

%% Operation
% All power values in kW, all energy values in kWh

P_w_exp = zeros(x,I,J);
P_w_chg = zeros(x,I,J);
P_w = zeros(x,J);
P_w_curt = zeros(x,I,J);

E_RAES = zeros(x,I,J);
P_RAES_dschg = zeros(x,I,J);
P_RAES_chg = zeros(x,I,J);
T_exp = zeros(x,I,J)+293;
eff_dschg = zeros(x,I,J);
eff_dschgT = zeros(x,I,J);
eff_chg = zeros(x,I,J);
av_eff_chg = zeros(I,J);
av_eff_dschg = zeros(I,J);
n_chg = zeros(I,J);
n_dschg = zeros(I,J);
mode = zeros(x+1,I,J);
```

```
modeX = 0;
kWh_t_kWh_e = zeros(x,I,J) + 0.9886;

E_TES = zeros(x,I,J);
T_TES = zeros(x,I,J);
T_TES(1,:,:) = 283;
TES_losses  = zeros(x,I,J);

P_d = zeros(x,I,J);
P_d_chg = zeros(x,I,J);
P_d_exp = zeros(x,I,J);
d_eff = zeros(x,I,J);
fuel = zeros(x,I,J);
d_heat = zeros(x,I,J);
startup_count = zeros(I,J);

P_d_b1 = zeros(x,1);
d_eff_b1 = zeros(x,1);
fuel_b1 = zeros(x,1);

P_d_b2 = zeros(x,1);
d_eff_b2 = zeros(x,1);
fuel_b2 = zeros(x,1);
P_w_b2 = zeros(x,1);

t_fuel = zeros(I,J);
av_eff = zeros(I,J);
cost = zeros(I,J);
cost_wwind = zeros(I,J);
f_savings = zeros(I,J);
savings = zeros(I,J);
payback = zeros(I,J);

%% Baseline case 1 - diesel only
for n = 1:x-1

     P_d_b1(n,1) = Load(n);
     d_eff_b1(n,1) = CAT_1010(P_d_b1(n,1), P_d_max);
     fuel_b1(n,1) = P_d_b1(n,1)*dt/d_eff_b1(n,1);
end

%% Baseline case 2 - wind and diesel only
P_w_b2 = wind;
for n = 1:x-1

    P_d_b2(n,1) = Load(n,1) - P_w_b2(n,1);
     if P_d_b2(n,1) < 0
         P_w_b2_curt(n,1) = P_d_b2(n,1);
         P_d_b2(n,1) = 0;
     else
     end
     d_eff_b2(n,1) = CAT_1010(P_d_b2(n,1), P_d_max);
     if P_d_b2(n,1) > 0
        fuel_b2(n,1) = P_d_b2(n,1)*dt/d_eff_b2(n,1);
     else
```

```
        fuel_b2(n,1) = 0;
     end
end

%% Energy storage case
for i = 1:1:I
    RAES_cap = cap(i);
    m_TES = RAES_cap/1000*33000;        %TES mass and heat loss depends
on Capacity
    loss = RAES_cap/1000*heatloss;
    E_TES(1,i,:) = m_TES*Cp_TES*T_TES(1,1,1)/3600;

    for j = 1:1:J
        W_pen = pen(j);
        P_w(:,j) = (pen(j)/100)*wind*(maxload/maxwind);

        for n = 1:x-1

                if P_w(n,j) >= Load(n)
                    P_w_exp(n,i,j)              =              Load(n);
%export wind to meet load
                    curtA = 0;
                    curtB = 0;

                    if P_w(n,j) - P_w_exp(n,i,j) > maxP
                        P_w_chg(n,i,j)              =              maxP;
%charge power limited by max power, so some curtailment is necessary
                        curtA    =    P_w(n,j)    -    P_w_exp(n,i,j)    -
P_w_chg(n,i,j);

                    elseif P_w(n,j) - P_w_exp(n,i,j) > minP
                        P_w_chg(n,i,j)  =  P_w(n,j)  -  P_w_exp(n,i,j);
%harge power is within power band, charge with all remaining wind power

                    else
                        P_w_chg(n,i,j)              =              0;
%remaining wind power is not within sotarge power band, so it must be
curtailed
                        curtA = P_w(n,j) - P_w_exp(n,i,j);

                    end

                    if  E_RAES(n,i,j)  +  P_w_chg(n,i,j)*dt*eff_chg_b  <=
RAES_cap
                        P_RAES_chg(n,i,j)       =       P_w_chg(n,i,j);
%there is remaining storage capacity
                    elseif  (RAES_cap  -  E_RAES(n,i,j))/(dt*eff_chg_b)>=
minP
                        P_RAES_chg(n,i,j)       =       (RAES_cap       -
E_RAES(n,i,j))/(dt*eff_chg_b);        %storage will reach SOC = 1, so
some curtailment is necessary
                        curtB  =  P_w_chg(n,i,j)  -  P_RAES_chg(n,i,j);
%ensure that available capacity can be charged within CAES storage
power band
                        P_w_chg(n,i,j) = P_RAES_chg(n,i,j);
```

```
                    else
                        P_RAES_chg(n,i,j)               =               0;
%storage will reach SOC = 1 but capacity will not work with power band
                        curtB = P_w_chg(n,i,j);
                        P_w_chg(n,i,j) = P_RAES_chg(n,i,j);
                    end

                    P_w_curt(n,i,j)      =      curtA      +      curtB;
%sum of the curtailments from low load and full storage limits

                else % (P_w < Load)

                    P_w_exp(n,i,j)              =              P_w(n,j);
%export all wind

                    %Prevent  rapid  charging  and  discharging  by  using
charge (1) and discharge (2) modes
                    if mode(n,i,j) == 1
                        %Cycle chaging
                        if cycle == 1
                            [         P_d(n,i,j),         P_d_exp(n,i,j),
P_d_chg(n,i,j),         P_RAES_chg(n,i,j)]         =         cycleCharge1(
Load(n),P_w_exp(n,i,j), minP, maxP, P_d_eff  );
                        elseif cycle == 2
                            [         P_d(n,i,j),         P_d_exp(n,i,j),
P_d_chg(n,i,j),         P_RAES_chg(n,i,j)]         =         cycleCharge2(
Load(n),P_w_exp(n,i,j), P_d_eff, cycleP  );
                        else
                        end

                        if  E_RAES(n,i,j)  +  P_d_chg(n,i,j)*dt*eff_chg_b
<= RAES_cap
                            P_RAES_chg(n,i,j)      =      P_d_chg(n,i,j);
%storage has capacity to accomodate cycle charging
                            mode(n+1,i,j) = 1;
                        elseif                  (RAES_cap                -
E_RAES(n,i,j))/(dt*eff_chg_b) >= minP
                            P_d_chg(n,i,j)       =       (RAES_cap       -
E_RAES(n,i,j))/(dt*eff_chg_b);     %ensure SOC = 1 is not exceeded
                            P_RAES_chg(n,i,j) = P_d_chg(n,i,j);
                            P_d(n,i,j)       =       P_d_exp(n,i,j)       +
P_d_chg(n,i,j);
                            mode(n+1,i,j) = 0;
                        else
                            P_d_chg(n,i,j)              =              0;
%SOC = 1, so do not charge
                            P_RAES_chg(n,i,j) = 0;
                            P_d(n,i,j) = P_d_exp(n,i,j);
                            mode(n+1,i,j) = 0;
                        end

                        t_d          =          t_d          +          dt;
%Keep track of how long DG has been on
                        if t_d >= runTime
                            mode(n+1,i,j) = 0;
                        else
```

```
                    end

                elseif      mode(n,i,j)      ==      2      &&
E_RAES(n,i,j)*eff_dschg_b/dt >= Load(n) - P_w_exp(n,i,j)

                    if Load(n) - P_w_exp(n,i,j) >= maxP
                        P_RAES_dschg(n,i,j)         =         maxP;
%discharge at max storage power and meet the remaining load with the
diesel generator
                        P_d(n,i,j)  =  Load(n)  -  P_w_exp(n,i,j)  -
P_RAES_dschg(n,i,j);
                        P_d_exp(n,i,j) = P_d(n,i,j);
                        mode(n+1,i,j) = 2;
                    elseif Load(n) - P_w_exp(n,i,j) >= minP
                        P_RAES_dschg(n,i,j)     =     Load(n)     -
P_w_exp(n,i,j);                         %storage is within power band and
capable of fully supplementing wind,
                        mode(n+1,i,j) = 2;
                    else
                        P_RAES_dschg(n,i,j)          =          0;
%Ignite DIESEL: remaining load is not within storage power band
                        P_d_exp(n,i,j) = Load(n) - P_w_exp(n,i,j);
                        P_d(n,i,j) = P_d_exp(n,i,j);
                        mode(n+1,i,j) = 0;
                    end

                else %Mode = 0
                    t_d = 0;

                    if  E_RAES(n,i,j)*eff_dschg_b/dt  >=  Load(n)  -
P_w_exp(n,i,j)              %there is available energy stored

                        if Load(n) - P_w_exp(n,i,j) >= maxP
                            P_RAES_dschg(n,i,j)       =       maxP;
%discharge at max storage power and meet the remaining load with the
diesel generator
                            P_d(n,i,j) = Load(n) - P_w_exp(n,i,j) -
P_RAES_dschg(n,i,j);
                            P_d_exp(n,i,j) = P_d(n,i,j);
                            mode(n+1,i,j) = 2;
                        elseif Load(n) - P_w_exp(n,i,j) >= minP
                            P_RAES_dschg(n,i,j)    =    Load(n)    -
P_w_exp(n,i,j);                         %storage is within power band and
capable of fully supplementing wind,
                            mode(n+1,i,j) = 2;
                        else
                            P_RAES_dschg(n,i,j)         =         0;
%Ignite DIESEL: remaining load is not within storage power band
                            %Cycle chaging
                            if cycle == 1
                                [    P_d(n,i,j),     P_d_exp(n,i,j),
P_d_chg(n,i,j),         P_RAES_chg(n,i,j)]         =         cycleCharge1(
Load(n),P_w_exp(n,i,j), minP, maxP, P_d_eff  );
                            elseif cycle == 2
```

```
                                    [    P_d(n,i,j),    P_d_exp(n,i,j),
P_d_chg(n,i,j),        P_RAES_chg(n,i,j)]        =        cycleCharge2(
Load(n),P_w_exp(n,i,j), P_d_eff, cycleP  );
                                else
                                end

                                if            E_RAES(n,i,j)            +
P_d_chg(n,i,j)*dt*eff_chg_b <= RAES_cap
                                    P_RAES_chg(n,i,j) = P_d_chg(n,i,j);
%storage has capacity to accomodate cycle charging
                                    mode(n+1,i,j) = 1;
                                elseif            (RAES_cap            -
E_RAES(n,i,j))/(dt*eff_chg_b) >= minP
                                    P_d_chg(n,i,j)    =    (RAES_cap    -
E_RAES(n,i,j))/(dt*eff_chg_b);     %ensure SOC = 1 is not exceeded
                                    P_RAES_chg(n,i,j) = P_d_chg(n,i,j);
                                    P_d(n,i,j)    =    P_d_exp(n,i,j)    +
P_d_chg(n,i,j);
                                else
                                    P_d_chg(n,i,j)          =          0;
%SOC = 1, so do not charge
                                    P_RAES_chg(n,i,j) = 0;
                                    P_d(n,i,j) = P_d_exp(n,i,j);
                                end
                            end

                        elseif E_RAES(n,i,j) > 0

                            if E_RAES(n,i,j)*eff_dschg_b/dt >= maxP
                                P_RAES_dschg(n,i,j)        =        maxP;
%discharge at max storage power
                                P_d(n,i,j) = Load(n) - P_w_exp(n,i,j) -
P_RAES_dschg(n,i,j);      %and meet the remaining load with the diesel
generator
                                P_d_exp(n,i,j) = P_d(n,i,j);
                            elseif E_RAES(n,i,j)*eff_dschg_b/dt >= minP
                                P_RAES_dschg(n,i,j)                    =
E_RAES(n,i,j)*eff_dschg_b/dt;                %discharge all remaining
power
                                P_d(n,i,j) = Load(n) - P_w_exp(n,i,j) -
P_RAES_dschg(n,i,j);      %and meet the remaining load with the diesel
generator
                                P_d_exp(n,i,j) = P_d(n,i,j);
                            else
                                P_RAES_dschg(n,i,j)          =          0;
%Ignite DIESEL: remaining load is not within storage power band
                                %Cycle charging
                                if cycle == 1
                                    [    P_d(n,i,j),    P_d_exp(n,i,j),
P_d_chg(n,i,j),        P_RAES_chg(n,i,j)]        =        cycleCharge1(
Load(n),P_w_exp(n,i,j), minP, maxP, P_d_eff  );
                                elseif cycle == 2
                                    [    P_d(n,i,j),    P_d_exp(n,i,j),
P_d_chg(n,i,j),        P_RAES_chg(n,i,j)]        =        cycleCharge2(
Load(n),P_w_exp(n,i,j), P_d_eff, cycleP  );
                                else
```

```
                            end
                            mode(n+1,i,j) = 1;
                        end

                    else

                        %Cycle chaging
                        if cycle == 1
                            [       P_d(n,i,j),       P_d_exp(n,i,j),
P_d_chg(n,i,j),         P_RAES_chg(n,i,j)]        =        cycleCharge1(
Load(n),P_w_exp(n,i,j), minP, maxP, P_d_eff  );
                        elseif cycle == 2
                            [       P_d(n,i,j),       P_d_exp(n,i,j),
P_d_chg(n,i,j),         P_RAES_chg(n,i,j)]        =        cycleCharge2(
Load(n),P_w_exp(n,i,j), P_d_eff, cycleP  );
                        else
                        end
                        mode(n+1,i,j) = 1;
                    end
                end
            end

            d_eff(n,i,j)       =       CAT_1010(P_d(n,i,j),P_d_max);
%calculate diesel generator efficiency

            if n > 1
                if   P_d(n-1,i,j)   ==   0   &&   P_d(n,i,j)   >   0
%calculate diesel startup fuel costs (kWh)
                    fuel_startup = startup;
                    startup_count(i,j) = startup_count(i,j) + 1;
                else
                    fuel_startup = 0;
                end
            else
            end

            if P_d(n,i,j) == 0
               fuel(n,i,j) = 0;
               d_heat(n,i,j) = 0;
            else
                fuel(n,i,j)       =       P_d(n,i,j)*dt/d_eff(n,i,j)+
fuel_startup;     %calculate disel fuel consumption (kWh)
                d_heat(n,i,j)   =   fuel(n,i,j)*(1-d_eff(n,i,j))*HR;
%calculate disel waste heat (kWh)
            end

            %Heat Recovery System
            if                HRS                ==                0
%Turn on/off HRS
                d_heat(n,i,j) = 0;
            else
            end

            T_TES(n,i,j)     =     E_TES(n,i,j)*3600/(m_TES*Cp_TES);
%Calculate temp in TES
```

```
                if P_RAES_chg(n,i,j) > 0;
                    eff_chg_P                =                interp1([0
maxP],eff_chg_P_b,P_RAES_chg(n,i,j));               %calculates  charge
efficiency as a function of power
                    eff_chg_SOC               =               interp1([0
RAES_cap],eff_chg_SOC_b,E_RAES(n,i,j));    %calculates charge efficiency
as a function of SOC
                    eff_chg(n,i,j) = (eff_chg_P + eff_chg_SOC)/2;
                    av_eff_chg(i,j) = av_eff_chg(i,j) + eff_chg(n,i,j);
%calculates average charge efficiency
                    n_chg(i,j) =  n_chg(i,j) + 1;
                else
                    eff_chg(n,i,j) = 1;
                end

                if P_RAES_dschg(n,i,j) > 0;
                    eff_dschg_P                =                interp1([0
maxP],eff_dschg_P_b,P_RAES_dschg(n,i,j));          %calculates discharge
efficiency as a function of power
                    eff_dschg_SOC               =               interp1([0
RAES_cap],eff_dschg_SOC_b,E_RAES(n,i,j));          %calculates  discharge
efficiency as a function of SOC
                    eff_dschg(n,i,j) = (eff_dschg_P + eff_dschg_SOC)/2;
%baseline efficiency
                    eff_dschgT(n,i,j)                                    =
(T_TES(n,i,j)/(T_amb(n)+dT))*eff_dschg(n,i,j);                %discharge
efficiency w/ temp compensation for TES
                    av_eff_dschg(i,j)      =      av_eff_dschg(i,j)      +
eff_dschgT(n,i,j);                          %calculates  average  discharge
efficiency
                    n_dschg(i,j) =  n_dschg(i,j) + 1;
                else
                    eff_dschgT(n,i,j) = 1;
                end

                %Calculate the total energy in the ESS
                E_RAES(n+1,i,j)         =         E_RAES(n,i,j)         +
P_RAES_chg(n,i,j)*dt*eff_chg(n,i,j)                                      -
P_RAES_dschg(n,i,j)*dt/eff_dschgT(n,i,j);

                if E_RAES(n+1,i,j) < 0
                    E_RAES(n+1,i,j) = 0;
                end

                if E_RAES(n+1,i,j) > RAES_cap
                    E_RAES(n+1,i,j)              =              RAES_cap;
%It is possible that this occurs by very small margins
                end

                TES_losses(n,i,j)   =   loss*(T_TES(n,i,j)   -   T_amb(n));
%Calculates thermal losses in the thermal storage tank

            if E_TES(n+1,i,j) < m_TES*Cp_TES*274/3600;       %Ensure TES
doesn't freeze.
```

```
                E_TES(n+1,i,j) = m_TES*Cp_TES*274/3600;
            else
            end

                E_TES(n+1,i,j)   =   E_TES(n,i,j)   +   d_heat(n,i,j)   +
P_RAES_chg(n,i,j)*eff_chg(n,i,j)*dt*kWh_t_kWh_e(n,i,j)                    -
P_RAES_dschg(n,i,j)/eff_dschgT(n,i,j)*dt*kWh_t_kWh_e(n,i,j)               -
TES_losses(n,i,j)*dt;

                %Ensure T_TES does not exceed maxTemp, otherwise diesel
cooling is not possible
                if E_TES(n+1,i,j)*3600/(m_TES*Cp_TES) > maxTemp
                    E_TES(n+1,i,j) = 348*m_TES*Cp_TES/3600;
                else
                end

                if E_TES(n+1,i,j) < E_TES(1,1,1)
                    E_TES(n+1,i,j) = E_TES(1,1,1);
                end
        end
        i %Informs user how program is progessing
        j
    end
end

%% Calculate statistics for each permutation
for j = 1:1:J
    cost_wwind(1,j) = (pen(j)/100)*maxload*WECcost;
end

for i = 2:1:I
    for j = 1:1:J
          cost_wwind(i,j)      =      (pen(j)/100)*maxload*WECcost      +
cap(i)*capcost + maxP*powcost;
    end
end

%This section calculates important statistics for analysis
t_fuel_b1_8mth = sum(fuel_b1)/10;
t_fuel_b2_8mth = sum(fuel_b2)/10;
t_wind_8mth = sum(wind)/4;
P_d_b1_t_8mth = sum(P_d_b1)/4;
P_d_b2_t_8mth = sum(P_d_b2)/4;

for i = 1:1:I
    for j = 1:1:J
        E_RAES_dschg(i,j)     =     sum(P_RAES_dschg(:,i,j))/4;     %RAES
throughput
        t_fuel(i,j) = sum(fuel(:,i,j))/10;      %total fuel consumption
in L
        av_eff(i,j)                                                    =
(av_eff_chg(i,j)/n_chg(i,j))*(av_eff_dschg(i,j)/n_dschg(i,j));
%average RT efficiency
        av_eff_dschg(i,j)  =  av_eff_dschg(i,j)/n_dschg(i,j);  %  average
discharge efficiency
```

```
        f_savings(i,j) = t_fuel_b1_8mth - t_fuel(i,j);   %fuel savings
compared to baseline
        savings(i,j) = f_savings(i,j)*diesel_price/0.58;        %dollar
savings
        payback(i,j) = cost_wwind(i,j)/savings(i,j);    %simple payback
for a wind/storage system
        curtailed(i,j) = sum(P_w_curt(:,i,j))/6;        %curtailed WEC
outout

    end
end
```

Cycle Charging Function

```
% RAES for Wind / Diesel Hybrid Systems
% Sebastian Manchester (sebmanchester@gmail.com)
% Copyright 2014 as part of the Renewable Energy Storage Lab
% Please direct inquiries to Dr. Lukas Swan

function [ P_d, P_d_exp, P_d_chg, P_RAES_chg] = cycleCharge1(
Load,P_w_exp, minP, maxP, P_d_eff )
%cycleCharge - calculates the level of cycle charging from a diesel
%generator

if Load - P_w_exp >= P_d_eff

    P_d = Load - P_w_exp;
    P_d_exp = P_d;
    P_d_chg = 0;

else
    if Load - P_w_exp + minP <= P_d_eff
        %run the optimal diesel efficiency point and cycle charge the
storage
        P_d = P_d_eff;
        P_d_exp = Load - P_w_exp;
        P_d_chg = P_d - P_d_exp;

        if  P_d_chg > maxP
            P_d_chg = maxP;     %don't overpower the storage during
charging
            P_d = P_d_chg + P_d_exp;
        else
        end
    else    %Condition 3C: ensure cycle charging at least meets minimum
storage power
        P_d_exp = Load - P_w_exp;
        P_d_chg = minP;
        P_d = P_d_exp + P_d_chg;
    end
end
```

Diesel Generator Function

```
% RAES for Wind / Diesel Hybrid Systems
% Sebastian Manchester (sebmanchester@gmail.com)
% Copyright 2014 as part of the Renewable Energy Storage Lab
% Please direct inquiries to Dr. Lukas Swan

function [ E ] = CAT_1010( P, Pmax )
%This function calculates the efficiency of a 1010 kW CAT diesel
generator based on
%its power output.
rated_power = 1010;
m = 60.35;
b = 33.683;

if P <= Pmax

    E = (P/Pmax)*rated_power/(((P*100/Pmax)*m/25+b)*9.7);
else

    P = P/2;
    E = (P/Pmax)*rated_power/(((P*100/Pmax)*m/25+b)*9.7);

end
```

APPENDIX B MATLAB Code for Constrained Grid Case Study

```
% Lightsail RAES for Wind / CHP System on a Capacity Constrained Grid
% Sebastian Manchester (sebmanchester@gmail.com)
% Copyright 2014 as part of the Renewable Energy Storage Lab
% Please direct inquiries to Dr. Lukas Swan


clc, clear;
tic;
%% Inputs
% Loads WEC output data, local temperature.
data1 = load('-mat','Data');
vars = fieldnames(data1);

for i = 1:length(vars)
    assignin('base', vars{i}, data1.(vars{i}));
end

x = 52560;                              %number of 10 min time steps in a
year

%choose WEC configuration
Wind = P_wec(25:52584,1);           % 3 X GE 1.6 MW WECs
T_amb = Temp_10min(1:x,1)+273;
dt = 1/6;                    %time step (hrs)

%% Operational Parameters
%Grid
gridlimit = 3600;                           %Maximum grid capacity under
COMFIT (kW)
FIT = 0.131;                            %COMFiT rate ($/kWh)
windcap = max(Wind);
%RAES system
maxcap = 20; %MWh
cap = [0.1;0.2;0.3;0.4;0.5;0.6;0.7;0.8;0.9;1]*maxcap*1000;
maxpow = 2; %MW
pow = [0.25;0.5;0.75;1.0]*maxpow*1000;
I = size(pow,1);
J = size(cap,1);
minP = 250;                             %rated minimum power
eff_chg_b = 0.8;
eff_dschg_b = 0.8;
eff_range_P = [0.67 0.81];              %efficiency range from 0 to 100%
for POWER
eff_range_SOC = [0.75 0.81];            %efficiency range from 0 to 100%
for SOC
eff_chg_P_b = eff_range_P;              %baseline charge eff for maxP
eff_chg_SOC_b = eff_range_SOC;          %baseline charge eff for SOC = 1
eff_dschg_P_b = eff_range_P;            %baseline discharge eff for maxP
eff_dschg_SOC_b = eff_range_SOC;        %baseline discharge eff for SOC =
1
dT = 32.6;                                  %(K) temperature rise during
compression
```

```
%TES system
HR_curt = 0;                %Capture curtailed wind as waste heat?
HRS = zeros(x,1)+1;
HRS(10945:37151,1) = 1;      %WHR from CHP only available between mid-
Oct and mid-Apr
steamtemp = 363;%273+155;
HR = 0.5;                   %heat recovery effectiveness
Cp_TES = 4.18;              %heat capacity (kJ/kg/k)
HX = 1 ;                    %heat exchanger efficiency
heatloss = 0.1;             %heat loss rate (kW/K)
maxTemp = 363;              %TES temp limit (normally 348 K)

%System Costs
capcost = 200;        %$/kWh
powcost = 2000;       %$/kW
windcost = 2275;      %$/kW

%% Operation
% All power values in kW, all energy values in kWh

P_w = Wind;
P_w_exp = zeros(x,I,J);
P_w_chg = zeros(x,I,J);
P_w_curtA = zeros(x,I,J);
P_w_curtB = zeros(x,I,J);
P_w_curt = zeros(x,I,J);

%Baseline values
P_w_exp_b = zeros(x,1);
P_curt_b = zeros(x,1);

E_RAES = zeros(x,I,J);
P_RAES_dschg = zeros(x,I,J);
P_RAES_chg = zeros(x,I,J);
T_exp = zeros(x,I,J)+293;
eff_dschg = zeros(x,I,J);
eff_dschgT = zeros(x,I,J);
eff_chg = zeros(x,I,J);
av_eff_chg = zeros(I,J);
av_eff_dschg = zeros(I,J);
av_effC = zeros(I,J);
av_effD = zeros(I,J);
n_chg = zeros(I,J);
n_dschg = zeros(I,J);
kWh_t_kWh_e = zeros(x,I,J) + 0.9886;

E_TES = zeros(x,I,J);
T_TES = zeros(x,I,J);
TES_losses  = zeros(x,I,J);
P_w_curt_heat = zeros(x,I,J);

%Stats
E_curt = zeros(I,J);
av_eff = zeros(I,J);
cost_RAES = zeros(I,J);
```

```
cost_system = zeros(I,J);
payback = zeros(I,J);
payback_system = zeros(I,J);
RAES_rev = zeros(I,J);
WEC_rev = zeros(I,J);
ave_T_TES = zeros(I,J);
ave_E_TES = zeros(I,J);
ave_E_RAES = zeros(I,J);
E_RAES_dschg = zeros(I,J);
E_RAES_chg = zeros(I,J);
E_WEC_exp = zeros(I,J);
empty = zeros(I,J);
%% Baseline case - no storage, curtail all wind

for n = 1:x-1
    if P_w(n,1) > gridlimit;
        P_curt_b(n,1) = P_w(n,1) - gridlimit;
        P_w_exp_b(n,1) = gridlimit;
    else
        P_w_exp_b(n,1) = P_w(n,1);
    end
end

E_WEC_exp_b = sum(P_w_exp_b(:,1))/6;
E_curt_b = sum(P_curt_b(:,1))/6;
WEC_rev_b = E_WEC_exp_b*FIT;
payback_b = windcap*windcost/WEC_rev_b;

%% Begin loops
for i = 1:length(pow)               %vary RAES power
    maxP = pow(i);


    for j = 1:length(cap)           %vary RAES energy
            RAES_cap = cap(j);
            m_TES = RAES_cap/1000*33000;        %TES mass and heat loss
depends on Capacity
            loss = RAES_cap/1000*heatloss;
            T_TES(1,i,j) = T_amb(1);
            E_TES(1,i,j) = m_TES*Cp_TES*T_TES(1,i,j)/3600;

        for n = 1:x-1

            if P_w(n,1) >= gridlimit;
                P_w_exp(n,i,j)              =               gridlimit;
%export wind to meet gridlimt
                curtA                       =                       0;
%Reset curtailment counters
                curtB = 0;

                if P_w(n,1) - P_w_exp(n,i,j) > maxP
                    P_w_chg(n,i,j)              =               maxP;
%charge power limited by max power, so some curtailment is necessary
                    curtA = P_w(n,1) - P_w_exp(n,i,j) - P_w_chg(n,i,j);
```

```
                elseif P_w(n,1) - P_w_exp(n,i,j) >= minP
                    P_w_chg(n,i,j)    =    P_w(n,1)    -    P_w_exp(n,i,j);
%charge power is within power band, charge with all remaining wind
power


                else
                    P_w_chg(n,i,j)                    =                    0;
%remaining wind power is not within sotarge power band, so it must be
curtailed
                    curtA      =      P_w(n,1)      -      P_w_exp(n,i,j);
%curtailed due to storage power
                end

                if   E_RAES(n,i,j)   +   P_w_chg(n,i,j)*dt*eff_chg_b   <=
RAES_cap
                    P_RAES_chg(n,i,j)          =          P_w_chg(n,i,j);
%there is remaining storage capacity
                elseif (RAES_cap - E_RAES(n,i,j))/(dt*eff_chg_b)>= minP
                    P_RAES_chg(n,i,j)        =        (RAES_cap        -
E_RAES(n,i,j))/(dt*eff_chg_b);        %storage will reach SOC = 1, so
some curtailment is necessary
                    curtB    =    P_w_chg(n,i,j)    -    P_RAES_chg(n,i,j);
%ensure that available capacity can be charged within CAES storage
power band
                    P_w_chg(n,i,j)          =          P_RAES_chg(n,i,j);
%curtailment due to storage capacity
                else
                    P_RAES_chg(n,i,j)                 =                 0;
%storage will reach SOC = 1 but capacity will not work with power band
                    curtB                =                P_w_chg(n,i,j);
%curtailment due to storage capacity
                    P_w_chg(n,i,j) = P_RAES_chg(n,i,j);
                end

                P_w_curtA(n,i,j) = curtA;        %Sum curtailment due to
storage power
                P_w_curtB(n,i,j) = curtB;        %Sum curtailment due to
storage capacity

            else % (P_w < gridlimit)

                P_w_exp(n,i,j)                =                P_w(n,1);
%export all wind

                if    E_RAES(n,i,j)*eff_dschg_b/dt    >=    gridlimit    -
P_w_exp(n,i,j)  %there is available energy stored to fill grid limit

                    if gridlimit - P_w_exp(n,i,j) >= maxP
                        P_RAES_dschg(n,i,j)            =            maxP;
%discharge at max storage power
                    elseif gridlimit - P_w_exp(n,i,j) >= minP
                        P_RAES_dschg(n,i,j)      =      gridlimit      -
P_w_exp(n,i,j);       %storage is within power band and capable of fully
supplementing wind,
                    else
```

```
                    P_RAES_dschg(n,i,j) = 0;
                end

            elseif E_RAES(n,i,j) > 0        %some energy, but not
enough to fill grid limit

                if E_RAES(n,i,j)*eff_dschg_b/dt >= maxP
                    P_RAES_dschg(n,i,j)           =           maxP;
%discharge at max storage power
                elseif E_RAES(n,i,j)*eff_dschg_b/dt >= minP
                    P_RAES_dschg(n,i,j)                                =
E_RAES(n,i,j)*eff_dschg_b/dt;                   %discharge all remaining
power
                else
                    P_RAES_dschg(n,i,j) = 0;
                end

            else         %no energy stored
                P_RAES_dschg(n,i,j) = 0;
            end
        end

        %Heat Recovery System
        %From CHP
        if              HRS(n)                 ==                0
%No steam from CHP
            T_TES(n,i,j)     =     E_TES(n,i,j)*3600/(m_TES*Cp_TES);
%Calculate temp in TES
        else
            T_TES(n,i,j)                  =                  maxTemp;
%Steam available from CHP
            E_TES(n,i,j) = maxTemp*m_TES*Cp_TES/3600;

        end
        %From Curtailed wind
        if HR_curt == 0
            P_w_curt_heat(n,i,j) = 0;
        else
            P_w_curt_heat(n,i,j)      =      (P_w_curtA(n,i,j)      +
P_w_curtB(n,i,j))*HR;
        end


        %RAES Efficiency
        if P_RAES_chg(n,i,j) > 0;
            eff_chg_P                  =                  interp1([0
maxP],eff_chg_P_b,P_RAES_chg(n,i,j));               %calculates  charge
efficiency as a function of power
            eff_chg_SOC                 =                 interp1([0
RAES_cap],eff_chg_SOC_b,E_RAES(n,i,j));             %calculates  charge
efficiency as a function of SOC
            eff_chg(n,i,j) = (eff_chg_P + eff_chg_SOC)/2;
            av_eff_chg(i,j)  =  av_eff_chg(i,j)  +  eff_chg(n,i,j);
%calculates average charge efficiency
            n_chg(i,j) =  n_chg(i,j) + 1;
```

```
            else
                eff_chg(n,i,j) = 1;
            end

            if P_RAES_dschg(n,i,j) > 0;
                eff_dschg_P                =                interp1([0
maxP],eff_dschg_P_b,P_RAES_dschg(n,i,j));          %calculates discharge
efficiency as a function of power
                eff_dschg_SOC               =                interp1([0
RAES_cap],eff_dschg_SOC_b,E_RAES(n,i,j));          %calculates discharge
efficiency as a function of SOC
                eff_dschg(n,i,j)  =  (eff_dschg_P  +  eff_dschg_SOC)/2;
%baseline efficiency
                eff_dschgT(n,i,j)                                        =
(T_TES(n,i,j)/(T_amb(n)+dT))*eff_dschg(n,i,j);                %discharge
efficiency w/ temp compensation for TES
                av_eff_dschg(i,j)       =       av_eff_dschg(i,j)       +
eff_dschgT(n,i,j);                          %calculates average discharge
efficiency
                n_dschg(i,j) =  n_dschg(i,j) + 1;
            else
                eff_dschgT(n,i,j) = 1;
            end

            %Calculate the total energy in the ESS
            E_RAES(n+1,i,j)          =          E_RAES(n,i,j)          +
P_RAES_chg(n,i,j)*dt*eff_chg(n,i,j)                                      -
P_RAES_dschg(n,i,j)*dt/(eff_dschgT(n,i,j));

            if E_RAES(n+1,i,j) < 0
                E_RAES(n+1,i,j) = 0;
            end

            if E_RAES(n+1,i,j) > RAES_cap
                E_RAES(n+1,i,j) = RAES_cap;    %It is possible that this
occurs by very small margins due to discrepencies between baseline and
actual efficiencies
            end

            TES_losses(n,i,j)    =    loss*(T_TES(n,i,j)    -    T_amb(n));
%Calculates thermal losses in the thermal storage tank


            E_TES(n+1,i,j)           =           E_TES(n,i,j)           +
P_RAES_chg(n,i,j)*eff_chg(n,i,j)*dt*kWh_t_kWh_e(n,i,j)                   -
P_RAES_dschg(n,i,j)*dt*kWh_t_kWh_e(n,i,j)/eff_dschgT(n,i,j)              -
TES_losses(n,i,j)*dt + P_w_curt_heat(n,i,j)*dt;

            %Ensure T_TES does not exceed maxTemp
            if E_TES(n+1,i,j)*3600/(m_TES*Cp_TES) > maxTemp
                T_TES(n+1,i,j) = maxTemp;
                E_TES(n+1,i,j) = maxTemp*m_TES*Cp_TES/3600;
            else
            end
```

```
            if E_TES(n+1,i,j) < m_TES*Cp_TES*274/3600;       %Ensure TES
doesn't freeze.
                E_TES(n+1,i,j) = m_TES*Cp_TES*274/3600;
            else
            end

            if E_RAES(n+1,i,j) <= 21              %Counter to determine
how much time RAES sits at SOC = 0.2
                empty(i,j) = empty(i,j) + 1;
            else
            end

        end
        %Calcultate the system cost
        cost_RAES(i,j) = RAES_cap*capcost + maxP*powcost;
        cost_system(i,j) = cost_RAES(i,j) + windcap*windcost;
        P_w_curt(:,i,j) = P_w_curtA(:,i,j) + P_w_curtB(:,i,j);
        i %Informs user how program is progessing
        j

    end
end
%%
E_WEC = sum(P_w(:,1))/6;
WEC_rev_NoRAES = sum(Wind(:,1))*3.6/4.86/6*FIT;
% Calculate analysis statistics
for i = 1:1:I
    for j = 1:1:J
        cost_system_inc(i,j)     =     cost_RAES(i,j)     +     (windcap-
3600)*windcost;    %Cost of the incremental WEC + RAES
        E_RAES_dschg(i,j)     =     sum(P_RAES_dschg(:,i,j))/6;     %RAES
throughput
        E_RAES_chg(i,j) = sum(P_RAES_chg(:,i,j))/6; %RAES charge energy
        E_WEC_exp(i,j) = sum(P_w_exp(:,i,j))/6; %WEC exported energy
        RAES_rev(i,j) = E_RAES_dschg(i,j)*FIT; % RAES revenue
        WEC_rev(i,j) = E_WEC_exp(i,j)*FIT;  %WEC revenue
        av_effC(i,j)   =   av_eff_chg(i,j)/n_chg(i,j);   %average   charge
efficiency
        av_effD(i,j)   =   av_eff_dschg(i,j)/n_dschg(i,j);   %   average
discharge efficicnecy
        av_eff(i,j)  =  (av_effC(i,j)*av_effD(i,j));         %average  RT
efficiency
        payback(i,j)  =  cost_RAES(i,j)/RAES_rev(i,j);   %simple  payback
for RAES only
        payback_system(i,j)                                              =
cost_system(i,j)/(RAES_rev(i,j)+WEC_rev(i,j));   %simple   payback   for
entire system
        payback_system_inc(i,j)                                          =
cost_system_inc(i,j)/(RAES_rev(i,j)+(WEC_rev(i,j)   -   WEC_rev_NoRAES));
%simple payback for excess WEC and RAES
        E_curt(i,j)  =  sum(P_w_curt(1:x,i,j))/6;        %total  curtailed
wind energy
        ave_T_TES(i,j) = mean(T_TES(:,i,j));
        ave_E_TES(i,j) = mean(E_TES(:,i,j));
        ave_E_RAES(i,j) = mean(E_RAES(:,i,j));
    end
```

```
end
empty = empty/6;

%% Count the duration of storage events (time between beginning and end
of curtailment)
i = 1;    %counter for duration matrix
duration = 0;
energy = 0;

for n=1:x
    if P_w(n,1) - gridlimit > 0
        duration(i,1) = duration(i,1) + 1;
        energy(i,1) = energy(i,1) + (P_w(n,1) - gridlimit)/6;
    end

    if duration(i,1) > 0 && P_w(n,1) - gridlimit <= 0
        i = i + 1;
        duration(i,1) = 0;
        energy(i,1) = 0;
    end
end

duration                          =                          duration/6;
%Convert to hours
d_bins = 5:5:60;
d_freq = histc(duration, d_bins)*size(duration,1)/100;


% Sum the bins for energy to determine what storage interval is most
useful.
energy = energy/1000;
int = 5;                                  %choose storage interval for
histogram
e_bins = 5:int:max(energy)+int;    %create bins
e_freq = histc(energy,e_bins);     %divide into bins

energy_binned = zeros(size(e_bins,2),1);

for m = 1:size(energy,1)      %sum the energy of the first bin
     if energy(m,1) <= e_bins(1,1)
         energy_binned(1,1) = energy_binned(1,1) + energy(m,1);    %sum
the event max bins, but in terms of event energy
     end
end


for n = 2:size(e_bins,2)    %sum the rest of the bins
     for m = 1:size(energy,1)
         if energy(m,1) <= e_bins(1,n) && energy(m,1) > e_bins(1,n-1)
             energy_binned(n,1) = energy_binned(n,1) + energy(m,1);
         end
     end
end
%%
Results1 = zeros(J+1,4);
```

```
i = 2;       %Choose capacity

Results1(:,1) = 0:2:20;
Results1(1,2) = E_curt_b;
Results1(2:J+1,2) = E_curt(i,:);
Results1(2:J+1,3) = E_RAES_dschg(i,:);
Results1(2:J+1,4) = RAES_rev(i,:);

Results1

toc;
```

APPENDIX C MATLAB Code for Miscellaneous Functions

Sample WEC Ouput Code

```
% Sebastian Manchester (sebmanchester@gmail.com)
% Copyright 2014 as part of the Renewable Energy Storage Lab
% Please direct inquiries to Dr. Lukas Swan

function [P] = wind_power_output(V)
%This function calculates the wind power output for an Windmatic 65 kW
wind turbine
% Copyright 2014 as part of the Renewable Energy Storage Lab
% Please direct inquiries to Dr. Lukas Swan

E33   =    [0   0;
            1   0;
            2   0;
            3   5;
            4   13.7;
            5   30;
            6   55;
            7   92;
            8   138;
            9   196;
            10  250;
            11  292.8;
            12  320;
            13  335;
            14  335;
            15  335;
            16  335;
            17  335;
            18  335;
            19  335;
            20  335;
            21  335;
            22  335;
            23  335;
            24  335;
            25  335;
            26  0];



x  = size(V,1)

for n = 1:x
P(n,1) = interp1(E33(:,1),E33(:,2),V(n,1),'cubic');              %Cubic
interpolation
end
end
```

Hub Height Correlation

```
%HubCorrect Correlates wind speeds to a proper hub height WEC hub
height
% Sebastian Manchester (sebmanchester@gmail.com)
% Copyright 2014 as part of the Renewable Energy Storage Lab
% Please direct inquiries to Dr. Lukas Swan

function [ Vhub ] = HubCorrect( V,z,zref )
%UNTITLED Correlates wind speeds to a proper hub height
                                                    %turbine hub height
alpha = 0.2;                                          %power law
exponent
Vhub = zeros(size(V,1),1);                          %Preallocate
array
for n = 1:size(V,1)
    Vhub(n,1) = V(n,1)*(z/zref)^alpha;
end

end
```